

STUDIES ON THE PREPARATION AND PROPERTIES OF NEUROFIBRILLARY  
TANGLES FROM BRAINS OF PATIENTS WITH ALZHEIMER-TYPE DEMENTIA

SUSAN HUSSEY

Ph.D THESIS

UNIVERSITY OF EDINBURGH

1988



## DECLARATION

This thesis has been composed by myself, Susan Hussey.

All the work described in this thesis has been performed by myself; with other contributions being only those specified below:

1. Initial screening assessment of all brains in MRC Brain Bank, using silver staining, were performed by Dr. Alexander Gordon.
2. Silver staining of brain sections were performed by Ms Linda McArdle.
3. Initial measurements of PHF in samples 1 and 2, in Chapter 3,, Part 1, using a graticule, were performed by Dr Peter Gibson. Measurements of PHF in samples 1 - 4, using an image analyser were performed by myself.
4. Technical operation of FACS IV 40 was by Mr Harris Morrison.
5. Computation of CD Spectra was performed by Dr. Steven Martin.

With thanks to:

Dr. Walter Gratzer

Mr. James Simpson

Dr. Alexander Gordon

Dr. Peter Gibson

Dr. Celia Yates

Professor George Fink,

Dr. Daryl Green

Dr. Peter Eagles

Dr. Robert Elton

Mrs. Anne Kelly

Mrs. Isobel Tait

## ABSTRACT OF THESIS

Alzheimer's disease and senile dementia of the Alzheimer type (Alzheimer-type dementia, ATD) are progressive dementing illnesses characterised histopathologically by the presence of neurofibrillary tangles and plaques. Ultrastructurally tangles are composed of paired helical filaments (PHF) (Kidd, 1963) of unknown origin. The purpose of this study was to investigate the biochemical and biophysical properties of tangles, and their constituent PHF. Investigation of tangle solubility by quantitative light microscopy of brain homogenates showed that a proportion of tangles, which varied between brains (ATD and Down's Syndrome with ATD pathology) were soluble in sodium dodecylsulphate (SDS) and NaOH. Tangle solubility in 1% SDS was inversely related to duration of dementia suggesting that patients with long standing illness have more fragile tangles.

Ultrastructural studies were carried out on tangle enriched fractions prepared by ultracentrifugation of supernatants from SDS treated brain homogenates, and by sucrose density gradient centrifugation of brain homogenates not treated with SDS. PHF in the former preparation were found to be longer with lengthened pitches compared to PHF in the latter preparation. PHF from another SDS treated preparation which was repeatedly freeze thawed (up to 25°C) were observed to lose their helical configuration. These electronmicroscopic observations suggest that the helical substructure of PHF may be subject to conformational change, whilst filament structure is retained.

Preparation of tangle enriched fractions from ATD brains was investigated using Percoll, sucrose gradient centrifugation and fluorescence activated cell sorting (FACS). Percoll proved unsatisfactory as a gradient medium for tangle separation; whereas sucrose density gradient centrifugation was found to be a successful method for preparing tangle enriched fractions. Tangle preparation using FACS was developed as a new technique, in which tangles labelled with the fluorescent dye, Congo red, could be sorted from ATD brain homogenate.

Partially purified tangle preparations were investigated using spectroscopy. The resulting spectra showed features consistent with an increase in  $\beta$  sheet in the tangle enriched versus the control fraction.



INDEX

	PAGE
CHAPTER 1 INTRODUCTION	
1.1 Epidemiology and clinical presentation of Alzheimer type dementia.	12
1.2 Pathology.	15
1.3 Morphometric studies in ATD.	18
1.4 Changes in the normal aged brain.	21
1.5 Other dementing diseases, a comparison with ATD.	22
1.6 Tangles and PHF in non-human species; and tangles produced experimentally.	25
1.7 Neurotransmitters in ATD.	27
1.8 Immunochemical studies on neurofibrillary tangles.	30
1.9 Genetic aspects of ATD.	32
1.10 Subunit structure of PHF.	34
1.11 Solubility of PHF.	35
1.12 Protein composition of PHF; and comparison with senile amyloid.	37
1.13 Intermediate filaments.	38
CHAPTER 2 MATERIALS AND METHODS	
2.1 MATERIALS	42
2.1.1 Human brain tissue.	42
2.1.2 Bovine extradural nerve roots.	43
2.1.3 Histological stains.	43
2.1.4 Percoll and calibration beads.	43
2.1.5 Electrophoresis calibration kits.	43
2.1.6 Electron microscopy materials.	43
2.1.7 Chemicals.	43

	PAGE
2.2. METHODS	44
2.2.1 Dissection of human brain.	44
2.2.2 Protein determination.	45
2.2.3 Dialysis.	46
2.2.4 Polyacrylamide gel electrophoresis (SDS-PAGE)	46
2.2.5 Electrophoretic procedure.	46
2.2.6 Gel filtration.	48
2.2.7 Light and fluorescence microscopy.	51
2.2.8 Electron microscopy.	52
2.2.9 Subcellular fractionation.	53
2.2.10 Histological staining techniques.	54
2.2.11 Fluorescence Activated Cell Sorting (FACS)	55
2.2.12 Spectral studies.	57
CHAPTER 3 MORPHOMETRIC AND SOLUBILITY STUDIES ON TANGLES AND PHF	
PART 1	59
3.1 INTRODUCTION	59
3.2 MATERIALS AND METHODS	61
3.2.1 Materials and staining techniques.	61
3.2.2 A quantitative comparison of Congo red and Silver Staining Methods.	61
3.2.3 Solubility of tangles and plaque cores in SDS and NaOH.	62
3.2.4 Comparison of Native and SDS treated PHF using electronmicroscopy.	64
3.3. RESULTS	67
3.3.1 Identification of tangles and plaques using histological staining techniques.	67
3.3.2 A quantitative comparison of Congo red and silver staining.	68

	PAGE
3.3.3 Solubility of tangles and plaque cores in SDS and NaOH.	72
3.3.4 A comparison of native and SDS treated PHF using EM.	77
3.4 DISCUSSION	82
3.4.1 Identification of plaques and tangles and comparison of Congo red and silver staining.	82
3.4.2 Solubility of tangles and plaque cores in SDS and NaOH, and the relationships to clinical factors.	85
3.4.3 A comparison between native and SDS treated PHF using electronmicroscopy.	87
PART 2	89
ULTRASTRUCTURAL OBSERVATIONS OF AN 'AGED' PREPARATION OF PHF	89
3.5 INTRODUCTION	89
3.6 METHODS	89
3.6.1 Preparation and examination of 'aged' PHF fraction.	89
3.6.2 Investigation of factors contributing towards morphological heterogeneity of PHF in the 'aged' preparation.	90
3.6.3 Quantitation of morphological changes in the 'aged' preparation.	92
3.7. RESULTS	94
3.7.1 A comparison of 'aged' and freshly prepared PHF fractions.	94
3.8 DISCUSSION	102
PART 3	
SDS POLYACRYLAMIDE ELECTROPHORESIS (SDS-PAGE) AND GEL FILTRATION OF ATD BRAIN HOMOGENATES AND TANGLE PREPARATIONS	104
3.9 INTRODUCTION AND METHOD	104
3.9.1 Gel electrophoresis.	104
3.9.2 Gel filtration.	105

	PAGE
3.10 RESULTS AND DISCUSSION	105
3.10.1 Gel electrophoresis.	105
3.10.2 Gel filtration.	106
CHAPTER 4 FLUORESCENCE ACTIVATED CELL SORTING (FACS) AS A SEPARATION METHOD FOR NEUROFIBRILLARY TANGLES	
4.1 INTRODUCTION	112
4.2 MATERIALS AND METHODS	113
4.2.1 Investigation of the fluorescence spectrum of Congo red.	113
4.2.2. Sample preparation and staining with Congo red.	119
4.2.3 Fluorescence Activated Cell Sorting Procedure.	125
4.2.4 Investigation of the effect of auto- fluorescence and non-specific staining.	127
4.3 RESULTS AND DISCUSSION	131
4.3.1 Comments on Figure 4.3.	131
4.3.2 Assessment of sorted fraction in final experiment.	139
4.3.3 Unresolved problems encountered during staining and sorting.	140
4.4 DISCUSSION	141
CHAPTER 5 THE PREPARATION OF NEUROFIBRILLARY TANGLES BY DENSITY GRADIENT CENTRIFUGATION	
5.1 INTRODUCTION	144
5.1.1 Centrifugation theory.	144
5.1.2 The use of density gradient centrifugation as a preparation method for intermediate filaments and PHF.	145
5.1.3 Percoll, a continuous self-forming gradient medium.	146
5.2 MATERIALS AND METHODS	147

	PAGE
5.2.1	The preparation of neurofibrillary tangles using Percoll. 147
5.2.2	The preparation of neurofibrillary tangles using sucrose density gradients. 150
5.2.3	The preparation of neurofibrillary tangles and PHF using a rapid denaturing method. 152
5.2.4	An investigation of Selkoe et al's (1982) PHF preparation method. 152
5.3	RESULTS AND DISCUSSION 155
5.3.1	The preparation of neurofibrillary tangles using Percoll. 155
5.3.2	The preparation of neurofibrillary tangles using sucrose density gradients. 157
5.3.3	The preparation of neurofibrillary tangles using continuous sucrose density gradient centrifugation. 167
5.3.4	Rapid denaturing method for the preparation of neurofibrillary tangles and PHF. 167
5.3.5	The preparation of neurofibrillary tangles using Selkoe's (1982) method. 167
5.4	DISCUSSION 168
CHAPTER 6	SPECTRAL STUDIES ON PURIFIED PREPARATIONS OF PHF
6.1	INTRODUCTION 172
6.1.1	Fluorescence spectra. 172
6.1.2	Circular dichroism. 173
6.1.3	Vibrational spectra - Infra red. 173
6.2	METHODS 174
6.2.1	Fluorescence spectra. 174
6.2.2	Circular dichroism. 175
6.2.3	Infra red spectra. 175
6.3	RESULTS 175
6.3.1	Fluorescence spectra. 175

	PAGE
6.3.2 Circular dichroism.	179
6.3.3 Infra red spectra.	182
6.4 DISCUSSION	184
SUMMARY	185
BIBLIOGRAPHY	187
APPENDIX TO BIBLIOGRAPHY	206
APPENDIX	207

## CHAPTER 1

### INTRODUCTION



## INTRODUCTION

### 1.1 Epidemiology and clinical presentation of Alzheimer type dementia

Dementia has been recognised clinically for many years. In 1902, Gowers hypothesised that some people showed a premature aging, or degeneration of the nervous system. The pathology of presenile dementia (Alzheimer's disease; AD) was described in 1907 by Alois Alzheimer, in a patient aged 51.

The pathology of the commonest form of dementia in older patients, i.e. senile dementia of the Alzheimer type (SDAT) was found to be similar to that of younger patients with AD (Simochowicz, 1910; Tomlinson, Blessed and Roth, 1970). Both senile and presenile diseases can therefore be referred to as Alzheimer-type dementia (ATD).

The diagnosis of ATD on the basis of psychiatric examination and psychological testing augmented by investigations such as brain scans, has progressed enormously over the last few years; however, identification of the histopathological changes at post mortem or very occasionally, by cerebral biopsy, still provide the definitive diagnosis. Amongst a group of 1,009 patients over 55 years of age presenting with dementia, Jellinger (1976) reported that the neuropathological diagnoses were: Alzheimer's disease 58%, cerebrovascular disease 22.5%, both Alzheimer changes and

cerebrovascular disease 13.6% and others 12%. Kay, Beamish and Roth (1964) reported the prevalence of senile dementia in a Newcastle survey, to be 2.3% for 65 - 70 year olds, 3.9% for 70 - 80 year olds and 22% for those aged over 80.

Therefore, the incidence of AD increases sharply with age, and it has been suggested that this relies on a predisposing autosomal dominant gene with age related penetrance which reaches approximately 40% by the age of 90 (Larsson et al., 1963). Also there is a rare autosomal dominant 'familial' form of AD (See section 1.9). Lastly, the histological and biochemical changes of AD occur in people with Down's syndrome from the age of about 40 onwards (Malamud, 1972; Ellis et al, 1974). As the population of Northern Europe and America has aged, due to increased life expectancy (12% of the US population were older than 65 years in 1980), dementia is a major cause of morbidity in these countries. The survival of severely demented patients is 33% - 50% that of age-matched controls, thus dementia is also a major cause of mortality.

The clinical symptoms and signs of AD are distressing, initially for the patient; and throughout by those who care for them. AD is also extremely disabling, and care of the dementing patient, particularly whilst still mobile, is very labour intensive, and the patient requires constant supervision. The International Classification of Diseases (ICD) defines the syndrome of dementia in ICD-10; this section is divided into 10 major rubrics, of

which, part F.0.1 defines Alzheimer's disease. In summary, dementia is defined as a decline in memory and intellect, with disturbances in other higher cortical functions, such as apraxia, aphasia and agnosia. Focal neurological signs are absent, though evidence of neurological damage, e.g. epilepsy, may occur. During the past 25 years, in order to provide data relating to the aetiology and pathogenesis of ATD, the main approach has been to investigate the biochemistry and pathology of the disease. Interest has focussed in particular on the neurofibrillary tangle, a distinctive, though not absolutely diagnostic feature of ATD, (tangles are found in small numbers in other organic brain syndromes, see section 1.5). The origin of the tangle is unknown. Although intraneuronal tangle formation correlates with the degree of dementia (Blessed et al, 1968; Tomlinson et al, 1970) it is not known whether it causes the symptoms and signs of dementia; or whether tangle formation is the result of another underlying process which gives rise to the clinical presentation of dementia. Also, the molecular structure of the paired helical filaments (PHF) which make up the tangle, is intermediate filaments normally present in neurons i.e. the micro tubule associated protein tau; though there may also be a contribution from protein/s not normally assembled into a filamentous structure. Knowledge of the constituent molecules, and assembly of the PHF will be the first step towards an understanding of the factors causing tangle formation.

## 1.2 Pathology

The pathological changes found in Alzheimer brains have been well defined qualitatively, and quantitative studies on plaques and tangles have been carried out. No single type of lesion is pathognomonic of the disease, and all changes may not be present, AD showing plaques only has been described by Ball (1985). However AD can be reliably diagnosed by histopathological assessment of the presence and distribution of the following lesions.

### 1.2.1 Senile plaques

By light microscopy, senile plaques may appear in three forms: amyloid cores, neuritic or neuritic with amyloid cores. Terry and Wisniewski (1970, 1972) hypothesised that this represented 3 stages of plaque formation: the first being the primitive plaque consisting of a number of distended neuronal processes "neurites" of mainly axonal origin, with little or no amyloid (Gonatas, Anderson and Evangelista, 1967). Some contain PHF (Wisniewski et al., 1983). Initially this type of plaque is only visible electromicroscopically. The second stage is the mature plaque with an amyloid core, surrounded by distended neurites, astrocytic processes, and occasional microglia. The last stage is the "burnt out" plaque consisting only of a dense amyloid core. This core is composed of 7.5nm amyloid fibrils, in bundles radiating from the centre. Each amyloid fibril consists of two 2.5-3nm filaments

arranged in a double helix of 150nm periodicity. Senile plaques will bind congo red and exhibit green birefringence (Divry, 1927), this property reflects the  $\beta$ -sheet conformation first proposed by Pauling and Corey (1951) (Cooper, 1974).

The origin of plaque amyloid is unknown. In addition, the connection between PHF and amyloid, if any, is unknown, and the presence of both PHF and amyloid in plaques has not been satisfactorily explained. The resemblance of senile amyloid to systemic amyloid is also unclear. However, amino acid sequencing of plaque cores (Masters et al., 1985a) correlates with the sequence of amyloid found in congophilic angiopathy (Glenner et al., 1984). Further work by Masters et al (1985b) has suggested that the proposed amyloid subunit (4 kDa), also constitutes the basic subunit of PHF.

Plaques are found in grey matter in the cerebral cortex, the hippocampus; and some deeper structures, including the amygdaloid nucleus, the corpus striatum and the diencephalon in general. They are rare in the brain stem and the cerebellum.

#### **1.2.2. Congo philic angiopathy**

It was first noted by Scholz (1938) that an amyloid-like substance was laid down in the walls of small cerebral vessels in some elderly people. It has been shown mainly to affect pial and intracortical arterioles, leptomenigeal vessels and occasionally intracortical capillaries. Amyloid is deposited around the media,

outside the elastic lamina of the vessel. Schlote (1965) confirmed that the ultrastructure of this amyloid was similar to that of plaque amyloid. Their chemical compositions have also been found to be similar (see previous section). However congophilic angiopathy may be absent in an ATD brain when plaques are present (Mandybur, 1975; Mountjoy, Tomlinson and Gibson, 1982).

### **1.2.3. Neurofibrillary tangles**

Neurofibrillary tangles, like amyloid, bind congo red and exhibit green birefringence. For this reason they were considered to be formed of intracellular amyloid, until electron microscopic studies (Kidd 1963; Terry, 1963) showed that they were formed of twisted filaments, 20-25nm maximum diameter narrowing to 10nm, with a 80nm repeat. They were first thought to be twisted tubules (Terry, 1963) but these authors subsequently rescinded, and agreed with Kidd's original postulate that they were two helically arranged filaments. More recently optical diffraction studies have suggested that the PHF is one twisted filament, the apparent gap between the "two" filaments representing a stain filled depression on the surface of the filament, and not a space between two filaments (see section 1.11).

Tangles are found in certain brain areas in ATD in a distribution similar to that of plaques. Ball (1985) showed that when tangles were present in brains, the hippocampus was always affected. This suggested that the hippocampus was the site at which tangles were first



formed. Previous work has also shown the hippocampus, parahippocampal gyrus, temporal cortex, amygdaloid nucleus to be severely affected areas (Moreland and Wildi, 1952; Yamada and Mehraein. 1968).

#### **1.2.4 Granulovacuolar bodies**

These bodies are found in hippocampal pyramidal cells, and rarely elsewhere (Woodard, 1962). Ultrastructurally they are seen as fine granular material within membrane bound vesicles (Hirano et al., 1961). They are of unknown origin.

#### **1.2.5 Hirano bodies**

These are paracrystalline bodies made up of 10nm membranes and filaments (Hirano et al., 1968). At EM they appear to lie adjacent to pyramidal cells in the hippocampus and are occasionally seen in the striatum lacunosum. They are probably sheets of membrane bound ribosomal particles, derived from rough endoplasmic reticulum (O'Brien et al., 1980).

#### **1.2.6 Lipofuscin**

Lipofuscin occurs in many aging cells. It occurs in large neurones in the normal aging brain, and is increased there in chronic, systemic and neurological disease.

### **1.3 Morphometric studies in ATD**

#### **Cell loss in ATD**

Brain volume is decreased in brains from patients with ATD compared to age-matched controls: however, in ATD cases over 80 years of age, cerebral volume is often within normal age limits (Hubbard and Anderson 1981a). In



addition, certain ATD brain areas show neuronal loss, compared to age-matched controls (Terry et al., 1981). Neurone loss in ATD has been well documented in the nuclei of three neurotransmitter systems, namely: the cholinergic, noradrenergic and 5-hydroxytryptaminergic systems. It occurs in the nucleus basalis (Pilleri 1966; Whitehouse et al, 1982). It also occurs in the locus coeruleus (Forno, 1978; Mann et al, 1980); and in the raphe nucleus (Mann et al., 1984).

Neuron loss in the temporal cortex and hippocampus has been more controversial, but it is now generally agreed that it does occur. Terry et al., 1981 and Mountjoy et al., 1983 demonstrated a loss of larger neurons in ATD compared with controls, from the mid frontal and superior temporal cortex. Mann et al., 1985 confirmed that pyramidal neurons were lost. Whereas, previously, Terry et al., 1977, had found no difference in counts between elderly demented and control patients. However, this could be explained by the finding of Mann et al (1985) that neurone loss was marked in presenile dementia patients, but the loss in the elderly SDAT patients could be largely attributed to age. They showed that pyramidal cell loss in the hippocampus and temporal cortex in ATD (when adjusted for loss normally due to age) correlated inversely with patient age.

Reports differ as to whether there is a statistical correlation between the numbers of plaques and tangles,

and cell loss. Ball (1977, 1978), has shown exponential inverse correlation between density of neurons in the hippocampus and the number of NFT in cases of ATD. Terry et al. (1981) did not find a correlation between plaques and cell loss in mid frontal, or superior temporal cortex, whereas Mann et al. (1985) reported weak positive correlations between plaques and cell loss; and tangles and cell loss, in both hippocampus and temporal cortex. The latter workers do, however, draw attention to the suggestion that plaques and tangles may be phagocytosed and removed from brain (Brun & Englund, 1981; Probst et al., 1982) and therefore a plateau of plaque and tangle numbers may occur.

In addition to neurone loss in ATD, there is also evidence of decreased protein synthesis. This is manifest by a reduction in the content of temporal lobe RNA, and a reduction in the ratio of RNA to DNA (Bowen et al. 1977). Also Sajhel-Sulkowska et al (1983) have shown functionally active mRNA to be lower in plaque and tangle containing areas of ATD cerebral cortex, than in control cortex. This decrease in protein synthesis in tangle-containing areas, can at least partly be accounted for, as tangle-containing neurons have been shown to have a reduced nucleolar size and RNA content as compared to non tangle-containing neurones (Dayan and Ball, 1973; Uermua and Hartmann 1978; Mann, Lincoln and Yates, 1981). It is not clear whether protein synthesis in ATD brain is affected in brain regions which do not show neuropathological

features of ATD. Another neuronal feature which appears to be altered in SDAT as compared with normal aging is the reduction in dendritic arborisation of neurons (Buell and Coleman, 1979; Scheibel and Scheibel, 1975).

#### **1.4 Changes in the normal aged brain**

The pathological features of ATD, that is, plaques, tangles, granulovacuolar degeneration, lipofuscin and neuronal loss, can be found in normal aged brain, although to a much lesser degree. For this reason and because the number of these features increases with age, ATD has been described as accelerated aging. This is probably not justified. For example, brains from cases of ATD show higher numbers of tangles in the younger cases (Constantinidis, 1978). Whereas this is not true in control brains, in which numbers of plaques and tangles increase with age. Therefore, younger ATD patients have a more severe pathology, and are more unlike age-matched controls, whereas elderly ATD cases become more like age-matched controls. It is possible that older patients are frailer and die more quickly from the disease, or that brains from older patients are less tolerant of pathology such that older patients show the same degree of dementia as younger patients with more severely affected brains, so the disease becomes evident earlier in its course. In normal old age, the brain reduces in volume, due to a reduction in both grey and white matter (Hubbard and Anderson, 1981b). Neuronal loss occurs; this was first

demonstrated in certain cortical brain areas by Brody (1955) in particular the superior temporal gyrus, to a lesser extent in the frontal lobes. Cell loss has also been demonstrated in the hippocampus (Miller and Corsellis, 1972) locus coeruleus, (Brody, 1976), corpus striatum and lentiform nucleus (Bugiani et al, 1978). However these cell losses are significantly greater in age-matched AD brains as discussed in the previous section.

The most striking difference between the effects of normal aging and AD are observed in the neurotransmitters one of which (dopamine) is decreased as an effect of aging, but not of AD; whilst others ChAT, noradrenaline, 5-HT, are decreased in AD, but not in normal aging (section 1.7).

### **1.5 Other dementing diseases, a comparison with AD.**

#### **1.5.1 Multi-infarct dementia**

This disease has similar presentation to AD. Multiple small infarcts or cerebral softenings are present at autopsy; although similar changes, with less destruction of brain tissue, may be present in elderly non-demented subjects (Tomlinson et al, 1968, 1970). Multi-infarct dementia can usually be distinguished clinically from AD by the presence of hypertension, peripheral vascular disease, and other accompanying neurological signs, particularly of the corticobulbar, and corticospinal tracts (Hachinski, Lassen and Marshall, 1974). The histopathological changes found in Alzheimer's disease are

not observed in multi-infarct dementia, except in cases where both conditions are present; and both, presumably, contribute towards dementia.

#### 1.5.2. Infective dementias

Creutzfeldt-Jakob disease and kuru, in man; and scrapie and mink encephalopathy in animals, are infectious subacute spongiform encephalopathies with very long incubation periods. The observation by Hadlow (1959) that the disease kuru histologically resembled scrapie, inspired further work which showed kuru to be transmissible (Gajdusek, Gibbs and Alpers, 1966). Later, Creutzfeld-Jakob disease was also shown to be transmissible to chimpanzees (Gibbs et al., 1968; Beck et al., 1969).

When examined neuropathologically, brains from patients or animals with these diseases, exhibit neuron loss, gliosis and amyloid plaque formation (Fowler and Robertson, 1959; Hadlow, 1959; Chou and Martin, 1971).

Neuron loss is seen in the cerebellum in kuru, scrapie, and mink encephalopathy, and in the cortex in Creutzfeld-Jakob disease (CJ). The amyloid plaques in these diseases resemble the plaques seen in ATD; although ultrastructurally they are not identical; for example the lack of neurites containing PHF, which are seen in ATD (Wisniewski, Bruce and Fraser, 1975; Masters et al., 1981). Whilst NFT are not observed in these diseases, twisted fibrils (scrapie - associated fibrils, SAF) have

been found in subcellular preparations of scrapie infected brains (Mertz et al, 1981) and from CJ affected brains (Mertz et al, 1983). SAF have not, however, been observed in histological sections from these brains. Although, both CJ and kuru have been experimentally transmitted by injection of infected brain tissue into the brains of chimpanzee. ATD has not been transmitted in this manner, and at present there is insufficient evidence to suggest an infective aetiology (Brown et al., 1982).

#### 1.5.3 Tangle-forming dementias - a comparison with ATD

This group consists of four dementia-parkinsonism complexes; post-encephalitic parkinsonism, amyotrophic lateral sclerosis, dementia-parkinsonism complex of Guam, and dementia pugilistica. The former has been seen following encephalitis epidemics. In these four conditions, tangles are found in subcortical nuclei, the substantia nigra, locus coeruleus, and reticular formation; plaques are not generally seen. Therefore, the distribution of tangles throughout the brain in these conditions is different to that seen in ATD. The symptoms of these disease complexes also differ from ATD, most notably in that Parkinsonism is usually present in the former group. The condition of dementia pugilistica or boxer's dementia was first described in Martland (1928). A 1969 study of 224 ex-boxers (Roberts, 1969) showed that 17% had a syndrome consisting of a neurological deficit, either cerebellar, pyramidal or extrapyramidal; and a psychological deficit consisting of decreased cognitive



function, particularly memory. The pathology of one case was described. A subsequent study by Corsellis (1973) confirmed their findings. In the latter study, it was interesting to note that all boxers demonstrating cerebral NFT formation, also had a history of alcohol abuse.

#### **1.6 Tangles and PHF in non-human species, and tangles produced experimentally**

PHF as defined by their EM appearance and dimensions have only been found in the brains of humans. There are models which produce tangles of filaments, or twisted filaments but not PHF. Aged animals do not show tangle or PHF formation, although twisted fibrils have been found in presynaptic boutons of aged rhesus monkey brains (Wisniewski et al., 1973). However, the pitch of these filaments is dissimilar to that of PHF.

De Boni and Crapper McLachlan (1985) have induced the formation of paired twisted filaments by adding glutamate and aspartate to culture media containing human fetal spinal cord neurones. In the presence of these substances they noted vaccolated neuronal somata and degenerating neuronal processes. These processes contained intermediate filaments which appeared to be arranged in helical pairs. However, interfilament distances and helical periods were different from those of paired helical filaments. The induced filaments consisted much more obviously of two filaments and the authors postulated that these were neurofilaments.



Animal models of neurofibrillary tangles in which the filaments are not ultrastructurally twisted has been produced using mitotic spindle inhibitors, (Schochet, Lampert and Earle, 1968) and substances which affect axonal transport e.g. Colchicine, which affects microtubules (Wisniewski and Terry, 1964).  $\beta,\beta$  iminodipropionitrile (IDPN) and aluminium have also been used. IDPN causes a focal enlargement of the intraparenchymal and proximal 5-10nm segments (Chou and Hartmenn, 1964; 1865) and probably disrupts the neurofilament/microtubule meshwork resulting in impairment of neurofilament (NF) transport, and NF accumulation in the proximal axon (Griffin et al., 1978, 1983). However, NF do not accumulate in the cell body. Aluminium phosphate was first used to produce intraneuronal tangles (by Terry and Pena, 1965; and Klatzo et al., 1965). Aluminium administered into the fourth ventricle in rabbits causes NF accumulation in both the cell body and proximal axon of anterior horn cells (Hirano, 1982). The mechanism for this was also postulated to be impairment of axonal transport (Bugani and Ghetti 1982; Troncosco et al. 1982). This was proved experimentally by Bizzi et al (1983) using (35S) methionine to label NF proteins. There is strong evidence that these experimentally produced tangles consist of neurofilaments, because of their polypeptide composition and immunostaining properties (Selkoe et al 1979; Dahl et al, 1982). However, the relevance of these models in which the induced filaments are not ultrastructurally twisted, to ATD is unclear.

### **1.7 Neurotransmitters in ATD**

Deficits have been found in a number of neurotransmitter systems in ATD (reviewed in Hardy et al., 1985). Some of these deficits are very striking, and indicate severe involvement of particular transmitter systems. The causal lesion resulting in a transmitter deficit has not been fully elucidated. The transmitter deficits appear to be related to loss of terminals in the area of deficit and loss of perikarya in the field of origin. Tangles are present in both cell body and cortical projection areas of affected neurotransmitter systems. However, this is not invariably true as they are not found in the caudate nucleus, which shows decreased ChAT and 5-HT. The primary lesion is more likely to be in the area of the field of innervation that is the cerebral cortex, than in the perikaryal field. The cell loss observed in the basal forebrain nucleus (BFN) in ATD, can be produced in animals by lesioning the cortex (Sofroniew et al., 1983). It has been shown by Ishii (1966) and Mann et al., (1984) that in the cholinergic and adrenergic systems, there is a higher tangle to plaque ratio in the BFN and locus coeruleus, than in the cortex. Hardy et al. (1985) hypothesise that plaques are the primary lesion, and tangles are found in neurons projecting to plaque containing areas. Though, this would imply that more than one mechanism for tangle formation exists, as tangles cannot be formed in this way in dementia pugilistica, where there are numerous tangles and extremely few plaques.

### **1.7.1 The cholinergic system**

Post mortem studies have shown a loss of choline acetyltransferase (ChAT) activity which is most marked in the temporal cortex and hippocampus, (Davies and Maloney, 1976; Bowen et al., 1976). Cortical biopsies also have reduced ChAT activity (Wilcock et al., 1982); and Smith et al (1983) have shown that acetylcholine synthesis is reduced in cortical biopsies from patients with AD. The cortical ChAT deficit has been shown to correlate with the degree of dementia (Perry et al., 1978) and with the numbers of plaques and tangles (Wilcock et al., 1982; Mountjoy et al., 1984). In addition, it has been shown that some tangles in the BFN occur in cholinergic cells (McGeer et al., 1984).

### **1.7.2 The noradrenergic system**

The depletion of noradrenaline in AD brain has been well established. The hypothalamus is particularly affected (Gottfries et al., 1976, 1983; Yates et al., 1981, 1983) with the caudate, putamen, cingulate, hippocampus and cerebral cortex showing less marked losses of noradrenaline (Berger et al., 1976; Carlsson et al., 1980). The activity of the synthetic enzyme for noradrenaline, dopamine  $\beta$ -hydroxylase, is reduced in the cortex and hippocampus (Cross et al., 1981; Perry et al., (1981). Noradrenaline uptake is also reduced in cortical biopsies from patients with AD (Benton et al., 1982). Although Adolfsson et al (1979) reported that the severity

of dementia was inversely correlated with levels of noradrenaline in the hypothalamus, Perry et al (1981) found that neither the degree of dementia nor plaque or tangle numbers were related to the activity of dopamine  $\beta$ -hydroxylase in the temporal lobe. Tangles have been found in noradrenergic cell bodies of the locus coeruleus (Mann et al, 1980).

#### **1.7.3 The dopaminergic and serotonergic systems**

These systems are less obviously affected than the cholinergic and noradrenergic systems.

There are few or no tangles in the substantia nigra in ATD (Ishii, 1966). Dopamine has variously been found to be decreased (Gottfries et al., 1976, 1983), and normal (Yates et al., 1979, 1983) in the caudate and hypothalamus. Conversely, there does seem to be a definite decrease in serotonin (Carlsson et al., 1980; Gottfries et al., 1983). Tangles are present in the raphe nuclei (Ishii, 1966).

#### **1.7.4. Peptide transmitters**

Of the peptide neurotransmitters measured in ATD brain, only somatostatin has been shown consistently, by several laboratories, to be reduced. This reduction occurs in the hippocampus and temporal cortex (Davies et al., 1980; Ferrier et al., 1983). Some somatostatin containing neurons have also been shown to contain tangles (Roberts et al., 1985).

### 1.8 Immunochemical studies on neurofibrillary tangles

Antibodies raised to both NFT and normal cell components have been used extensively in immunohistochemical and Western Blotting studies. In particular, antibody cross-reactions between intermediate filaments and NFT have been investigated. Some polyclonal antisera raised to neurofilaments or their constituent polypeptides also stain NFT (Ishii et al., 1979; Gambetti et al, 1980; Dahl et al, 1982). Anderton et al. (1982) showed immunohistochemical labelling of tangles by monoclonal antibodies to anti-200 Kd and anti 150 Kd (neurofilament subunits). Rasool et al (1984) isolated NFT which showed cross-reaction with anti-NF antibodies only after treatment with SDS, thus the antigenic site had been exposed by this process. Other polyclonal antisera raised to neurofilaments have not labelled NFT (Gambetti et al, 1980; Grundke-Iqbal et al, 1984; Yen et al, 1981). However, absorption experiments show that the antibody has been raised to a polypeptide, possibly MAP-2, which co-purifies with microtubules (Kosik, 1984). Ihara et al (1983) showed that antibodies to vimentin cross-react with NFT.

Grundke-Iqbal et al (1984) applied Western blotting to SDS polyacrylamide gels of PHF preparations from ATD brain, and control fractions prepared from normal brain, using antisera to NFT preparations. A complicated pattern of labelling occurred in which there was diffuse binding to the PHF preparation, with labelling of a variable



number of bands in the 45,000-70,000 kDa range with strong labelling of a 50,000 kDa band. There was no staining below 20kDa. Material from the top of the stacking gel also bound the antibody and a 20,000 MW polypeptide did so occasionally. The identically prepared control fraction did not bind the antibodies, although it must be noted that 10 times more PHF protein than control fraction protein was applied to the gel. Absorption of the anti-PHF antisera occurred with any of the PHF polypeptides separated by electrophoresis: the PHF preparation; the control preparation at 40 times the concentration of the PHF preparation; and ATD brain homogenate. Microtubule and neurofilament preparations only absorbed the antibody very slightly. Absorption did not occur with normal brain homogenate, and only to an extremely small extent with glial filament preparation. Wang et al (1984) raised monoclonal antibodies to NFT. Binding of these antibodies to tangle preparations was not eliminated by treatment of the tangles with 2% SDS. Cross-reactivity of these antibodies with various other organelles occurred e.g. cytoplasm, nuclei, although binding to either neurofilaments or microtubules did not occur. Yen et al (1985) also produced monoclonal antibodies to NFT. Their study, interestingly, showed that some of these antibodies stained some but not all tangles. Six of the antibodies stained 100% of methanol-fixed tangles, three stained 70-80%, and one stained less than 30%. Formalin fixation altered this

pattern; so that three of the antibodies did not stain at all, three stained weakly and four stained strongly. Using Western blotting, nine of the antibodies reacted with material at the top of the stacking gel in gels of NFT preparations. Polypeptides of 58,000, 66,000 and 70,000 MW bound two of the antibodies in electrophoresed preparations from both ATD and normal brains, and two other antibodies only bound to bands from ATD brain. One antibody showed no labelling at all.

Recently, numerous immunocytochemical studies have implicated the microtubule associated protein, tau, as a surface component of PHF (Brion et al, 1985; Grundke-Iqbal et al, 1986; Ihara et al, 1986; Kosik et al, 1986). Immunoelectronmicroscopy has shown that neurofilament and microtubule epitopes are located on the PHF (Perry et al., 1985; Miller et al., 1986). The latter group has shown that antibodies raised to neurofilament side-arms will bind to PHF. They also found that immunodecoration at the ultrastructural level is still observed after strong detergent treatment (also Perry et al., 1985), although anti-tau antibodies do not label plaque core or vascular amyloid (Kosik et al, 1986); Selkoe et al., 1986).

### 1.9 Genetic aspects of ATD

There appears to be a significant genetic component as a risk factor in ATD. An increased incidence of ATD has



been reported in the relatives of ATD cases (Sjogren et al, 1952; Larsson et al., 1963; Heston et al, 1981). This finding becomes less significant with increasing age of the ATD patient. Autosomal dominant inheritance does occur although this is very rare (Wheelan, 1959; Feldman et al, 1963); if one of a pair of identical twins is affected, the other does not always develop the disease (Kallman and Sander, 1949; Jarvik et al, 1980). Efforts to link A4 or  $\beta$ -protein amyloid gene responsible for the production of vascular and plaque amyloid to the genetic defect in familial Alzheimer's disease have shown a failure to segregate (Tanzi et al., 1987; Van Broeckhoven et al, 1987). However, vertical transmission of an infectious 'slow virus' type agent cannot be excluded (Masters et al, 1981). The strongest evidence for a genetic contribution can be seen in Down's syndrome. Cases of Down's syndrome develop hippocampal and cortical plaques and tangles by the age of forty (Malamud 1872; Burger and Vogel, 1973). It is not clear whether the onset of dementia in Down's syndrome is invariable (Ropper and Williams, 1980; Thase et al 1982).

An additional link between Down's syndrome and Alzheimer's disease was noted by Heyman (1983), who found that the incidence of Down's syndrome was three times that expected in the general population, in a survey of the families of 1,200 patients with Alzheimer's disease.

### 1.10 Subunit structure of PHF

Many structural models for PHF have been postulated. The original model of the "twisted tubule" (Terry 1963) was replaced by the "paired helical" filament (Kidd 1964) later confirmed by Wisniewski, Narang and Terry (1976). Negative staining techniques have improved resolution at EM, and this has been further improved by the recent development of supra-ultrathin sectioning techniques (Wisniewski and Wen, 1985). The visualisation of 4 protofilaments within the PHF has been widely reported (Wisniewski et al., 1984). In transverse section, the supra ultra-thin sectioning technique of Wisniewski and Wen revealed eight protofilaments i.e. two sets of four protofilaments each set forming one of a pair of filaments. The eight protofilaments are globular in appearance with connecting longitudinal bars, and the protofilaments are also connected by transverse bars. The 'globules' measure  $3.2 \pm 0.4\text{nm}$ , and the longitudinal bars measure  $4.7 \pm 0.6\text{nm}$ . This is larger than the measurements of similar ultrastructural features in neurofilaments by the same group.

A slightly different approach has been taken by Wischik et al (1985). Using high contrast electron micrographs, they produced optical diffraction patterns showing a number of interesting features. The main ones were that the PHF consisted of subunits of very limited axial extent arranged along two left-handed helical strands. Using an autocorrelation function, an axially displaced pair of

peaks corresponding to lines in the image, of approximately 3nm apart were noted. Therefore they proposed an axial subunit of 3nm. Computation of the structure normal to that axis showed that the PHF was composed of 2 c-shaped subunits, in transverse section, each one showed a cleft which divides the subunit into two domains. Therefore the apparent "tramlines" are produced by clefts between structural domains rather than complete divisions between filaments. In addition they successfully modelled the varying 3-4 tramline appearance, and the strapwork appearance, showing that the latter subunit structure is unlike that of neurofilaments and the authors conclude that although neurofilament protein may be involved, PHF do not derive from a helical aggregation or cross-linkage of neurofilaments.

### 1.11 Solubility

The work of Selkoe et al (1982) was the first work to suggest that PHF were remarkably resistant to solubilising agents. In particular, resistance to SDS, 0.2M NaOH, and urea was noted. It was therefore postulated that the bonding in the PHF was by non-disulphide cross links. Subsequently, Kosik et al (1984) have tested numerous solvents of varying nature including 0.2M HCl and 20% Trifluoro-acetic acid (TFA), and found that numbers of tangles are not significantly reduced by these treatments. However, when 5M LiBr was used, a depletion of tangles occurred but PHF were still seen at EM. 7M LiBr

abolished cross polarisation birefringence, suggesting breakdown of conformation; and PHF were not seen at EM, however amorphous fibrous structures remained. Also these workers found that enzymatic treatment including trypsin, papain, elastase, pronase and proteinase K had no significant effect on tangles. In contrast to this, Yen and Kress (1983) achieved a 20-40% tangle depletion with 3-stage pronase treatments. Subsequent incubation of the same sample reduced tangle numbers by a further 20-40%. If this step was replaced by 70% formic acid, an 85-90% reduction was achieved. The paired helical filament ultrastructure of tangles appeared to be lost with pronase/pepsin treatment. Formic acid also destroyed PHF ultrastructure but tangle 'ghosts' were still seen on light microscopy. Yen and Kress too, concluded that any bonds present were non-disulphide. Masters et al, (1985) showed that more than 90% of PHF were soluble in formic acid, as determined by quantitative amino acid analysis. Iqbal et al (1984) also showed a significant reduction in tangle numbers with repeated SDS treatment and sonication. The proportion of tangles lost varied enormously between individual brains. This group postulated a sparing solubility, rather than an insolubility of PHF in SDS. In a more recent study, Iqbal et al (1985) compared a PHF preparation method previously developed in their laboratory, with a PHF preparation method devised by Ihara et al (1983). The former method

does not extensively use denaturing agents, whilst the latter does. Iqbal et al found that PHF prepared by a non-denaturing method appear to be more readily soluble than those prepared under prolonged denaturing conditions. They concluded that their findings did not support the presence of a  $\gamma$ -glutamyl- $\epsilon$ -lysine cross link as the bond responsible for the stable structure of PHF. They argued that this bond would not be susceptible to the measures they used to solubilise PHF. They also postulated that the insolubility of PHF may be artefactually induced due to either micelle formation or sheet formation induced by heating.

#### **1.12 Protein composition of PHF; and a comparison with senile amyloid**

The protein of plaque amyloid and congophilic angiopathy has been characterised and analysed. The latter has been characterised by Glenner and Wong (1984); the former by Masters et al (1985), who found that plaque core and congophilic angiopathy protein are almost identical in terms of molecular mass, amino acid composition and  $\text{NH}_2$  terminal sequence, though the plaque core proteins have ragged  $\text{NH}_2$  termini. The constituent protein consists of an aggregated polypeptide with a subunit mass of 4kDa. Masters et al. (1985b) subsequently applied similar analytical techniques to PHF and found the same 4kDa peptide to be a subunit. They demonstrated that antibodies raised against synthetic peptides have (in



different regions of the molecule) epitopes for neurofibrillary tangles and plaque core or vascular amyloid. Masters et al also found the PHF NH<sub>2</sub> termini to be more ragged than those of plaque core amyloid. They hypothesised that the degree of terminal heterogeneity reflected the age of the protein. Developing this theory, they postulated that A4 protein is manufactured in the neuron and deposited there first, from whence it leaks out to form a plaque core, finally being transported to blood vessels where it forms congophilic angiopathy. Kidd (1985) has also suggested a common subunit for plaque amyloid and PHF. However, the findings of Masters et al could be criticised on the grounds that amyloid plaque cores were one of the major contaminants of their NFT preparation.

To date the most consistent findings relating to the nature of the protein composition of PHF, come from immunocytochemical studies implicating the microtubule associated protein tau (see section 1.8).

### **1:13 Intermediate filaments, microtubules and microfilaments.**

There are three major types of fibrillar proteins in neurons (Wuerker and Kirkpatrick, 1972). These are: microtubules which have hollow cylinders with a diameter of 24 nm and a 6nm thick wall; microfilaments which consist of a 6nm diameter actin filament; and neurofilaments which are 10nm diameter filaments. Neurofilaments have been carefully considered as



candidates for the origin of PHF. They share antigenic determinants with PHF (section 1.8) and their diameter is similar to the smallest diameter of PHF.

Together, these filaments form the cytoskeleton which facilitates, and is closely associated with, axonal transport. The microtubule associated proteins (MAPS) are part of this skeleton; and the protein tau belongs to this group. The observation that phosphorylation of tau impedes microtubule assembly (Lindwall et al, 1984) and therefore affects axonal transport, is possibly a significant factor in tangle formation. Neurofilaments are synthesised in the cell bodies of neurons and then travel distally up the axon in the slow component of axonal transport (Sca), (Black and Lasek, 1980; Norton and Goldman, 1980). In the disease category; giant axonal neuropathies and amyotrophic lateral sclerosis, neurofilaments accumulate in cell bodies and axons (Norton and Goldman 1980), indicating an impairment of axonal transport.

Mammalian neurofilaments are composed of three main polypeptides, with molecular weights of approximately 200,000, 160,000 and 70,000 (Hoffman and Lasek, 1975; Schlaepfer and Freeman, 1978). The probable arrangement of neurofilament triplet is that the 70,000 M.W. polypeptide is central, and the 160,000 and 200,000 polypeptides more peripherally situated; their 'core' regions fixed to the central filament and the COOH terminal regions of the 200,000 probably form the

side-arms seen at electron microscopy (Willard and Simon, 1981; Sharp et al, 1982; Geisler and Weber, 1981). These COOH terminal regions from the 200,000 and 160,000 polypeptides can be cleaved from neurofilaments, using trypsin leaving a still intact 10nm filament (Chin et al, 1983).

It has been shown that there are close homologies of primary sequence for a peptide from the smallest triplet polypeptide of porcine NF and related sequences from  $\alpha$  helical regions of other IF polypeptides, and of wool keratins.

The variability between intermediate filaments is accounted for by differences in the COOH terminal regions and this may confer the different biological properties of the different intermediate filaments (Fuchs and Hanko 1983). For example the difference between the NF 70,000 kDa polypeptide and 52,000 kDa desmin, is almost all accounted for by a longer C-terminal peptide (Geisler et al, 1981; 1982). The close homology of these sequences probably accounts for some cross-reactivity between antibodies raised to certain intermediate filaments and PHF; and, therefore, all such experiments must be interpreted carefully. However, these experiments do strongly suggest that intermediate filament sequences are present in, or attached to, PHF. So tangle formation is likely to be related to an abnormality of the cytoskeleton.

## CHAPTER 2

### MATERIALS AND METHODS

## MATERIALS AND METHODS

### 2.1 MATERIALS

#### 2.1.1. Human brain tissue

Human brain tissue collected over a period of seven years by the MRC Brain Metabolism Unit was used for experiments described in this thesis. The brains were obtained at post-mortem from cases of clinically suspected ATD, Down's syndrome (all with trisomy 21 anomaly), and controls who had no clinical signs of central nervous system abnormality. The cadavers were refrigerated prior to post-mortem within four hours of death, and autopsies carried out within 45 hours and in most cases within 25 hours of death. The brains were sectioned in the mid-sagittal plane. The right hemisphere of all ATD and Down's cases, and most control cases was fixed in 10% formalin in tap water for at least two weeks before histological examination by Dr. A. Gordon, (Consultant neuropathologist, Edinburgh University and Western General Hospital). The left hemisphere was either frozen at  $-70^{\circ}\text{C}$  or dissected and the dissected samples frozen at  $-70^{\circ}\text{C}$ . A case was diagnosed as ATD by the presence, on neuropathological examination, of increased numbers of senile plaques and neurofibrillary tangles in the frontal and temporal cortex and hippocampus and a clinical history of dementia. Cases in which an ATD pathology was accompanied by other pathological changes, such as cerebral infarcts, were excluded. Control brains which were examined

histologically appeared normal. For reasons of laboratory safety, brains were not accepted from patients with clinical or pathological evidence of jaundice, massive blood transfusion, or disseminated bacterial infection.

#### **2.1.2 Bovine extradural nerve roots**

Bovine spinal cords including nerve roots were obtained fresh from a slaughterhouse and processed within a few hours. Neurofilament preparations (Carden et al, 1983), used in this thesis as molecular weight markers, were performed by Mrs R Rao and stored at 4°C prior to use.

#### **2.1.3. Histological stains**

These were obtained from Gurr (BDH Chemicals Ltd).

#### **2.1.4. Percoll and calibration beads**

The colloidal silica gradient medium used was Percoll (Pharmacia (Great Britain) Ltd., Hounslow, Middlesex). The density gradient calibration kit (same supplier) was used in conjunction with this.

#### **2.1.5. Electrophoresis calibration kits**

The 'high molecular weight' and 'low molecular weight' protein mixtures, from Pharmacia were used to calibrate polyacrylamide gels for molecular weight estimations.

#### **2.1.6. Electron microscopy materials**

Grids and fixatives used for electron microscopy were obtained from TAAB Laboratory Equipment Ltd., Reading, Berks.

#### **2.1.7. Chemicals**

Unless specifically stated otherwise, all chemicals used

were from Sigma (Poole, Dorset) or British Drug Houses (Poole, Dorset), and were 'Analar' grade (where applicable).

## 2.2 METHODS

### 2.2.1. Dissection of human brain

Several brain dissection methods were used, depending on the amount of tissue required, brain area and factors relating to the brain bank, such as organisation of storage space.

#### (a) Dissection of fresh left hemisphere

Tissue samples taken from the fresh hemisphere had been stock-piled in the BMU Brain Bank before the start of this thesis. After sagittal sectioning, the left hemisphere was kept on ice and the meninges removed. Frontal cortical grey, mid-temporal cortical grey, and the grey matter of the para-hippocampal gyrus were scraped from the brain surface. All samples were stored at  $-70^{\circ}\text{C}$ .

#### (b) Dissection of coronal slices from frozen left hemisphere

The left hemisphere was stored at  $-70^{\circ}\text{C}$ . It was then sliced in the coronal plane in an antero-posterior direction, using a Bosch electronic meat slicer to give 2- 5 mm thick slices which were taken and immediately transferred to a Cambion cold plate at  $-10^{\circ}\text{C}$ . Between slicings, the brain was returned to the  $-20^{\circ}\text{C}$  freezer. Slices were numbered by notches. The hippocampus was easily identified, and dissected from the appropriate slices. Grey matter from the temporal, parietal and frontal cortex was also dissected from the appropriate slices.



### **Dissection of frozen left hemisphere**

Large quantities of frontal and temporal grey matter were scraped, using a scalpel, from the surface of hemispheres equilibrated overnight at  $-20^{\circ}\text{C}$ .

#### **2.2.2. Protein determination**

Protein concentrations were determined using bovine serum albumin (Sigma fraction V) as the standards. Four methods were used:

(a) The method of Peterson (1977) based on the method of Lowry et al (1951) was used for estimation of protein in tissue homogenates. The assay is inaccurate in the presence of sucrose, urea, SDS or phenol.

(b) The method of Bradford (1976) was used in experiments when sucrose, urea or SDS were present in samples, and the method of Peterson could not be used.

(c) A technique involving protein spotting and Coomassie R-250 Brilliant Blue binding, was used to estimate protein in column eluates which contained phenol/acetic acid/water (1:1:1 vol); (adaptation of method of Bramhall et al, 1969; Carden M.J-PhD thesis, 1983). 1-10 $\mu\text{g}$  of protein in 10ml was spotted on to filter paper (Whatman's grade S4). This was air dried then stained with gel stain (see appendix) for 30 min. It was destained (see appendix) for 30 mins, and air dried. Squares of identical size which included the protein spots were cut out, and the coomassie blue was eluted for 30 minutes in 4ml methanol. The absorbance was read at 595nm.

(d) Protein concentration in some gel filtration eluates, in

which phenol or urea were not present, was assayed spectrophotometrically, by absorption at 280nm.

### 2.2.3 Dialysis

Samples were dialysed prior to protein estimation and electronmicroscopy in 0.5cm diameter dialysis tubing. Where it was important to conserve exact sample volumes, perspex dialysis cassettes, with a taut circular dialysis membrane (King's College Biophysics Workshop) were used.

### 2.2.4 Polyacrylamide gel electrophoresis (SDS PAGE)

Using the discontinuous system of Laemmli (1970) proteins were separated electrophoretically on the basis of molecular weight. SDS is an ionic detergent and will dissociate most proteins into their polypeptide subunits. When the negatively charged SDS is bound to the protein in the presence of excess SDS, the charge of the protein is insignificant in comparison to the charge of the bound SDS. Therefore, proteins separate on the SDS gel according to molecular weight rather than charge.

### 2.2.5 Electrophoretic procedure

All samples were dialysed prior to gel electrophoresis and protein measurement. Protein measurement was carried out by the method of Peterson (1977). Sample preparation was carried out as described in this section. The resolution of polypeptides according to molecular weight was performed using linear gradient 3-12% and 5-15% SDS polyacrylamide gels. Marker proteins consisting of bovine neurofilament,

and commercial marker protein preparations (Pharmacia Ltd) were electrophoresed; and molecular weights were determined according to the method of Weber and Osbourn (1979). Gels were stained with Coomassie Brilliant Blue R250 and/or with silver. Slab gels (150 x 120 x 1.5mm) were cast in batches of 8 using an LKB gradient mixer. 3-12% linear gradient gels with a 2.5% stacking gel, or 5-15% gels with a 4.2% stacking gel were used. The lower percentage acrylamide gels were used as these can resolve proteins of molecular weights of between 20,000-400,000kDa, and polypeptides of molecular weight 800,000 will migrate into the stacking gel. The 5-15% gels resolve proteins over a slightly lower molecular weight range, of between 15,000-300,000kDa.

Gels were run at 300v for 5 min; then at 200v through the stacking gel, until the dye front was at the top of the slab gel; then at 60v constant voltage for about 14 hours in a vertical running tank (Kings College Biophysics workshop), using an LKB power pack. Running buffer was similar in composition to that of Laemmli (1970) (appendix).

#### **Gel staining**

(a) Coomassie blue. Simultaneous fixing and staining of the protein was achieved by gently shaking >6 hours in gel stain (appendix).

The gel was then destained (appendix), changing the destaining solution when necessary.

(b) Silver. Silver staining was performed using the method of Morrissey (1981).

### **Sample preparation**

Samples were prepared for electrophoresis by adding at least 20% of the total volume as dissolving buffer. The dissolving buffer used was similar in composition to that of Laemmli (1970) (appendix). After dissolving buffer had been added, samples were heated for 5 minutes in a boiling water bath. Samples were then centrifuged for 30 seconds at  $8,000 \times g$  in an Eppendorf centrifuge, before loading on to the gel.

### **Sample application**

Samples were applied to the wells in the stacking gel using a Gilson pipette. The Gilson C-100 plastic nozzle was adapted for gel loading by attaching a 2cm piece of 1mm bore teflon tubing. This ensured that samples could be directly loaded into the well bases, preventing overflow into adjacent wells.

### **2.2.6 Gel filtration**

Gel filtration as a technique for macromolecular separation was first used by Porath and Flodin (1959). In experiments described here, gel filtration has been used to separate proteins on the basis of molecular size. The value of this technique was that it could be easily and successfully used with various solvents which were unsuitable for use in electrophoretic systems. Gels are formed by cross-linking dextran with epichlorohydrin, lower range gels are more highly cross linked, and are therefore, very stable. The separation is based on the principle that the gel contains pores of a particular size, depending on its type. Gel

types are chosen so that the large molecules which cannot enter the pores pass straight through the gel in the elution volume. Smaller molecules spend a proportion of the time inside the pores. This depends on size, the small molecules have easiest access and so spend most time in the pores. Therefore, molecules elute in order of decreasing size. Three gel types, covering a wide molecular weight fractionation range were used; G-75 superfine (3000-80,000)kDa M.W.) G-50 fine (1,500-30,000kDa M.W.) and G-25 superfine (1,000-5,000 kDa M.W.), (Sephadex, Pharmacia). **The preparation of Sephadex gel columns; and the fractionation procedure**

The gel was left to swell in excess eluting solvent; 6 hours for G-25 and G-50, 24 hours for G-75. It was then degassed under vacuum, left to settle for 30 minutes then excess solvent poured off. The gel was packed in one operation through 2-3 column volumes of solvent under 400 mm solvent pressure. The sample was then applied to the top of the column and eluted at 300 mm solvent pressure. Samples volume was kept small enough (1-5% bed volume) to be insignificant in comparison with the elution volume. The void volume was ascertained in each column by dissolving 50-100mg of Dextran blue in 0.25-0.5ml of the appropriate solvent, applying this to the column, and eluting at 300mm solvent pressure. Dextran blue, being a large molecule, was eluted at the void volume. Then, calibration proteins in the appropriate size range were dissolved in solvent and applied to the column. In experiments using formic acid as



the solvent, the eluate was collected in 50 drop (0.5ml) fractions, using a Pharmacia fraction collection with a drop sensor device. In experiments in which phenol/acetic acid was used as the solvent, the plastic drop sensor device could not be employed. Therefore fractions of about 0.5ml were collected for timed intervals of 30 minutes. The volumes of these fractions were measured using 0.5ml and 1 ml glass pipettes. For fraction collection, siliconised rubber tubing and glass test tubes were used.

In each experiment the same column was used for both ATD and control samples. Identifical amounts of protein from ATD and control samples were (separately) loaded. The columns were washed between samples by running through 3-4 times the elution volume of solvent.

#### **Preparation of tangle-enriched samples**

Tangle enriched samples were prepared by discontinuous density sucrose gradient centrifugation in the presence of SDS (section 5.3.1). Samples were dialysed against distilled water overnight, and protein concentrations were measured using the Peterson protein assay. Solvent constituents were then added to the sample, so that the sample was in a solvent identical to the eluting solvent. For example when using a phenol/acetic acid/water solvent (1:1:1) (W/V/V), 100 $\mu$ l of acetic acid and 100mg of phenol were added to 100 $\mu$ l of sample (in distilled water), to achieve the correct final solvent composition. The resulting solution containing the sample was incubated at room temperature for one hour before loading on to the



column. In one experiment, the tangle preparation was first heated to 90°C in a small volume of trichloroacetic acid for 5 minutes before incubation at room temperature in eluting solvent; however this pre-filtration treatment was found to hydrolyse all protein in the samples, and so was subsequently abandoned.

#### **Protein detection**

Detection of protein in fractions containing formic/acetic acid was carried out spectrophotometrically at 280 nm (uv cord, Pharmacia Ltd). Detection of protein in fractions containing phenol/acetic acid was performed during the protein spotting Coomassie blue binding technique.

#### **2.2.7 Light and fluorescence microscopy**

A Zeiss Universal microscope fitted with a 12 volt lamp and crossed polarisation filters, was used for routine checking of brain sections, smears and preparations. This microscope was also used for plaque and tangle counting experiments. A Zeiss inverted microscope with a 100 watt mercury source was used for fluorescence microscopy. Zeiss filter combination No. 9 (BP450-490; LP515) was used, with congo red as the fluorochrome. The Zeiss inverted microscope was used for light, crossed polarisation, and fluorescence photography; colour slides were taken on 160 ASA Tungsten film (Kodak Laboratories), using a Contax 139 camera. Congo red fluorescence was investigated using a Model SF1/B photomultiplier (EMI) (on stained tangles); and an Aminco Bowman spectrophotometer (on congo red solutions).



### **Tangle and plaque counting**

When counting tangles and plaques in tissue suspensions, a glass Sedgewick rafter cell (Graticules Ltd.) was used.

### **2.2.8 Electron microscopy**

Hitachi 600 and Phillips 200 electronmicroscopes were used. PHF were visualised using negative staining, for which Pioloform, Formvar, and carbon coated grids were used.

### **Carbon coating**

This was carried out using an Edwards Speedivac coating unit. The method used was similar to that described by Bradley (1961): mica sheets were coated with a thin layer of carbon, this was floated off on to meniscus of distilled water, positioned over a number of 200-mesh grids placed on a metal grill which was then brought into contact with the carbon coat, and air dried. The grids were then kept under vacuum until ready for use.

### **Negative staining**

The method used was a modification of the method first devised by Huxley (1963) and adapted to suit the negative staining of PHF by Iqbal et al (1984).

PHF preparations in distilled water were diluted to a concentration of approximately 0.1mg protein per ml. A 10 $\mu$ l drop was applied to the supporting film and left for one minute. Excess fluid was then gently drawn off to one side using filter paper. A drop of stain (2% w/v phosphotungstic acid pH 7, or 1% W/V uranyl acetate) was then applied to the grid and drawn off after 20 seconds.

### **Platinum shadowing**

A PHF preparation was eluted to approximately 0.5 mg per ml protein concentration, with distilled water. This suspension was sprayed on to sheets of newly cleaved mica. The mica pieces were then shadowed unidirectionally with platinum at an angle of 1 in 4 (adapted from the method of Elliot and Offer, 1978), in an Edwards Speedivac Coating Unit. On top of the platinum, a thin layer of carbon was deposited. The complete film was then floated off on to a meniscus of distilled water, and mounted on 200-mesh grids. Grids were viewed after 24 hours.

### **EM photography**

Using the Phillips EM 200 electronmicrographs were taken at magnifications of X55,000 and X71,000, and, using the Hitachi 600 electron micrographs were taken at X50,000; on Ilford EM film. Negatives were developed in Kodak D19 developer for 3 min. 45 sec. at 20°C, stopped in 2.5% (v/v) acetic acid, fixed in Ilford Hypam rapid hard fix for 4 min, and washed in tap water for 30 min.

### **2.2.9 Subcellular fractionation**

Experimental subcellular fractionation techniques are described in Chapter 5.

All low speed centrifugations (<1,500 x g) were performed in a Centra 7R centrifuge (Daman/IEC Division). Middle speed centrifugations were carried out in either an Eppendorf centrifuge with a fixed r.p.m. equivalent to 8,000 x g; or a Burkard Koolspin bench top centrifuge (Burkard Scientific Ltd). High speed centrifugations, used for the formation of

percoll gradients (see section 5.1.3), were performed in an MSE 18 High Speed centrifuge, in an 8 x 70ml fixed angle rotor (with 15 ml adaptors). Ultracentrifugation was performed in a Beckman L2-65B ultracentrifuge using a selection of swing bucket rotors.

### **Gradients**

Unless otherwise stated, discontinuous sucrose gradients were made up 6 hours before use, and refrigerated for this period, in order to allow some merging of the interfaces. 0.001% sodium azide was added to all sucrose solutions. Percoll gradients were prepared in 0.15M sodium chloride. Gradients were prepared in pairs of tubes; to one tube a selection of calibration beads was added. Centrifugation conditions were varied, as described in Chapter 5.

### **2.2.10 Histological staining techniques.**

#### **Tissue sections**

Tissue sections of fixed ATD brain were routinely stained with Von Braunmuhl's Silver Technique (1957) or Puchtler et al's alkaline Congo red technique (1962). When the latter method was used, haematoxylin was used as a nuclear counterstain if required.

#### **Fresh tissue smears, homogenates and preparations**

The Congo red method of Puchtler et al (1962) was not used to stain fresh brain smears or brain preparations. The reasons for this were twofold. Firstly, Puchtler et al's method involved a number of prolonged stages; and when attempting to stain small amounts of unfixed tissue, the tissue tended to float off the microscope slide. Secondly,

it was not necessary to achieve selective staining of plaques and tangles when crossed polarisation microscopy was being used for routine scanning of preparations. Therefore, the following simple technique was used:

**Aqueous Congo red**

Fixative	None or ethanol
Solutions:	1% Congo red aqueous
Technique	<ol style="list-style-type: none"><li>1. Drop Congo red solution on to tissue - 2 min.</li><li>2. Drain slide and dehydrate through graded alcohols to 100%</li><li>3. Clear in xylene, and mount in DPX.</li></ol>

**2.2.11 Fluorescence Activated Cell Sorting (FACS)**

Sorting was carried out in a FACS IV 40 (Becton Dickenson). In order to comply with category B tissue handling regulations, a vacuum exhaust was attached to the sorting chamber, and bubbled through two sealed jars of chlorox connected in relay. A single argon laser was used during sorting, with an output of about 0.2 watts at 457.9nm.

The actual sorting procedure used was experimental and is discussed in Chapter 4. The basic principle of the equipment is as follows: Individual cells or particles are shot through the nozzle in a sheath of phosphate buffered saline (PBS). The nozzle vibrates, and this causes the stream to break up into droplets and a charge is conferred upon them. The amount of PBS sheath fluid is varied so that one particle is contained in one drop. To avoid the inclusion of more than one particle per droplet, many drops contain no particles. After emerging from the nozzle, each

droplet crosses the path of the laser and is viewed with regard to its fluorescent and light scattering properties by the appropriate detectors. If the properties of a particular particle fall into the 'window' the FACS has been programmed to select, the electromagnet is switched on to deflect the particle to one side into a separate collecting vessel. Droplets not selected fall straight down into a waste container. Analytical and sorting profiles can be represented on the electronics console in a number of ways.

The sorter can be set to 'trigger' on scatter or fluorescence. The former setting is used for analysis as every particle is registered. The latter setting will only register fluorescent particles and can be used for sorting.

Forward angle light scatter approximately corresponds to the size of a particle. Therefore the FACS can be calibrated with fluorescent beads of a known size; 1.5  $\mu\text{m}$  diameter beads were used in these experiments. Some beads stick together and a plot of number of particles vx forward angle scatter reveals peaks at 1.5, 3, 6, 9 $\mu\text{m}$  etc. Channel numbers are then noted. However, due to different scattering properties of different particles, the calibration is only accurate if the forward angle light scatter of the experimental cells or particles corresponds to size; this cannot be assumed and must be proven. Therefore size calibration in these experiments was used only as an approximate estimation of the order of size of the particles collected.



### **2.2.12 Spectral studies**

Tangle preparations from ATD brains, and control fractions from control brains were prepared by SDS sucrose discontinuous density gradient centrifugation. Samples for fluorescence spectroscopy and circular dichroism were dialysed against 10mM sodium phosphate buffer pH 6.8 with 0.1M sodium chloride, in a glass beaker, for a minimum of 4 hours, in order to remove azide, which interferes with absorbance. Samples for infra-red studies were dialysed against D<sub>2</sub>O. Studies were performed on sample supernatants or suspensions, with the exception of infra red spectroscopy which was performed on a dried film of the preparation.

#### **Ultraviolet spectra**

Samples were viewed in a 1 cm light path quartz cell. Spectrophotometry was carried out in a Perkin-Elmer Coleman 575 spectrophotometer.

#### **Infra red spectra**

Samples were smeared and air dried on to calcium fluoride windows. Spectrophotometry was carried out using a Grubb Parsons 'Spectromaster'.

#### **Circular dichroism**

Circular dichroism was performed using a Cary 61 Spectropolarimeter. This was flushed with nitrogen gas for 30 minutes before use. Protein was measured, prior to spectrophotometry, using the method of Tonbs et al (1959).

## CHAPTER 3

### MORPHOMETRIC AND SOLUBILITY STUDIES ON TANGLES AND PHF

## MORPHOMETRIC AND SOLUBILITY STUDIES ON TANGLES AND PHF

### PART 1

#### 3.1 INTRODUCTION

The identification of neurofibrillary tangles depends upon recognition of their appearances using light microscopy, and visualisation of their constituent PHF using EM. Similarly, plaques can be recognised by their light microscopic appearances, and by visualisation of their ultrastructural constituents, using EM. Plaques and tangles are argyrophilic (Alzheimer, 1907) show dichroic birefringence with congo red (Divry 1927) and yellow fluorescence with thioflavine. The constituent proteins of PHF and amyloid are currently under investigation (see Sections 1:8-1:12), therefore the presence of plaques and tangles in tissue sections and preparations must be monitored using microscopy. A selective, simple and adaptable method for staining plaques and tangles in tissue sections and brain extracts was required, in order to monitor the separative procedures (Chapter 5) and to study the solubility characteristics of plaques and tangles. Congo red was found to be a suitable histological stain. Semi-quantitative assessment of plaques and tangles in the contralateral hemisphere of brains stored in the MRC Metabolism Unit brain bank had previously been performed by Dr. A Gordon,

Consultant Neuropathologist, using tissue sections stained by Von Braunmuhl's silver impregnation method. An initial experiment was performed: (1) To compare the visualisation of plaques and tangles by silver impregnation and congo red staining methods.

Both plaques cores and tangles have been reported to be insoluble in protein solubilising agents such as SDS and 0.2M NaOH (Allsop et al., 1983; Selkoe et al., 1982, respectively). However, Iqbal et al (1984) reported tangles to be partially soluble in SDS. In view of the widespread use of this reagent in the preparation and biochemical analysis of tangles, two further experiments were performed;

(ii) To investigate the solubility of tangles and plaque cores, in SDS and NaOH, in brains from cases of ATD and Down's syndrome.

(iii) To collate the results from this study with clinical data collected on the cases; in order to determine if the numbers and solubility of tangles and plaque cores were related to clinical parameters.

An observation had been made by Wischik et al (1985) that treatment with NaOH caused PHF to untwist or straighten. Therefore, in order to determine whether SDS also had an untwisting effect on PHF, a fourth experiment was carried out.

(iv) To investigate the effect of SDS treatment on the total and repeat length of PHF.

### 3.2 MATERIALS AND METHODS

#### 3.2.1 Materials and staining techniques

Sections from the right cerebral hemisphere, from control and ATD brains, fixed in 10% saline/tapwater for longer than 4 weeks, were cut from tissue blocks. All silver staining was performed by Ms L McCardle, all other staining by myself. Fresh frozen brain tissue from the left cerebral hemisphere, from control brains and cases of ATD, was obtained from the MRC brain bank. Clinical data on each case were assessed from the case notes by Dr J.E. Christie, Consultant Psychiatrist. Tissue sections, brain smears and homogenates, were prepared and stained as described in Section 2.

#### 3.2.2. A quantitative comparison of Congo red and silver staining methods.

Five brain areas; and parahippocampal gyrus, mid temporal cortex, frontal cortex, parietal cortex, and hippocampus, from the right hemisphere of ATD brain B138 were studied. Twenty serial (or consecutive) 10 $\mu$ m sections were cut on a freezing microtome. Alternate sections were stained by von Braunmuhl's silver technique, and Congo red (Puchtler et al., 1962); using an eyepiece graticule (Graticules Ltd), plaque and tangle counts were performed over 10 fields (at x 160 magnification), in each brain area, in all sections. This gave 100 fields for each stain, in each of the five areas.

### 3.2.3 Solubility of tangles and plaque cores in SDS and NaOH.

Samples from the left temporal lobes from twenty five cases of ATD were selected from the brain bank, on the basis of semi-quantitative assessments of severe ATD pathological changes in sections from the right temporal lobes. These assessments were performed by Dr A Gordon, Consultant Neuropathologist. Smears of the left temporal cortex from these brains were stained with Congo red and inspected under the light microscope. Fourteen brains observed to contain significant numbers of tangles were selected for study. The six cases of Down's Syndrome, all aged over 50 years, showed an Alzheimer pathology, in silver stained sections of the fixed right temporal cortex and in Congo red stained smears of the unfixed left temporal cortex, of a severity similar to the fourteen ATD cases.

Sex, age at death, post mortem interval (the interval between death and autopsy), duration of terminal illness, and duration of dementia, of these twenty subjects are given in Fig. 3.3. The cause of death was bronchopneumonia (7 cases of ATD and 4 cases of Down's Syndrome), coronary atheroma or myocardial infarction (2 cases of ATD), aspiration of stomach contents (one case of ATD), torsion of ovarian cyst (one case of ATD) and unknown (2 cases of ATD and one case of Down's Syndrome). All patients were hospitalised and confined to bed for at least the last few days of life.



### 3.2.3.1 Tangle and plaque core counts and solubility

One gram of temporal cortex was dissected from the frozen left hemisphere of each brain and homogenised (20 strokes, glass on glass) in two volumes of distilled water. Four aliquots of 125 $\mu$ l were further homogenised (5 strokes) with 875 $\mu$ l distilled water, 1% SDS, 5% SDS, and 0.1M NaOH respectively; with 0.1%  $\beta$ -mercaptoethanol included in the SDS solutions. The samples were incubated at room temperature for 5 mins. Distilled water (5 ml) was then added, the samples centrifuged at 8,000xg for 5 mins and the supernatant reserved. Each pellet was suspended in 1.0 ml 0.05% (w/v) Congo red to stain plaques and tangles, left for 2 mins and centrifuged at 8,000xg for 5 mins. The supernatant was discarded and the pellet washed twice in 1.0 ml distilled water to remove excess stain and centrifuged as before. The final pellet was re-suspended in 1.0 ml distilled water (3 strokes of homogeniser) and transferred to a 1.0 ml (1000x1 $\mu$ l) glass rafter cell counter, covered with a cover slide and left for 30-60 mins to allow the tissue particles to settle. The number of tangles and plaque cores were counted under crossed polarisation microscopy (at x 160 magnification) in 50 x 1 $\mu$ l divisions of the rafter cell, using 50 sets of regularly spaced co-ordinates on the microscope stage. All co-ordinates were at least 5 squares from the edge of the rafter. Tangles and plaque cores were recognised by their green-red birefringence and form, under crossed polarisation microscopy; and plaque cores were distinguished

by their maltese cross shape. Centrifugation of the 8,000xg supernatant from the 1% SDS and 5% SDS homogenates, from four brains and two brains respectively, at 200,000xg for 2 h, produced pellets which did not contain plaques or tangles. This indicated that centrifugation at 8000xg was sufficient to pellet these structures.

#### 3.2.3.2 Correlation of counts with clinical data

The Wilcoxon rank sum test was used to compare counts in the ATD and Down's groups and in males and females counts in the four treatment groups were compared by Friedman two-way analysis of variance, and differences between pairs of treatments were tested by multiple comparison tests (Daniel, 1978). Associations between counts and other quantitative variables were tested using Spearman rank correlation,

#### 3.2.4. Comparison of native and SDS treated PHF using electronmicroscopy

Sample 1. SDS insoluble PHF: Temporal cortex from ATD brain No. 11 was homogenised as described for light microscopy; 250 $\mu$ l of homogenate was further homogenised with 750 $\mu$ l 1% SDS containing 0.1%  $\beta$ -mercaptoethanol. This was incubated at room temperature for 5 mins, and 3.0ml distilled water was added. The sample was centrifuged at 8,000xg for 5 mins and the pellet, which contained tangles and plaque cores was discarded. The supernatant was diluted to 5.0ml and centrifuged at 200,000xg for 2 h to give a PHF-containing high speed pellet which was suspended in 200 $\mu$ l distilled water.

Sample 2. Native PHF: These could not be prepared by the above method because, without SDS extraction, PHF would not be released in large numbers into the 8,000xg supernatant; and in any case, would be obscured by other tissue components on the EM grid. A sucrose gradient method was therefore used: temporal cortex (0.5g) from brain ATD No. 14 was homogenised in 1.0ml 5mM Tris pH 7.0, layered onto a discontinuous density gradient of 4ml each of 2M, 1.6M, 1.4M and 1.2M sucrose in a 17 ml centrifuge tube, and centrifuged, using a swing bucket rotor, at 50,000 xg for 50 h. (See Chapter 5). 1.0ml of the 1.6M interface fraction, which was rich in tangles, was dialysed overnight against distilled water.

Samples 3 and 4 Quantification of the effect of SDS on PHF: Two 0.5g portions of temporal cortex from brain ATD No. 21 were homogenised in 1.0 ml 5mM Tris pH 7.0, and in 2.0ml 1% SDS containing 0.1%  $\beta$ -mercaptoethanol, respectively. The homogenates were applied to discontinuous density gradients prepared as above, with 0.1% SDS and 0.1%  $\beta$ -mercaptoethanol present throughout the gradient used for the SDS homogenate. The two gradients were centrifuged as before and tangle rich samples (approximately 1.0 ml) at the 1.6-2M interphase from the native non-SDS (Sample 3) and SDS (Sample 4) gradients dialysed overnight against distilled water.

Measurement of PHF length (L) and number of repeats per PHF (N): For samples 1 and 2 a magnifying glass containing a graticule was employed to measure the lengths of 245 PHF in 27 fields (sample 1) and 208 PHF in 11 fields (sample 2) photographed at  $\times 25,000$ ,  $\times 50,000$  and  $\times 80,000$  with a resolution of 2, 1 and 0.6nm respectively. Measurements by graticule were performed by Dr. P.H. Gibson. In randomly selected fields of samples 1 and 2, the length, and the number of repeats between the first and last constriction of each PHF measured, were determined using an image analyser (Zeiss MOP-Videoplan). Thirty-five PHF in 10 fields (sample 1) and 32 PHF in 7 fields (sample 2), photographed at  $\times 50,000$  and enlarged by  $\times 2$  were investigated. The same technique was used to determine PHF length and the number of repeats per PHF of 45 in 24 fields of sample 3, and 50 PHF in 24 fields of sample 4.

Variation in PHF length (L), number of repeats per PHF (N) and mean repeat length per PHF (L/N) between different fields of the same preparation was examined using the Kruskal-Wallis test. In samples 1 and 2, multimodality in the distribution of PHF length was examined by the method of Silverman (1981). In samples 3 and 4, proportionality of PHF length and mean repeat length was tested by Kendall rank correlation of the product and the ratio of these two measurements. PHF Length, and mean repeat length in samples 3 and 4 were compared using the Wilcoxon rank sum test. All analyses were performed by computer.

### 3.3 RESULTS

#### 3.3.1 Identification of tangles and plaques using histological staining techniques

The amyloid stains, Congo red and silver, were used to stain tangles and plaques. It was possible to stain plaques and tangles in tissue sections and brain smears or preparations, using the methods of Puchtler et al (1962) and an aqueous Congo red method (section 2.2.9 this thesis), respectively. However the silver method of von Braunmuhl was difficult to apply to brain smears and preparations, and was therefore, only used on tissue sections.

Using these staining techniques it was possible to identify clearly the following structures:

i) Amyloid core plaques -

These were demonstrated as dense black deposits using silver. Congo red staining showed green red birefringence, under crossed-polarisation, with a 'maltese cross' appearance.

ii) Amyloid core plaques plus surrounding neurites - The cores of these structures were identical to those described in i). These cores were surrounded by neurites, which appeared as densely stained black bundles of fibrils, using silver. Congo red demonstrated the neurites as slender green/red birefringent spicules, with a fibrillar texture.

iii) Neuritic plaques (without cores) -

These consisted of a radial arrangement of neurites, which stained as described above.



iv) Tangles -

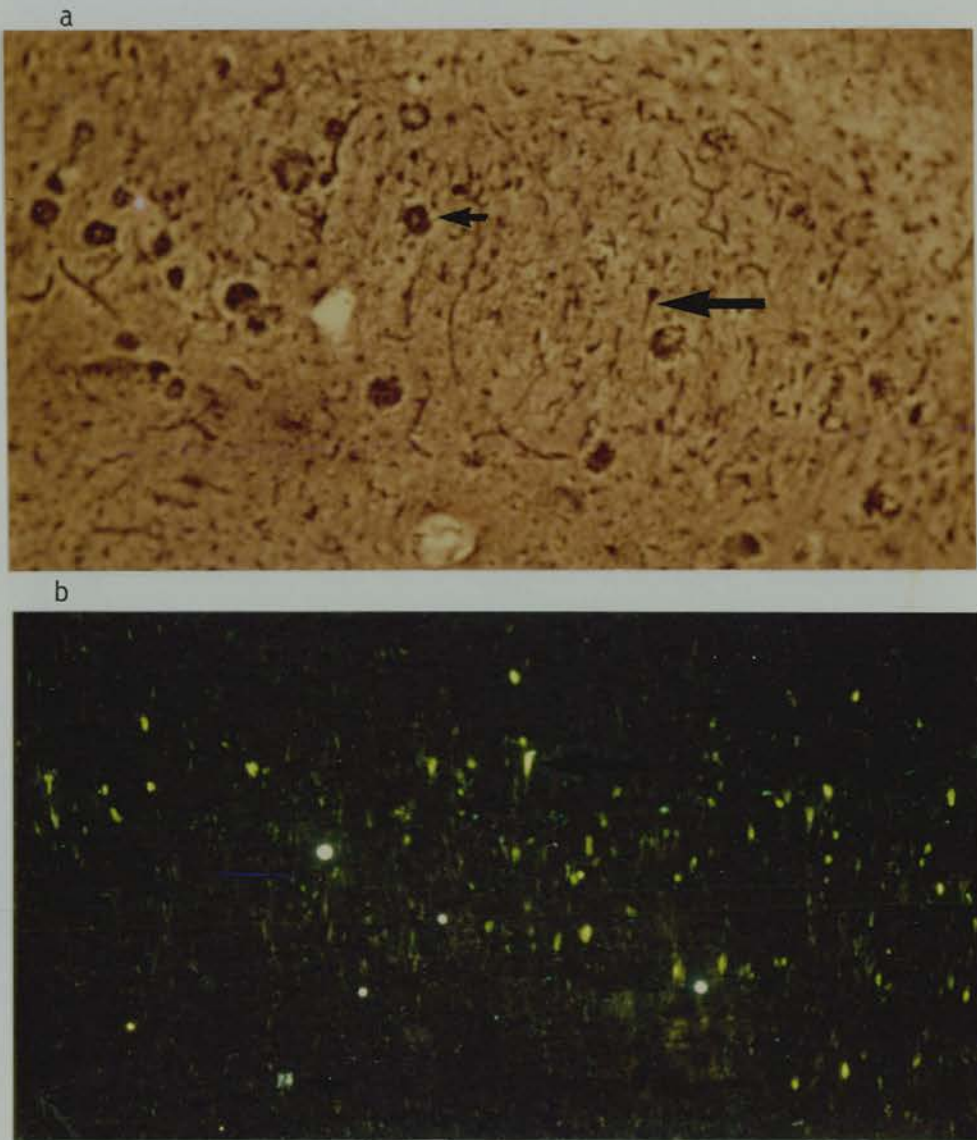
Using silver staining, tangles appeared as dense black structures with a fibrillar consistency. Congo red staining showed green/red birefringent structures. With both stains, identification of tangles depended heavily on the morphological appearances, these were a neuronal shape (a complete, or part of, a cell body); with the tangle fibrils apparently orientated around the cell perimeters; with or without a central nuclear space; with or without the appearance of extension of the tangle into dendrites, or into the proximal axon.

**3.3.2 A quantitative comparison of Congo red and silver staining**

The results of this study shown in figs. 3.1 and 3.2 revealed that plaque cores and tangles were better identified by Congo red staining than silver staining. In particular, tangles in pyramidal cells in the hippocampus were better demonstrated by Congo red. Neuritic plaques and plaque cores with surrounding neurites were better identified by silver staining. Occasionally, structures which were slightly ambiguous in appearance were noted when using Congo red staining. These possessed most of the features of tangles, and probably represented slightly atypical tangles. However, numbers of these were noted separately and included in brackets in the table.



Figure 3.1 CONSECUTIVE SECTIONS OF HIPPOCAMPUS STAINED WITH  
a) SILVER AND b) CONGO RED



a) Hippocampus stained with silver, von Braunmyhl's method. Neuritic plaques are clearly seen (small arrow), whereas neurofibrillary tangles are more difficult to discern (large arrow).

b) A consecutive section of the same hippocampus stained with Congo red, (Puchtler et al's method). Here tangles are clearly seen (large arrow) whereas large neuritic plaques are not well demonstrated; though amyloid plaque cores are visible (small arrow)

Magnification x 125

Fig 3.2

A comparison of Congo Red and  
Von Braunmuhl Silver Staining using  
serial sections of an ATD brain.

	Brain area	Plaque cores	Plaque cores + 'halo' of neurites	Neuritic plaques	Tangles*
Congo Red	Mid temporal cortex	5	19	163	535(90)
	Frontal cortex	16	11	176	184(31)
	Hippocampus- sommers sector	70	29	93	1,768(10)
	Parietal cortex	9	12	128	483(127)
	Parahippo- campal gyrus	90	21	97	690(57)
Von B.	Mid temporal cortex	4	41	227	254
	Frontal cortex	3	19	193	156
	Hippocampus- sommers sector	35	97	244	655
	Parietal cortex	5	23	237	283
	Parahippo- campal gyrus	14	25	382	447

Congo red : Von B, ratio

Plaque cores	3.16
Plaque cores + 'halo'	0.45
Neuritic plaques	0.5
Tangles	1.8

\* Numbers in brackets refer to slightly ambiguous structures, which appear to be tangles but do not meet all the criteria for tangle recognition (Page 68). The adjacent larger tangle numbers are inclusive of the figures in brackets.

Figure 3.2 A COMPARISON OF THE NUMBERS OF PLAQUES AND TANGLES USING CONGO RED AND SILVER STAINING IN CONSECUTIVE SECTIONS.

Table showing numbers of plaques and tangles counted under light microscopy in five different brain areas, in 20 consecutive sections stained alternately with Congo red (Puchtler et al) and silver (Von Braunmuhl).

Underneath the table the numbers of structures recognised using Congo red staining have been divided by the numbers recognised using silver staining, producing a ratio for each of the 4 structures (3 types of plaque + tangles). Averaging the 5 brain areas examined, these ratios demonstrate that Congo red staining shows up plaque cores and tangles more readily; whereas silver staining shows up neuritic plaques and plaque cores plus a 'halo' of neurites more readily.

### 3.3.3 Solubility of tangles and plaques cores in SDS and

#### NaOH

After treatment with SDS/ $\beta$ ME or NaOH, brain homogenates were centrifuged at 8,000 g x 5 minutes. The resulting low speed pellets contained tangles and plaque cores which were counted (Fig. 3.3). When these supernatants were centrifuged at high speed, this resulted in a "high speed" pellet which contained no tangles or plaque cores under light microscopy. However, this pellet did appear to be faintly birefringent. Under electron microscopy PHF were seen in both low and high speed pellets. There were no obvious morphological differences between the PHF in the two pellets.

The number of tangles in the water-treated (control) homogenate varied enormously between brains (range 15-653, median 107, per mg wet weight) and was not related to age, sex, duration of dementia, duration of terminal state or post-mortem interval. Smaller numbers of plaque cores (range 3-47, median 9, per mg wet weight), also unrelated to clinical factors, were found in the control homogenates. Wide variation in plaque and tangle numbers between brains has been previously reported (Gibson, 1985; Wilcock and Esiri, 1982). Plaque and tangle numbers before treatment with SDS or NaOH did not correlate with any of the clinical data collected in this study. It has previously been shown that plaque and tangle numbers correlate with the degree of dementia (Blessed et al, 1968; Tomlinson et al, 1970). Therefore, it is possible that the variation in plaque and

Figure 3.3

Clinical details and tangle and plaque core counts in homogenates (water, 1% SDS, 0.2 M NaOH of temporal cortex from cases of Alzheimer-type dementia (ATD) and Down's syndrome													
Brain	Clinical details				Tangle (T) and plaque core (P) counts per 3 mg wet wt								
	Age/Sex	Duration of dementia (years)	Duration of terminal state (days bed-ridden)	Post-mortem interval (h)	Water-treated Control	1% SDS	5% SDS	0.2 M NaOH					
					T	P	T	P	T	P	T	P	P
Down's													
1	56/M	1	7	20	380	28	290	31	200	33	172	24	
2	57/M	3	180	12	715	35	292	33	235	40	117	15	
3	60/M	6	730	19	354	25	225	27	144	21	21	9	
4	61/M	3	30	22.5	752	98	406	88	382	80	251	37	
5	63/F	3	30	24	288	43	189	39	72	29	294	50	
6	67/F	4	49	21.5	85	14	98	18	35	17	33	30	
ATD													
7	59/M	2	7	12	769	21	539	23	235	19	268	21	
8	64/F	2	14	9	253	96	191	97	105	77	46	79	
9	66/M	6	2	3.5	358	27	227	25	248	29	133	30	
10	69/M	7	30	23	695	141	376	151	206	171	201	131	
11	70/M	8	3	30	279	15	77	13	100	16	60	6	
12	70/M	6.5	30	3	240	19	75	13	98	13	75	16	
13	71/M	10	30	16	90	12	30	10	20	9	54	8	
14	74/F	4.5	<1	44	1960	131	1067	63	838	62	933	77	
15	76/M	5	5	10.5	1018	138	996	140	930	125	166	50	
16	76/F	5	21	6.5	131	12	35	13	50	12	37	8	
17	76/F	-	<1	12	79	8	35	10	42	8	15	5	
18	77/F	-	<1	19	46	15	35	19	28	11	31	17	
19	81/F	4	30	38	268	27	108	26	76	21	81	20	
20	82/F	10	14	55	942	65	203	41	248	46	462	54	
21	81/F	-	-	28.5	-	-	-	-	-	-	-	-	

<sup>a</sup> Interval between death and autopsy, cadavers refrigerated within 4 h of death; -, No data; SDS, sodium dodecylsulphate



Figure 3.3 A STUDY OF PLAQUE AND TANGLE SOLUBILITY IN ATD AND DOWNS BRAINS.

Clinical details and solubility experiments on 20 brains (14 ATD, 6 Down's). Homogenates of each of the 20 brains were subjected to 4 treatments: water, 1% SDS, 5% SDS, and 0.2M NaOH. The number of plaques and tangles insoluble in these treatments were recorded, for each brain. Results were analysed as described in the text.

As one gram of temporal cortex was homogenised in 2ml of water, plaque and tangle counts in the 125 $\mu$ l aliquots were representative of a large volume of brain. Reproducibility of counts was confirmed on a pilot study of 4 water-treated (control) aliquots of 2 brains (7 and 8). These counts showed no significant differences ( within each brain).

There were wide variations between plaque and tangle numbers between brains (see section 3.3.2). Tangles were found to be significantly soluble in 1% SDS 5% SDS and 0.2M NaOH ( $p < 0.01$ ,  $p < 0.001$ ,  $p < 0.001$  respectively), as compared to the water-treated sample. Plaque cores were found to be significantly soluble in 0.2M NaOH ( $p < 0.05$ ), as compared to water-treated and 1% SDS treated samples. Tangles were proportionally more soluble than plaque cores (see Fig. 3.4).



Figure 3.4

THE PERCENTAGE OF TANGLES AND PLAQUE CORE INSOLUBLE IN 1% SDS, 5% SDS AND 0.2M NaOH.

For each brain the numbers of tangles and plaque cores after treatment with (i.e. insoluble in) 1% SDS, 5% SDS and 0.2 NaOH was expressed as a percentage of the number in the aqueous homogenate (zero treatment). Mean  $\pm$  S.D. for 20 brains.

Treatment	% Tangles insoluble	% Plaque Cores insoluble
1% SDS	57 $\pm$ 25	97 $\pm$ 21
5% SDS	43 $\pm$ 17	90 $\pm$ 21
0.2M NaOH	37 $\pm$ 22	72 $\pm$ 21

tangle numbers between brains seen here, reflects the correlation with the degree of dementia. The degree of dementia was not looked at as a clinical co-ordinate in this study, as it was felt to be too difficult to assess accurately, in retrospect, from the case notes.

There was no significant difference between the cases of Down's syndrome and ATD in plaque and tangle counts of the pellets in the four treatment groups. Data from all cases were therefore, pooled for co-variate analysis. Treatment with 1% SDS, 5% SDS and 0.2M NaOH did not alter the morphological appearance of tangles and plaque cores as viewed by crossed polarisation microscopy. Tangle counts after treatment with 1% SDS, 5% SDS and 0.2M NaOH, were significantly less ( $p < 0.01$ ,  $p < 0.001$  and  $p < 0.001$  respectively) than the tangle count in the control homogenates. There were no significant differences between treatment groups. Plaque core counts after treatment with 0.2 M NaOH were significantly less than both control counts  $p < 0.05$ , and counts after treatment with 1% SDS ( $p < 0.05$ ). The mean tangle and plaque core counts after 1% SDS, 5% SDS and 0.2 M NaOH expressed as a percentage of counts in the control homogenates, showed that tangles were more soluble than plaque cores (Fig. 3.4). The percentages of tangles and plaque cores insoluble in 1% SDS, 5% SDS and 0.2M NaOH were not significantly correlated with the number of tangles in the control brain homogenates, not with the clinical co-variables; age, sex, duration of terminal state or post-mortem interval. However, the percentage of tangles

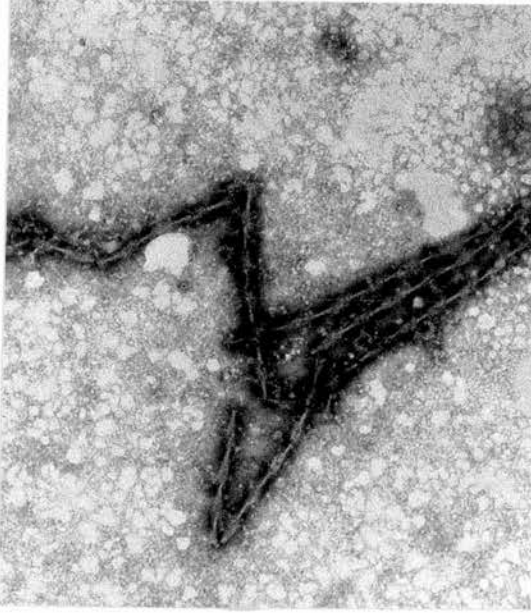
insoluble in 1% SDS was found to be inversely correlated with duration of dementia ( $r = -0.49$ ,  $p < 0.01$ , Fig. 3.5d). That is the proportion of insoluble tangles was greater in early dementia, or tangle solubility in 1% SDS was increased with increasing duration of dementia. This relationship was also significant ( $r = -0.52$ ,  $p < 0.05$ ) when only the ATD cases were considered. Duration of dementia was not significantly correlated with the percentage of tangles insoluble in 5% SDS or 0.2M NaOH, or with the percentage of plaque cores insoluble in all three treatments.

#### 3.3.4 A comparison of native and SDS treated PHF using EM

PHF prepared under native and SDS denaturing conditions were of similar appearance, under EM. PHF in all samples appeared twisted with a maximum diameter of 20-30 nm narrowing to about 10 nm approximately every 70-80 nm. Very occasionally PHF with a longer repeat length of about 120 nm were observed in the SDS preparation (fig. 3.5). In both preparations the smallest PHF recognisable, measured about 30 nm in length; such filaments usually, but not invariably, were constricted at both ends. Pieces of longitudinally aligned PHF with short intervening gaps, probably formed as a consequence of breakdown of a long PHF during grid preparation were observed in both native and SDS preparations. All breaks in filaments were transverse and longitudinal cleavage of any description e.g. separation into two filaments, was not observed. There were significant differences between photographic fields of samples 1 and 2 measured using the graticule with respect

Figure 3.5

a



b



c

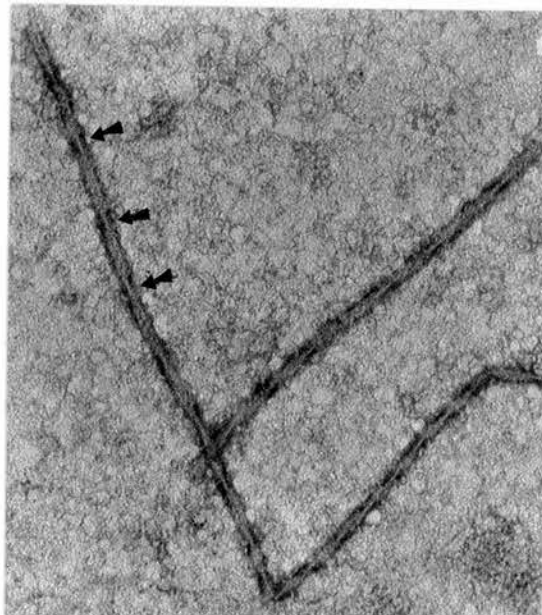
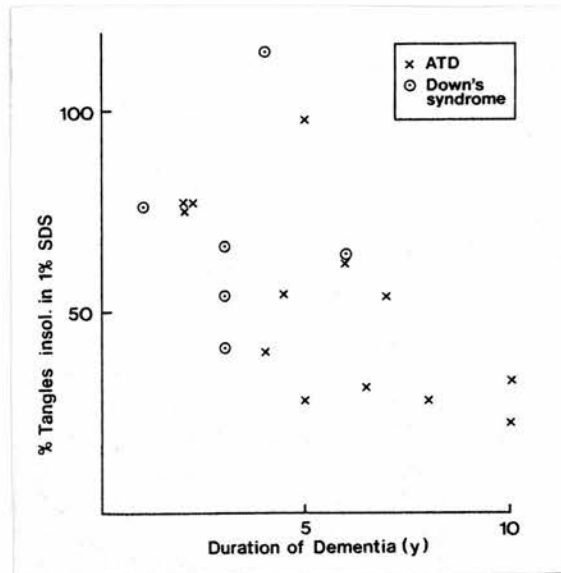


Figure 3.5 ELECTRONMICROGRAPHS OF NATIVE AND SDS TREATED PHF (a-c). GRAPH SHOWING % TANGLES INSOLUBLE IN 1% SDS vs DURATION OF DEMENTIA (d).

d



a) Native PHF, (from sample 3, brain No. 15).

b) and c) SDS treated PHF, (from sample 4, brain no. 15).

c) shows PHF with a lengthened repeat (arrows).

d) Percentage of tangles insoluble in 1% SDS versus duration of dementia; showing inverse correlation. That is, tangles from brains with a short duration of dementia are proportionally less soluble in 1% SDS than tangles from brains with a longer duration of dementia.

Magnification x 76,000

Figure 3.6

SAMPLE	BRAIN NO.	TREATMENT	NO. OF PHF MEASURED	MEAN + SD	PHF LENGTH (nm)	MEAN REPEAT LENGTH PER PHF (nm)
1	11	SDS	35	595±190		74.9±4.5
2	14	Native	32	465±336		66.8±3.2
3	21	Native	45	585±375		68.9±6.9
4	21	SDS	50	745±266*		79.1±9.8**



Figure 3.6 LENGTH AND MEAN REPEAT LENGTH OF PHF ISOLATED IN THE PRESENCE (SDS), AND ABSENCE (NATIVE), OF 1% SDS.

Samples 3 and 4 were compared statistically (see section 3.3.4). These were SDS and native preparations of the SAME brain. The results show that SDS treated PHF have a longer mean repeat and total length, than native PHF.

For sample No. 4: \*  $p < 0.05$  vs sample No. 3  
\*\*  $p < 0.001$  vs sample No. 3.

to PHF length ( $p < 0.001$ ;  $p < 0.05$ ) and suggestion of heterogeneity with respect to PHF length and mean repeat length between samples 3 and 4 measured by image analysis. The mean values of PHF length and mean repeat length per PHF for each field were therefore used for all further analysis. No significant multimodality was found for the length (mean  $\pm$  S.D) of 245 SDS treated PHF (sample 1,  $449 \pm 202\text{nm}$ ) or 205 native PHF (sample 2,  $177 \pm 55\text{nm}$ ). Mean repeat length was not significantly correlated with PHF length in samples 3 and 4. PHF length ( $P < 0.05$ ) and mean repeat length ( $p < 0.001$ ) were greater in the SDS treated sample (3) compared with the native sample (4) (fig. 3.6). The mean repeat lengths were very similar for native PHF obtained from two brains (samples 2 and 3) and similar for SDS treated PHF from two brains (samples 1 and 4).

### 3.4 DISCUSSION

#### 3.4.1. Identification of plaques and tangles, and comparison of Congo red and silver staining

The size and shape to the tangle may be dictated, at least in part, by the shape of the neurone within which it is contained. As tangles are contained in different type of neurones e.g. cortical neurones, pyramidal neurones, and these are different in appearance, tangles vary in size and appearance, e.g. 'globose', 'comma' and 'flame' shaped tangles. This variation is present both between tangles in different brain areas, and tangles within brain areas.

The tangle appearances found in the cortex appear to consist

mainly of the 'comma' and 'globose' types. Many tangles in the subcortical nuclei are similar to those found in the cortex, having a globose appearance. Whereas, hippocampal tangles show up as flame shapes extending down into the axon, (fig. 3.2). As tangles presumably form over a period of time, early tangles must be present within ATD brains. These have been previously described (Wisniewski et al, 1982) as starting around the outside of the cytoplasm. It is possible that the birefringent spicules visualised in Congo red stained sections and preparations, may, in part, represent these early tangles.

The results in fig. 3.2. show that tangles are demonstrated better by Congo red than by silver staining. This is particularly apparent in the hippocampus, where the Congo red stain shows a tangle in almost every pyramidal neurone, these tangles are much less easily seen using silver staining.

Plaques are also variable in appearance. The sequence of events of plaque formation is not proven, but Terry and Wisniewski (1972) describe three types of plaque and suggest that the neuritic plaque, develops an amyloid core, ultimately progressing to a 'burnt out' core of tightly packed amyloid, without surrounding neurites. Whether or not this is correct, three types of plaque can be easily recognised both by silver and Congo red staining. The results in fig. 3.2 show that amyloid plaques are better demonstrated by Congo red than by silver staining, although neuritic plaques are better demonstrated by silver staining.

The identification of tangles and plaques within tissue sections does not present much difficulty, as other features in the tissue, for example, nuclei, can be used for orientation. However, it is sometimes more difficult to identify plaques or tangles in tissue preparations or homogenates, particularly when other features are absent. Most tangles survive the homogenisation process intact and can be recognised in most cases. Likewise amyloid core plaques survive intact. However, neuritic plaques which seem to be more loosely packed, appear to break up during homogenisation to release birefringent neurites. At a light microscope level, it is possible that these are identical to the spicules representing partly formed or fragmented tangles. Therefore, within a homogenate it is not possible to say whether a 'spicule' originates from a neuritic plaque or a tangle. Those from neuritic plaques could be expected to consist either of PHF or amyloid (Wisniewski et al, 1983). Therefore within a Congo red stained homogenate or preparation any green/red dichroic birefringent particle could be identified as one of the following: tangle, amyloid plaque core, spicule, or neuritic plaque. The only other birefringent objects were bundles of connective tissue. These were different in shape and tended to be parallel sided, larger than tangles and they demonstrated a red/yellow-white birefringence. The presence of connective tissue in tangle preparations was minimised by careful dissection of tissue and, in some cases, by discarding the 'blood vessel' portion of the tissue pellet (see Chapter 5).

### 3.4.2 Solubility of tangles and plaque cores in SDS and NaOH, and its relationship with clinical factors.

Absolute numbers of tangles and plaque cores in temporal cortex homogenates were extremely variable between brains from cases of ATD and Down's Syndrome, and did not correlate with patient age. Considerably variation in tangle counts has been reported in ATD brain homogenates (Iqbal et al, 1984), and in tissue sections (Wilcock et al, 1982); and variation in plaque core number in tissue sections has also been reported (Gibson 1985). However, other workers have found that pathology is more severe in younger cases of ATD (Wilcock et al, 1982; Mann et al, 1985). The absence of a relationship between age and pathology in the study described here, is probably due to the selection of cases on the basis of severe Alzheimer pathology. The observation that tangle and plaque core counts were unrelated to post-mortem interval or to duration of terminal state, assessed by the number of days the patient was bed-ridden before death, suggests that tangles and plaque cores, at a light microscopic level are unaffected by pre and post mortem conditions. The excess of tangles over plaque cores (core numbers were approximately 10% of tangle numbers) was in accordance with the work of Gibson (1985) who also found that plaque core numbers were about one tenth of tangle numbers. Tangles were variably soluble in SDS and NaOH, whilst plaque cores were insoluble in SDS, as reported by Allsop et al (1983) and Masters et al (1985), and slightly soluble in 0.2M NaOH. The estimate of mean tangle

solubility in 1% SDS from all cases studied here was 43%. Iqbal et al (1984) in a study of twelve brains, in which they counted fewer tangles, reported a mean tangle solubility in 2% SDS of 38%. The hypothesis investigated here was that variability in tangle solubility between brains could be related to clinical factors, in particular those which may reflect the stage of the illness, such as duration of dementia or duration of terminal state. The only correlation between tangle solubility and clinical parameters was the inverse correlation between the percentage of tangles insoluble in 1% SDS and duration of dementia. That is, the percentage of soluble tangles increases with increasing duration of illness. If tangle solubility is related to the packing density of constituent PHF, as suggested by Iqbal et al (1984), the observed increase in solubility may reflect a change in the state of the tangles, such as, transformation from intracellular to extracellular tangles. The latter are less dense than intracellular tangles, and show infiltration by astrocytic processes (Probst et al, 1982), and therefore may well be composed of more loosely packed PHF.

The degree of dementia has been found to be related to plaque (Blessed et al, 1968) and tangle (Wilcock and Esiri, 1982) numbers in silver impregnated sections of cerebral cortex. Degree of dementia was not investigated in this series.



### 3.4.3 A comparison between native and SDS treated PHF using electron microscopy

Treatment with 1M NaOH has been reported to untwist PHF to give ribbon-like structures with sharp transverse ends, or more rarely longitudinal fractures (Wichik et al, 1985). This is manifest by an increase in repeat length. This observed increase in mean repeat length was not related to the absolute PHF length. The untwisting induced here in vitro may occur in vivo, since straight filaments (15nm diameter) have been found to be a major constituent of extracellular tangles (Okamoto et al, 1983), and have also been observed in continuity with classically twisted PHF in sections of cerebral cortex (Yoshimura, 1984). If this process does occur in vivo the factor initiating untwisting would probably be an endogenous biological substance such as a protease. For, although proteases in cells are usually within lysosomes; in cell damage, there is an increase in non-lysosomal proteases. That is, the disintegration of the cell around the tangle would release proteases which may act on the PHF forming the tangle. The significant difference in PHF length and mean repeat length between different fields of the same grid could either, be due to differences between PHF within one preparation, or could be related to local conditions on the grid.

Although tangles were not seen in the 8,000g supernatants of the SDS and NaOH treated homogenates using light microscopy, PHF were seen in these supernatants using EM. Therefore the treatments with SDS and NaOH were causing tangles to break

up into their constituent PHF. Although, it is not possible to say, from the results of this experiment, whether PHF themselves were being solubilised by these treatments.

The isolation of PHF with greater length in the presence of 1% SDS could be caused by SDS loosening PHF bundles, with the release of long PHF. Whereas, PHF from untreated tangles may be more tightly packed and more likely to be broken up into shorter lengths when separated from tangle aggregates.

No significant multimodality in the lengths of native and SDS treated PHF was observed. This suggests that within the limits of accuracy of the measurements, the axial subunit is small, compared to the repeat length. This is in accord with the  $< 5\text{nm}$  subunit proposed by Wischik et al (1985). Therefore, the observed untwisting of PHF without separation into two filaments, may represent a realignment of axial subunits.

## PART 2

### ULTRASTRUCTURAL OBSERVATIONS OF AN 'AGED' PREPARATION OF PHF

#### 3.5 INTRODUCTION

A PHF fraction prepared by SDS sucrose density gradient centrifugation, stored at  $-40^{\circ}\text{C}$  for approximately 1 year, was subjected to intermittent defrosting and sampling, for other experimental purposes, such as gel electrophoresis. After a year, a portion of the sample was viewed under electronmicroscopy. It was noted that PHF of unusual appearance, including partially twisted and untwisted forms, were present (fig 3.8). Grids of the same sample, made up immediately subsequent to the preparative centrifugation were retrieved and compared quantitatively with the 'aged' fraction. It was noted that the widths of the unusual filaments appeared to differ from those of more conventional PHF. In order to investigate this, the widths of filaments of three differing appearances were measured and compared,

#### 3.6 METHODS

##### 3.6.1 Preparation and examination of 'aged' PHF fraction

A PHF fraction prepared by SDS sucrose density gradient centrifugation (section 5.2.2), and dialysed against

5mM Tris 0.001% sodium azide overnight, was stored for 1 year at  $-40^{\circ}\text{C}$ . During this time, portions were periodically removed from the sample, for other experimental purposes. Each time, the preparation was defrosted (up to  $25^{\circ}\text{C}$ ), and frozen again within 30 minutes. The thawing and refreezing process was carried out 9 times. The fifth time, the whole sample was diluted with 9 volumes of distilled water before refreezing. After a period of 1 year, this 'aged' preparation was examined by EM and light microscopy; and compared with grids of the same sample made up one year previously.

### **3.6.2 Investigation into the nature of the factors**

**contributing towards morphological heterogeneity of  
PHF in the 'aged' preparation.**

In the method described above (3.6.1.), it was not clear which of the conditions related to storage and treatment of the sample may have contributed to the production of heterogeneous PHF. Four variables were identified and investigated as follows: on dialysed PHF preparations:

#### **Freeze-thawing**

Two PHF preparations were observed under EM to contain 'classical' twisted PHF. They were then subjected to freeze-thawing in which the samples were frozen at  $-40^{\circ}\text{C}$  for an hour, thawed, and immediately refrozen, for 6 cycles. EM was subsequently carried out on these samples. The appearances of the PHF had not changed. No more straight or non-twisted forms were seen than on the original grids.

#### **Bacterial contamination**

Two PHF fractions were prepared from two brains by the SDS

sucrose gradient centrifugation method without adding sodium azide. The fractions were divided into two aliquots each, and one aliquot from each brain was dialysed against 5mM Tris 0.001% sodium azide (as before). The remaining aliquots were dialysed against 5mM Tris without azide. Both fractions were left exposed to air at 4°C. After 7 days they were examined by EM. Numerous bacteria were seen in the fractions without azide; these were associated with clusters of PHF. As the PHF were in clusters, quantitative assessment of their morphology was not possible, however some non-twisted and straight forms were noted. When the samples were left for a further 7 days, intense bacterial contamination and protein clumping made the samples impossible to assess. The fractions containing azide were examined by EM and shown to contain classical twisted PHF.

#### **Aging of sample**

Two samples frozen at -40°C, but left undisturbed for several months, were viewed by EM. The PHF did not show increased heterogeneity. However other PHF fractions which had been stored for over a month and occasionally defrosted, did show less well preserved PHF; in particular the wide portions of the filament were more ragged.

#### **Heating of PHF preparations**

One dialysed PHF preparation was divided into six aliquots. Five portions were heated in water baths for 10 minutes, one to 100°C, one to 80°C, one to 60°C, one to 40°C and one to 30°C. The remaining aliquot was kept on ice. Negatively stained grids were made up from each aliquot. All five portions heated for 10 minutes failed to show PHF and very

little other protein was seen; whereas, the unheated sample showed numerous PHF. Failure to see PHF on grids made up from the heated samples, was due to aggregation of protein during heating, and subsequent failure of protein to bind to the EM grids during negative staining.

The exact conditions in which increased numbers of PHF of unusual morphology occur were not reproduced. It is probable that these altered forms were caused by a combination of factors, possibly including bacterial contamination, and repeated thawing of the sample, up to 25°C. Other authors (Selkoe et al, 1982; Iqbal et al, 1984) have reported EM visualisation of PHF in SDS buffer, after heat treatment, up to 100°C; although, Iqbal et al (1984) describe repeated heating in SDS, with sonication, as a method for solubilising PHF.

Although the casual factors were not established, the opportunity was taken to study these unusual filaments. However, in future preparations in which PHF preservation was desirable, 0.001% azide was added to the sample. Also when sampling was carried out, PHF fractions were refrigerated at 4°C immediately after thawing and not allowed to warm up to room temperature during grid preparation.

### **3.6.3 Quantitation of morphological changes in the 'aged' preparation.**

#### **a) Counting of PHF**

Five grids of aged PHF, prepared as described in Section 3.6.1., were made up and negatively stained using PTA. On



each grid, using the EM scan mode, an area of grid squares with intact carbon film was chosen. Commencing randomly on one grid square, all recognisable PHF were counted and their appearance recorded. Then PHF on adjacent grid squares were counted, until 50 PHF per grid had been analysed and recorded. Numbers of PHF per grid square ranged from 0 to 17 (only 2 squares containing no PHF) and the average number of grid squares counted per grid was 5.6. A count on the retrieved grids of a fresh preparation of the same sample was carried out in a similar fashion, as a control.

**b) Measurement of PHF widths**

Forty-seven electron micrographs of PHF were taken, from seven grids of the 'aged' prep. The fields were chosen to include well preserved PHF of three appearances: 'classical' twisted PHF, periodically constricted (apparently untwisting) PHF and straight filaments. From the micrographs, 50 'classical', 45 periodically constricted, and 36 straight filaments were chosen. The criteria for choosing filaments was that at least 4 turns, or the equivalent length of straight filaments, had to be sufficiently well preserved and distinct from other filaments, to be measurable. The widest and narrowest portions of the filaments were measured using an optical defractometer; two measurements of the latter were taken to include the width between the inner borders of stain, and the outer borders of stain. The reason for this, was that while the filament edges at the wide portions were distinct, the filament edges at the narrow portions were obscured by

stain, presumably due to banking up of stain due to the filament shape. The average widths for the wide and narrow portions of each filament were calculated. For straight filaments, measurements at 25nM intervals were made along the filament; these were also averaged for each filament.

### 3.7 RESULTS

#### 3.7.1 A comparison of 'aged' and freshly prepared PHF fractions

##### 3.7.1.1 'Aged' PHF fractions

Examination of the 'aged' sample under light microscopy showed tangles which were qualitatively similar to those seen in slides of the fresh preparation. Examination of the 'aged' sample under EM revealed considerable changes in some PHF, which overall showed a heterogeneous appearance. The main morphological types and their percentage contribution to recognisable filaments, as assessed by the method described in Section 3.6.3.a, is shown in fig. 3.7. These results show that, compared to the fresh preparation, the 'aged' preparation contained a far smaller percentage of regularly twisted 'classical' PHF. Instead the 'aged' preparation contained a large proportion of other forms, all of which were less regularly twisted than 'classical' PHF. In fig 3.7 filaments have been divided up into three main categories. These are: twisted filaments; twisted/non-twisted filaments, in which a helical structure is suggested but not clearly observed; and untwisted filaments, in which there is no suggestion of a helical

Figure 3.7

Percentages of Morphological types of PHF:-

"Aged" preparation versus fresh preparation

Morphological type of PHF	Percentage of identifiable PHF in "aged" preparation (n=250)	Percentage of identifiable PHF in fresh preparation (n=250)
PHF TWISTED		
1. Twisted, regular repeat	21.6	86.0
2. Twisted, irregular repeat, ragged loops	23.6	4.0
3. Twisted/not twisted	26.0	3.6
PHF NOT TWISTED		
1. Periodically constricted	10.8	0.4
2. Straight	5.2	0.4
3. Fragmented	13.2	5.6

Figure 3.7. MORPHOLOGICAL TYPES OF PHF IDENTIFIED IN  
'AGED' AND FRESH PHF PREPARATION (see fig. 3.8).

PHF - TWISTED

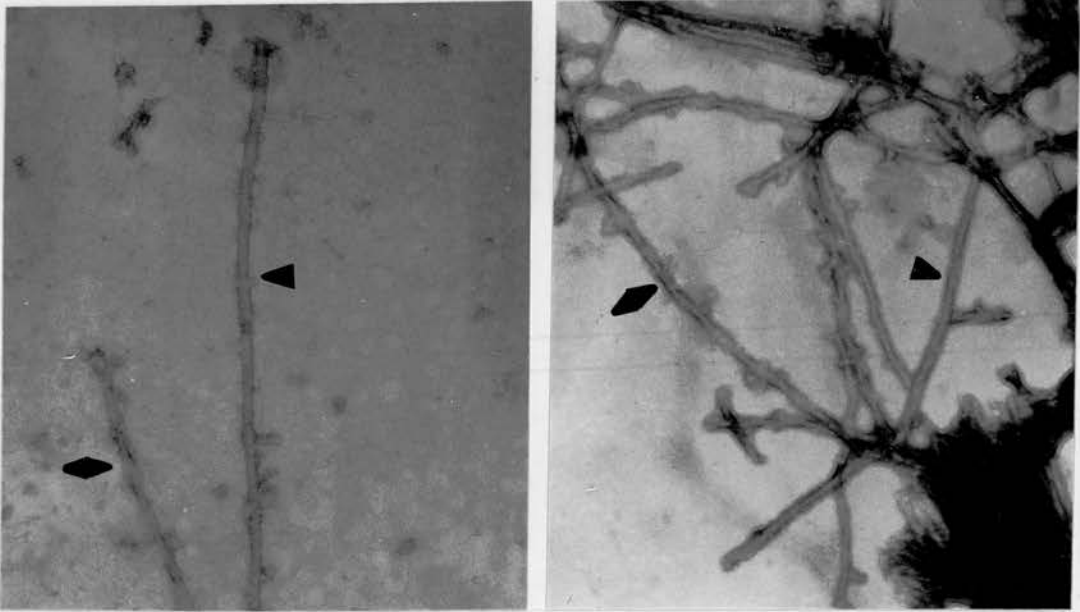
1. Twisted, regular      - PHF consisting of two helically wound filaments. Repeat only slightly variable.
2. Twisted, irregular    - PHF consisting of two repeat ragged tops helically wound filaments. Repeat very variable. Outlines of PHF ragged in the loop regions, amounting to small projections from some loops.
3. Twisted/not twisted PHF    - Filaments in which it cannot be clearly identified whether or not they are twisted. Some have small projections along their sides, often bilaterally opposing.

PHF - NOT TWISTED

1. Periodically constricted    - Filaments which do not appear to consist of two helically wound filaments, but instead have periodic bilateral constrictions.
2. Straight                    - Filaments which appear parallel sided, with no evidence of helical structure.
3. Fragmented                - Filaments with variable structure, which appear to be breaking up and disintegrating, losing their filamentous form.

Figure 3.8

a



b

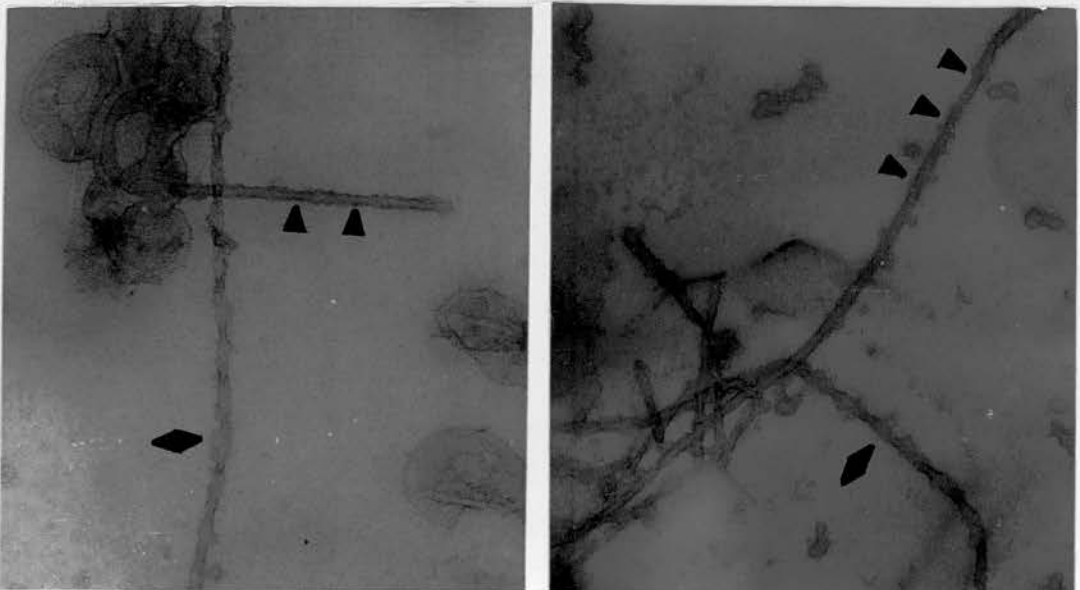
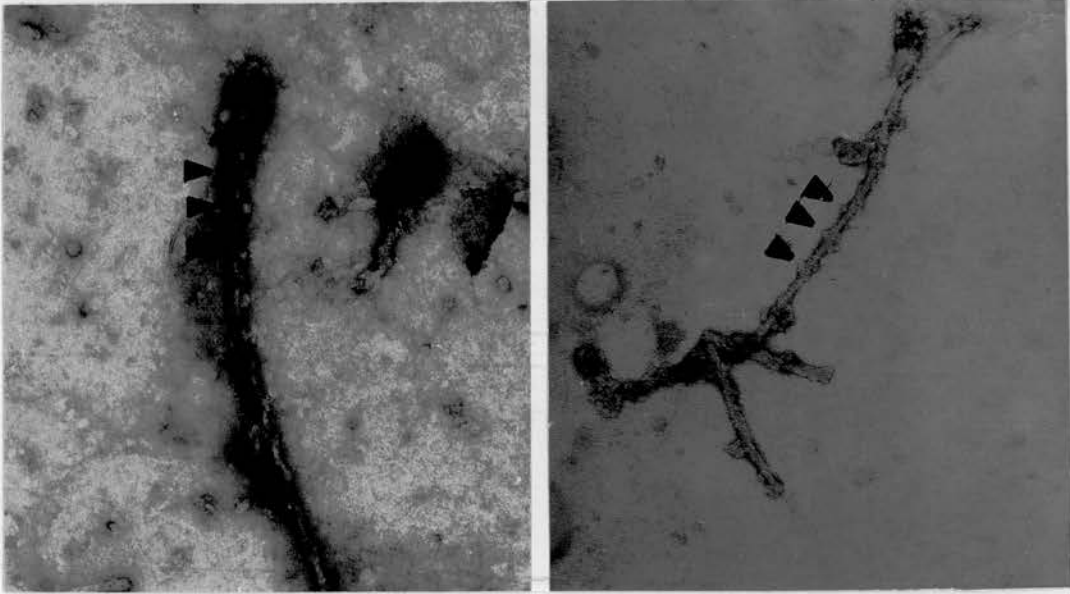


Figure 3.8

c



d

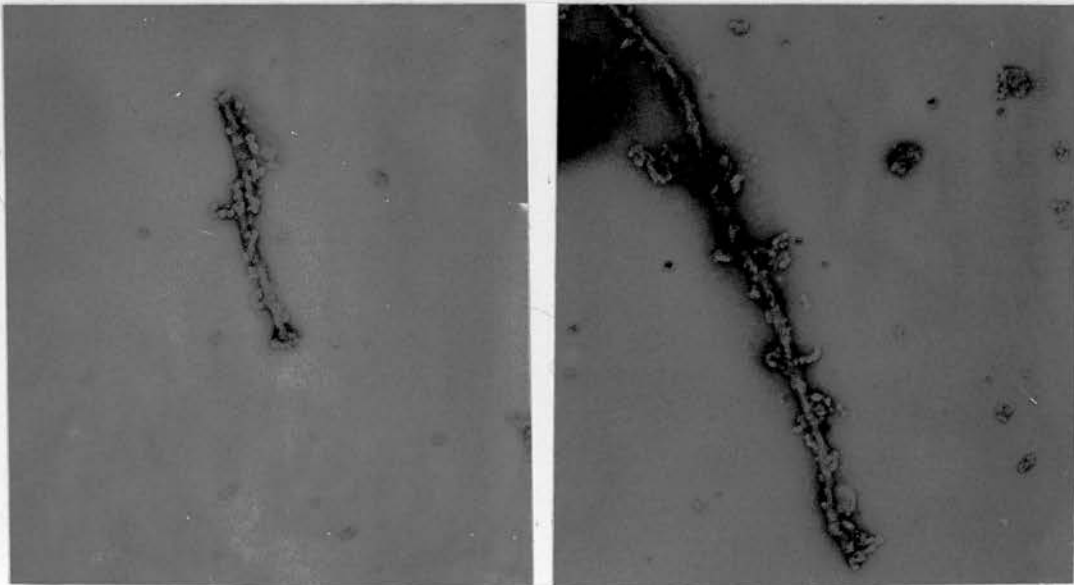




Figure 3.8

e

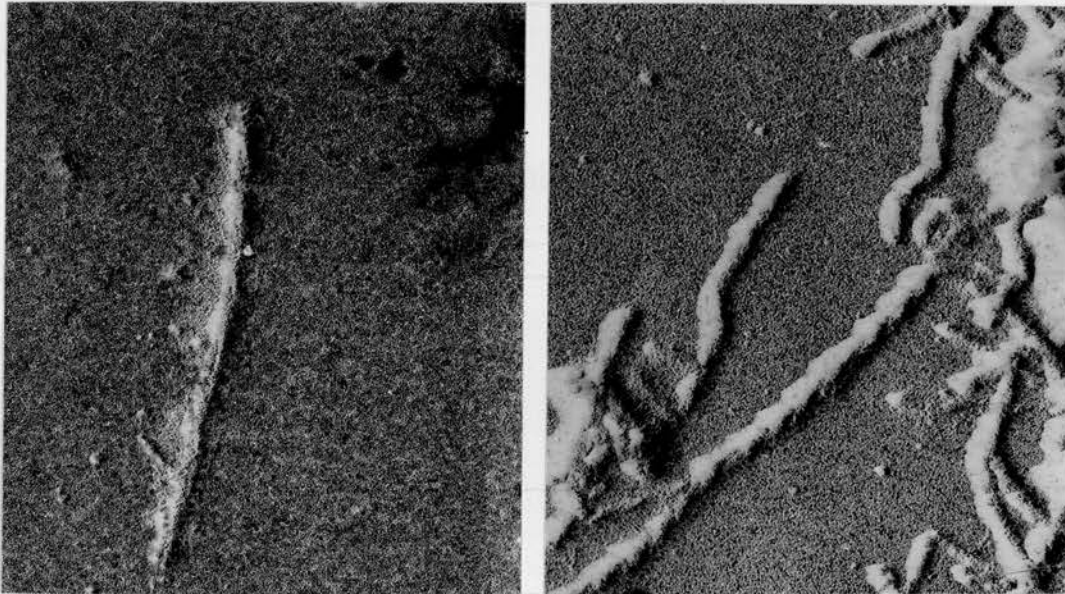


Figure 3.8 PHF WITH UNUSUAL MORPHOLOGY

- a) Straight filaments; (indicated by an arrow).
- b) Periodically constricted filaments; (constrictions indicated by arrows)
- (a) and (b) also show ragged twisted PHF; (indicated by diamond-headed arrows).
- c) Filaments showing bilateral "projections". The left hand PHF is obviously twisted, and the projections appear to be attached to the 'loops' of the PHF. The right hand filament is not obviously helical. ('projections' are indicated by arrows).
- d) Disintegrating filaments
- e) The 'aged' fraction, viewed after platinum shadowing.

Magnification x 71,000

conformation. Of particular interest in the 'aged' fraction were twisted filaments which showed bilateral projections situated on the widest portions (or loops) of the filament repeats.

#### **3.7.1.2 Freshly prepared PHF fraction**

Re-examination of grids of the freshly prepared fraction, originally made up 1 year previously, showed numerous PHF, with occasional collagen and amyloid fibrils and very little other protein. Morphologically these PHF appeared similar to the PHF prepared by denaturing methods described by other authors. However, when these PHF were carefully examined and counted, as described in Section 3.6.3.a, occasional unusual forms were noted, similar to smaller quantities (fig. 3.7).

#### **3.7.1.3 Measurements of widths of 3 or the morphological varieties of PHF in the 'aged' preparation**

Measurements were carried out as described in section 3.6.3.b. The results, shown in fig. 3.9, revealed that compared to the classical twisted PHF, partially untwisted or periodically constricted filaments had similar maximum widths; but significantly larger minimum widths (nm) ( $19.55 \pm 2.77$  VS.  $14.73 \pm 2.43$ ). Also, the straight or untwisted filaments observed, were significantly narrower than the widest portions ( $21.12 \pm 3.122$  VS  $28.52 \pm 4.87$ ) but wider than the narrowest portions ( $21.12 \pm 3.122$  VS  $14.73 \pm 2.43$ ) or 'classical' PHF. Widths of filaments with projections along their sides were not measured, as exact boundaries were difficult to define when such projections were present.

Figure 3.9 WIDTH MEASUREMENTS ON THREE MORPHOLOGICAL TYPES OF FILAMENT (TWISTED, PERIODICALLY CONSTRICTED, AND STRAIGHT FROM THE 'AGED' PREPARATION.

Average width (nm)	Twisted filaments	Periodically constricted filaments	Straight filaments
Widest portion	28.52 $\pm$ 4.87	29.27 $\pm$ 6.53	21.12 $\pm$ 3.12*
Narrowest portion:-			
a) between outer borders of stain	14.73 $\pm$ 2.43	19.55 $\pm$ 2.77*	
b) between inner borders of stain	9.99 $\pm$ 2.04	13.92 $\pm$ 2.61*	13.84 $\pm$ 2.98*

\* The difference between the mean value and the mean value calculated for Twisted PHF was significant,  $p < 0.001$ .

Three morphological types of filament from the 'aged' preparation (see fig. 3.7) were identified, and their widths were measured.

Measurements were performed as described in Section 3.6.3.b.

n = 50 for twisted filaments  
n = 45 for periodically constricted  
n = 36 for straight filaments.

### 3.8 DISCUSSION

PHF in a sucrose density gradient preparation may change or 'age' with the passage of time. The changed PHF may appear twisted, or not twisted; and within these two categories, may show a range of appearances. It is possible that these appearances represent stages in a spectrum of PHF degeneration. However it was not possible to reproduce or identify the mechanism by which these heterogeneous PHF were produced. Other authors have described the appearances of PHF breaking up; unwinding into two separate filaments has been described by Metuzals et al (1984), Gorevic et al (1986); sharp transverse breaks, with short PHF fragments of 30nm in length have been observed by Wischik et al (1985). They have also noted an axial repeat ( $< 5\text{nm}$ ) in twisted filaments. From this they postulated that the filament is composed of short structural subunits and is not an extended fibrous molecule (see section 3.4 Discussion). However, it must be noted that a repeat of this order of size is approaching the limits of resolution of the microscope, and may possibly be artefactual. Longitudinal striations in PHF have been reported by many authors (Wisniewski et al, 1984; Wischik et al 1985). Wisniewski et al (1985) described 8 'protofilaments' seen on negative staining and seen in cross section by ultra thin section. In fact the PHF appear to be polar; 4 longitudinal divisions can be seen at one end of the wide part of the PHF and 3 can be seen at the other.

This has been modelled by Wischik et al (1985) and subsequently reconstructed by using optical diffraction (Crowther et al, 1985).

Straight (15nm) filaments are also seen within tangles (Metuzals et al, 1981) although their relationship to PHF is unknown.

The significance of the observation that 'untwisted; PHF have narrower wide portions, and wider narrow portions than 'classical' PHF is unclear. Computer modelling of this finding may provide some insight. It is possible that these changes in dimensions are related to the appearance of projections along the sides of degenerating PHF. These projections somewhat resemble the collapsed side arms seen on neurofilaments. However, unlike neurofilaments, sidearms are not seen at EM in transversely sectioned PHF. Recently immunohistochemical evidence has suggested that the protein 'tau' is a component of PHF (Brion et al, 1985; Kosik et al, 1986; Grundke-Iqbal et al, 1986). (See section 1.8).

It is possible that the 'projections' noted in this study, represent a re-location of proteins, possibly related to tau which are normally peripherally situated on PHF. This relocation may occur prior to these proteins being lost altogether, resulting eventually in a narrower filament, with concurrent untwisting of the filament, producing the morphological variants of PHF seen in this study.

## PART 3

### SDS POLYACRYLAMIDE GEL ELECTROPHORESIS (SDS-PAGE) AND GEL FILTRATION OF ATD BRAIN HOMOGENATES AND TANGLE PREPARATIONS

#### 3.9 INTRODUCTION AND METHOD

##### 3.9.1 Gel electrophoresis

Many workers have tried to identify PHF protein by SDS-PAGE of ATD brain, and tangle preparations; with inconclusive results (see below). After the observation in part 1 of this chapter, that a large percentage of tangles are soluble in SDS/ $\beta$  Mercaptoethanol, gel electrophoretic studies were performed in order to see if PHF protein could be detected in this manner.

ATD and control brains were repeatedly solubilised, using the following method: 1g each of ATD and control brain was homogenised (20 strokes glass on glass) into 5ml of 1% SDS/0.1%  $\beta$ ME. After incubation at 100°C for 10 minutes the homogenate was centrifuged at 200,000 x g for 2 hours. This procedure was repeated with the pellet, 7 times. Protein was measured by the paper spotting technique. Samples were not dialysed. A 200 $\mu$ l aliquot of each supernatant was reserved and mixed with dissolving buffer, ready for electrophoresis.

SDS-PAGE of tangle fractions produced by SDS sucrose density gradients was performed. These showed no consistent or significant differences from fractions identically prepared using control brains. (Gels from these experiments are not shown in this thesis).



### 3.9.2 Gel filtration

Although PHF were not seen in the final pellet produced by method 3.9.1 (see section 3.10.1), it was still possible that SDS/ $\beta$ ME was failing to completely solubilise the filaments. Therefore, gel filtration was chosen as a technique which could be used easily with protein solubilising agents other than SDS. The aim (as with gel electrophoresis) was to try and breakdown PHF protein and identify the polypeptide subunits. Although the evidence concerning the nature of the polypeptide subunit is conflicting, Iqbal et al (1984) versus Masters et al (1985b), there is no evidence that this subunit is very large. Therefore two gel columns were run initially; one on G-75 superfine sephadex (fig. 3.10b) (separation range 3-70kD) and the other on G-50 superfine sephadex (fig 3.10c) (separation range 1.5-30kD) using formic/acetic acid/water 1:4:45 (v/v/v), and phenol acetic acid/water 1:1:1 (w/v/v), respectively as the eluting solvents. PHF and control brain preparations were run on each column. PHF and control fractions for gel filtration were prepared by SDS discontinuous sucrose density gradient centrifugation (section 5.2.2),

## 3.10 RESULTS AND DISCUSSION

### 3.10.1 Gel electrophoresis (fig. 3.10a)

Gel electrophoresis of the repeat extraction supernatants showed an apparent loss of protein in one of the ATD lanes,

A3. It is possible that the sparing soluble PHF protein accounted for this discrepancy (as identical amount of protein, measured by the Peterson assay, were loaded). Sections of the final pellet (P7) did not show PHF when viewed under electronmicroscopy. The supernatants, A5 and 7 and C5 and 7, showed two protein bands at 62 and 67kDa, only detectable by silver staining. These bands occurred in approximately the same molecular weight range as those seen by Iqbal et al (1984) (62 and 57 kDa). Although Iqbal et al found that the amount of these proteins were much greater in ATD than in control fractions, the uniform nature of the bands seen here (fig. 3.10a) is difficult to explain, and it is possible that these bands are contaminating proteins. Borthwick et al (1985) found a loss of 55kD tubulin in ATD as compared to control brains; this was thought to be correlated to neurone loss in ATD brains, rather than to the presence of tangles. Selkoe et al (1982) found no proteins attributable to PHF in gels of PHF versus control preparations, but found that structurally intact PHF could be seen at the top of the gel.

### **3.10.2 Gel filtration**

Gel filtration, using solvents other than SDS, also showed no features attributable to the presence of PHF, in ATD fractions. Recovery of protein from these columns was found to be 90% on average. Large amounts of protein (in G-75 and G-50) in both ATD and control fractions, were eluted in the void volume. Therefore, results from SDS-PAGE and gel filtration, in concurrence with those of other authors would

suggest that PHF are composed of a protein that is either: not resolved on G-75 to G-25 sephadex and 3-12% PA gels: or is not soluble in any of the solvents used (except TFA at 90°C) or is normally present within whole brain and preparations of ATD and control brain, i.e. is a protein normally present within neurons.

Figure 3.10

a

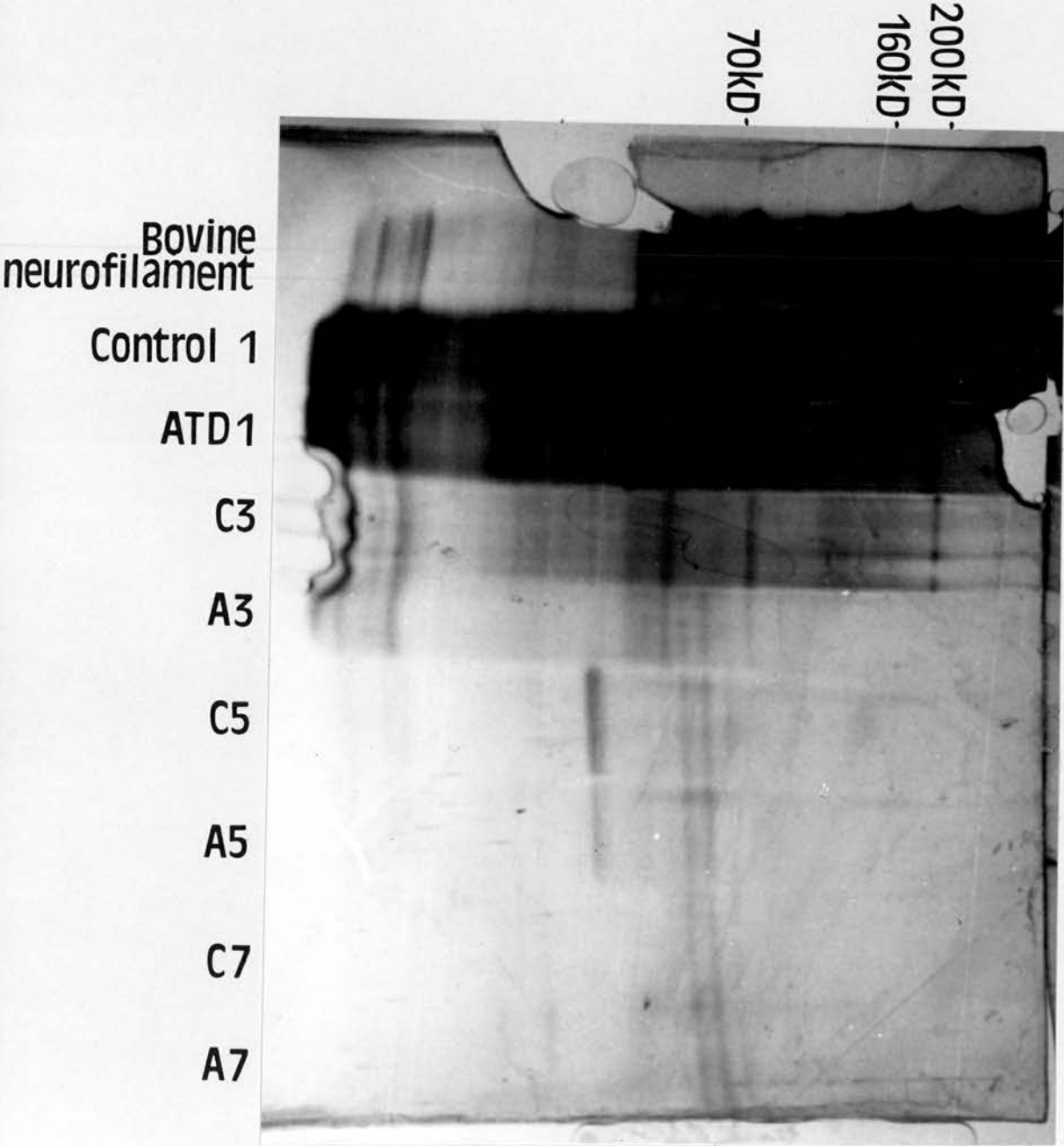


Figure 3.10

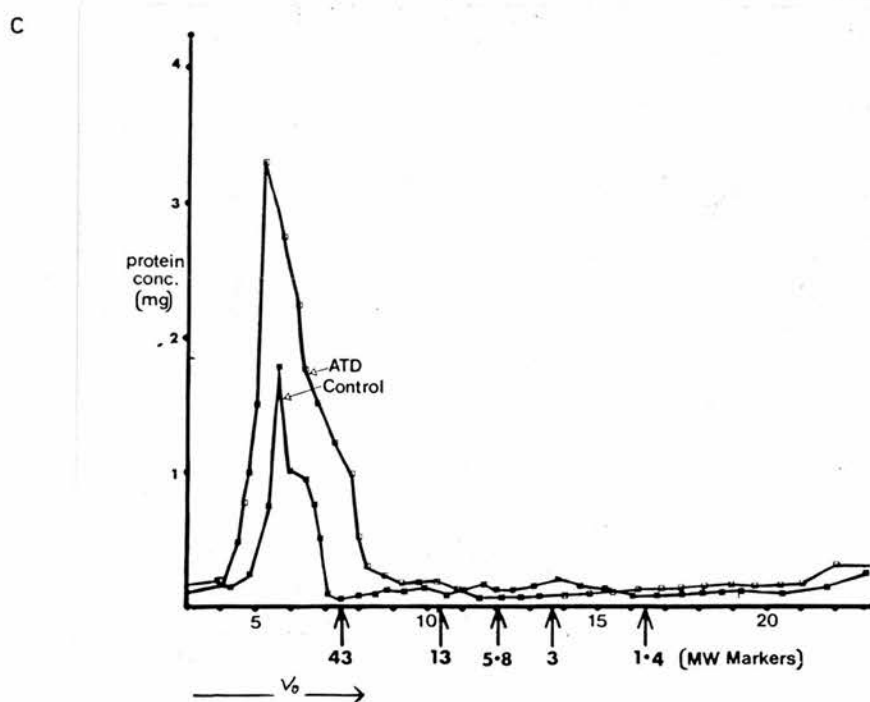
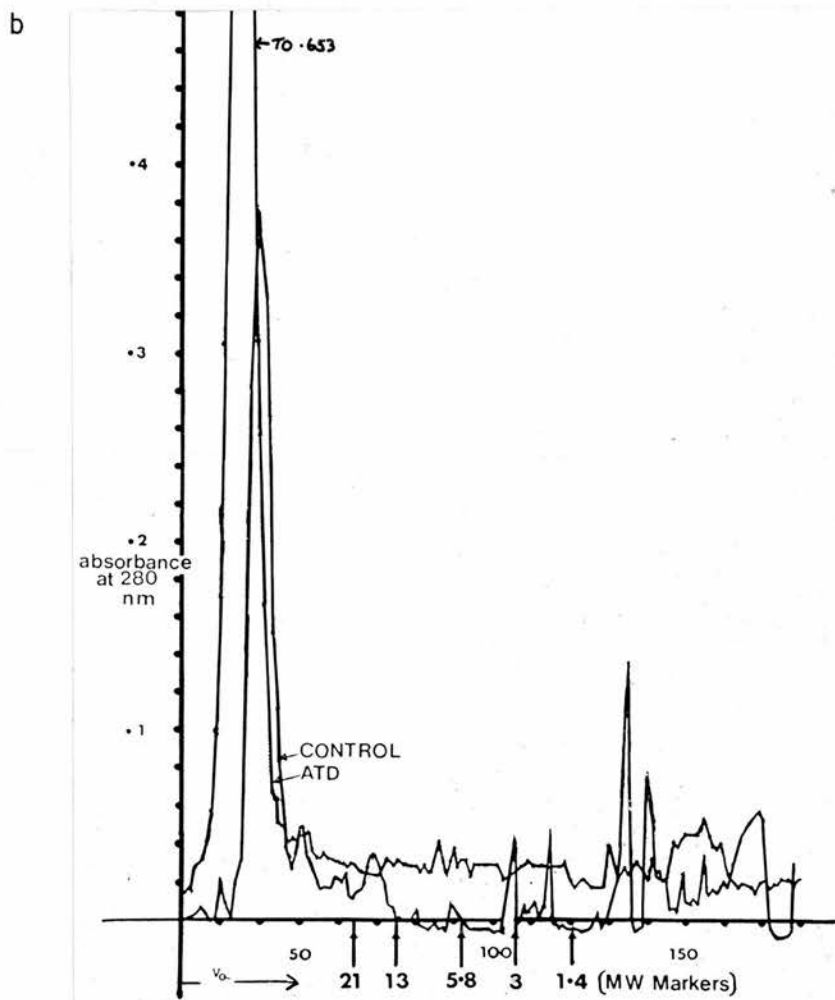


Figure 3.10 SDS PAGE AND GEL FILTRATION OF ATD AND CONTROL BRAIN PREPARATIONS

- a) Gel electrophoresis of repeated SDS/ $\beta$ ME extracted ATD and control brains. (Silver staining). Seven extractions were performed on ATD and control brains (A1-7 and C1-7) respectively. Two protein bands at 62 and 67 kDa are prominent in extractions 5-7, in both ATD and control brains.
- b) Sephadex G-75 superfine gel. A comparison of tangle-enriched and control brain fractions, using formic/acetic acid as the eluting solvent. Protein eluted was measured using absorbance at 280nm.
- c) Sephadex G-50 superfine gel. A comparison of tangle-enriched and control brain fractions, using phenol acetic acid as the eluting solvent. Protein eluted was measured using the protein spotting Coomassie blue binding technique.



CHAPTER 4

FLUORESCENCE ACTIVATED CELL SORTING (FACS) AS A SEPARATION  
METHOD FOR NEUROFIBRILLARY TANGLES

## FLUORESCENCE ACTIVATED CELL SORTING (FACS) AS A SEPARATION METHOD FOR NEUROFIBRILLARY TANGLES.

### 4.1. INTRODUCTION

The observation by Selkoe et al (1982) that PHF were resistant to the denaturing agent Sodium dodecyl sulphate (SDS), enabled the development of separative centrifugation methods, yielding fractions of high purity; due to the dissolution of most other co-sedimenting proteins by the use of SDS in the gradient (Chapter 5, this thesis). However, as shown in Chapter 3, variable proportions of NFT are lost from ATD brain, during treatment with SDS; up to 78.5% in one of the 20 brains studied, (Figure 3.3). It was, therefore, important to devise methods for preparing native tangles; and FACS was considered for use as a preparation method.

During fluorescence activated cell sorting, cells, or cell particles are usually, though not invariably, first fluorescently labelled. They are then analysed and sorted according to the light scattering or fluorescence characteristics they exhibit (see section 2.2.9). A set of experiments was designed to see if tangles could be sorted from other cell particles in this way. The experimental format could be divided into the following sections.

1. Investigation of the fluorescence spectrum of Congo red.

2. Sample preparation and staining with Congo red:
  - (i) Choice of brain tissue
  - (ii) Investigation of staining methods
  - (iii) Preparation of stained sample for FACS
  - (iv) Methods employed to increase the proportion of NFT in the homogenate
  - (v) Microscopy
3. Fluorescence activated cell sorting  
Procedure:
  - (i) Analysis
  - (ii) Sorting parameters
  - (iii) Sorting

#### **4.2. MATERIALS AND METHODS**

##### **4.2.1 Investigation of the fluorescence spectrum of Congo red.**

###### **4.2.1.1 Choice of Congo red as the fluorescent label**

Plaques and tangles can be demonstrated with the same histological stains (Divry et al, 1927). A combination of both selective and intensive staining can be achieved with the histological and fluorescent dye, Congo red; the method was first developed by Bennhold, (1922). Congo red is a diazo dye of the benzidine type and has a strong affinity for amyloid and tangles. It is a sulphonated poly-azo dye, which forms a linear molecule with a chain of conjugated double bonds along its long axis. The polar groups are distributed symmetrically, with the sulphonic acid groups on

one side of the molecule, and amino groups on the other side. Resonance along the chain of conjugated double bonds favours co-planarity of the aromatic ring structures. Hydrogen bond formation with suitable groups, and planarity of the molecule is facilitated by the formation of chelate hydrogen bonds between ortho-amino and azo groups. This enables the elongated Congo red molecule to lie parallel to linear structures. Much work has been done on the use of Congo red as a direct cotton dye binding to cellulose. It has been found that Congo red can form hydrogen bonds between its amino, azo and hydroxyl groups and a substrate molecule. These groups in the dye must be separated at intervals which co-incide with the distribution of reactive groups along the fibre, to permit alignment for hydrogen bond formation. At least two hydrogen bonds are required for substantivity. Congo red seems to bind to the hydroxyl groups of amyloid. This is suggested by experiments on the staining of amyloids in the presence of deaminating, acetylating or oxidising agents (Puchtler et al, 1962). The hydrogen bonding between amyloid and Congo red is highly selective and Congo red probably binds to PHF in the same way. Congo red can also bind non-selectively to many tissue components by the formation of ionic bonds between the sulphonic acid groups of the dye and basic groups in the tissue.

To summarise, Congo red can be bound to tissue by both ionic and hydrogen bonds; Congo red is bound to plaques and tangles by hydrogen bonding. Therefore, to increase the

specificity of the staining, the equilibrium can be shifted in favour of hydrogen bonding by using a high concentration of ions (NaCl) in an ethanolic alkaline dye solution (Bennhold, 1922; Highman, 1946). Pre-treatment of tissue with ethanolic alkaline solutions containing NaCl reveals more sites for covalent bonding, whilst formalin fixation decreases Congo red staining of amyloid probably by binding to the same groups (Puchtler et al, 1962).

Another strongly fluorescent dye, thioflavine T, which also binds to plaques and tangles was considered as a fluorescent label for FACS. It has been recommended by Vassar and Culling (1959), as the fluorochrome of choice for demonstrating amyloid. However, initial experiments on histological sections using both stains, confirmed the findings of Rogers et al (1965), who found thioflavine T to be unselective for amyloid with binding to many other types of tissue. Whereas, using the techniques described above to favour hydrogen bonding, Congo red was seen to be more specific for tangles and plaques than thioflavine T.

#### **4.2.1.2 Investigation of the fluorescence characteristics of Congo Red**

Congo red is a blue/red indicator dye with a bright fluorescence. It has an excitation spectrum in the Ultra Violet/blue range and an emission spectrum in the orange/red range. The excitation and emission spectra of Congo red in solution were investigated using a spectrophotometer. The excitation and emission spectra of Congo red bound to tissue

Figure 4.1

Set Wavelength (Å)	λ of peak measured	Rel. height of peak	Dye solution-C, Red content
Emission. 600	None	-	None (aqueous neutral)
" "	475	0.1	.001 ( " " )
" "	450	0.1	.01 ( " " )
" "	None	-	.1 ( " " )
" "	490	0.2	.001 (aqueous alkaline)
" "	450	0.1	.01 ( " " )
" 575	None	-	.01 ( " " )
" 600	None	-	.1 ( " " )
" 600	None	-	None (80% alcohol/aq. neutral)
" 600	450	1.0	.001 ( " " )
" "	475	0.2	.01 ( " " )
" "	400	0.9	.1 ( " " )
" "	475	0.1	.001 (80% alcohol/aq. alkaline)
" "	460	0.5	.01 ( " " )
" 590	460	.7	.1 ( " " )
Excitation 400	600	1.5	.01 (80% alcohol/aq. alkaline)
" 450	600	1.8	.01 ( " " )
" 500	590	1.6	.01 ( " " )



Figure 4.1 SPECTROPHOTOMETRIC INVESTIGATION OF CONGO RED

The table shows the peak wavelengths of excitation and emission spectra obtained from different solutions of Congo red. Congo red content was varied from 0.001 to 0.1% (w/v) and the solvent was varied with regard to the aqueous/ethanol content and pH. Alkaline solutions were produced by adding NaOH, to pH10. The excitation peak varied between 400 and 490 nm. The emission peak was constant at 590 - 600 nm.

were checked, on Congo red stained brain smears, using a fluorescence microscope and photomultiplier. Congo red solutions were made up, with a range of dye concentration, ethanol concentration and pH. The fluorescence spectrum of each solution was determined using the fluorescence spectrophotometer. The results in fig. 4.1 show that the excitation wave length which produced maximum fluorescence of Congo red varied with alterations in dye concentration, ethanol concentration and pH. Fluorescence was, however, maximal at an emission wavelength of approximately 600nm. Congo red stained brain smears (method of Puchtler et al, 1965) and Congo red stained brain homogenate (method described in Section 2.2.9) were viewed with the fluorescence microscope. Various filter combinations were tried using excitation filters with maximum wavelengths ranging between 375nm and 500nm, and barrier (emission) filters allowing the passage of wavelengths ranging from > 450 nm to > 550 nm. It was found that plaques and tangles were viewed optimally using an excitation filter BP450 - 490 (Zeiss). The barrier filter used was less critical, the LP515 (Zeiss) giving good results.

As a result of these findings, the FACS laser was used with a barrier (emission) filter of 515 nm, and excitation wavelengths of 480, 457.9 or 370 nm. The production of suitable excitation wavelength by the argon laser, was limited to these three values.

#### **4.2.2 Sample preparation and staining with Congo Red**

##### **4.2.2.1 Choice of brain tissue**

Grey matter was dissected from the left temporal cortex of a frozen half brain from a case of ATD (no. 20), containing 314 tangles and 22 amyloid core plaques per mg tissue (mean value) i.e. tangle to plaque ratio = 14.3:1 Clinical data, on brain no. 20 has been previously documented in Chapter 3.

##### **4.2.2.2. Investigation of staining methods**

Methods described in the literature for staining tissue sections with Congo red proved unsuitable for staining homogenates. Different experimental staining methods were, therefore, applied to the brain homogenates with the aim of improving the specificity of the Congo red stain for plaques and tangles.

Four staining methods, which yielded four labelled brain suspensions, were investigated. Three of these methods used counterstains plus Congo red, (a); and one method used Congo red and a differentiating solution (b). The aim of the staining methods was to produce a tissue suspension containing plaques and tangles labelled with Congo red, with minimal background staining. For each of the four methods, the duration of counterstaining and differentiation was optimised. This was done by staining, and counterstaining or differentiating a sample of brain homogenate for a fixed time period; then, removing portions at selected intervals and making slides of these portions. The slides were then compared microscopically, with regard to the selectivity of tangle staining obtained.

**(a) Counterstaining methods:**

These experiments were carried out with each of the three counterstains; toluidine blue (1%) methylene blue (0.1%) and alum haematoxylin.

Approximately 0.25g of ATD grey matter was homogenised in 10 volumes of phosphate buffered saline (PBS), then washed, by dispersal in 10 volumes of distilled water, and centrifuged. The pellet was dispersed in 5 volumes of counterstain. Portions of this homogenate were removed at time zero, and at minute intervals for 10 minutes, centrifuged, and the pellet immediately washed by dispersal in 10 volumes of distilled water. After two washings, each portion was stained with 0.1% aqueous Congo red for 5 minutes, centrifuged, washed, dehydrated and mounted for viewing by light and fluorescence microscopy. Each 0 - 10 minute counterstaining procedure was repeated a further five times, in which the period of Congo red staining was extended to 10, 15, 30, 45 and 60 minutes. All slides were examined, and for each counterstain, the best combination of staining times was noted and subsequently used.

All centrifugations were carried out at 8000 x g for 5 minutes in an Eppendorf centrifuge. All washings involved redispersal of pellets, using a fine glass pipette. Dispersal of the pellets into stain, was carried out using 10 strokes in a glass on glass homogeniser.

After staining, a small portion of each pellet was smeared on to a slide, dehydrated through ethanol, cleared in xylene, and mounted in DPX. The remaining portion of the pellet was prepared for FACS as described in Section 4.2.2.3.

### Congo Red and Toluidine Blue

Solutions Toluidine Blue 1% aqueous,  
Congo red 0.1% aqueous, pH10 (with NaOH)

- Technique
1. Centrifuge homogenate, wash pellet in water. Centrifuge.
  2. Disperse pellet in toluidine blue for 3 minutes.
  3. Wash twice in water.
  4. Disperse pellet in about 10 vol Congo red for 45 minutes.
  5. Centrifuge, wash twice in water. Centrifuge.

### Congo Red and Methylene Blue

Solutions: Methylene blue 0.1% aqueous, red 0.1% aqueous, pH10 (with NaOH).

- Technique:
1. Centrifuge homogenate, wash pellet in water. Centrifuge.
  2. Disperse pellet in methylene blue for 3 minutes 15 seconds.
  3. Wash twice in water.
  4. Disperse pellet in about 20 vol Congo red for 20 minutes.
  5. Rehomogenise (10 strokes) and leave for a further 10 minutes.
  6. Centrifuge, wash twice in water. Centrifuge.

### Congo Red and Haematoxylin

Solutions: Haematoxylin (Harris's solution)  
Congo Red 0.1 aqueous, pH10 (with NaOH)

- Technique:
1. Centrifuge homogenate, wash pellet in water. Centrifuge.
  2. Disperse pellet in Haematoxylin.
  3. Centrifuge immediately.

4. Differentiate in 0.5% lithium carbonate for 2 min.
5. Disperse in about 20 vol. Congo red for 30 minutes.
6. Centrifuge, wash twice in water. Centrifuge.

It was difficult to achieve reproducibility of staining by the above methods in which two stains were employed, i.e. Congo red and a counterstain. Therefore a method using Congo red alone with a differentiation procedure, was devised.

(b) Congo red stain with alkaline differentiation:

Highman (1946) adapted Bennhold's (1922) Congo red staining method, using potassium hydroxide in 80% ethanol as the differentiating solution. Puchtler et al (1962) developed a staining method which involved pretreatment of the section with acid/ethanol solution, then with alkaline/ethanol solution containing a high concentration of salt.

None of these methods was suitable for the purposes of FACS, as alcohol could not be used when staining a homogenate, because the tissue particles formed an aggregate which could not be redispersed for analysis by FACS. Ethanol was therefore omitted from the differentiating solution. Despite the absence of ethanol, the weak alkaline high salt solution used as a differentiator in the following method, favoured selective staining of tangles and plaques.

Solutions: Stain Congo red 0.5% aqueous containing 1% w/v NaCl, pH 9 (with NaOH).

Differentiator 0.01M NaOH



Buffer	1% w/v NaCl, 50mM Na <sub>2</sub> HPO <sub>4</sub> (PBS); pH9
Technique:	<ol style="list-style-type: none"><li>1. Homogenise brain in 10 vols Congo red. Leave 10 minutes.</li><li>2. Centrifuge. Wash twice in water.</li><li>3. Congo red staining of the pellet was differentiated by dispersing in 0.01M NaOH (10vol) for approximately 1 minute until background staining was minimal and tangles selectively stained, as viewed by light-fluorescence and crossed polarisation.</li><li>4. Centrifuge wash in buffer.</li><li>5. Centrifuge.</li></ol>

#### 4.2.2.3 Preparation of sample for FACS: basic method

In order to produce a tissue suspension suitable for FACS, the pellet produced by one of the four staining methods described in 4.2.2.2, was washed by dispersal in approximately 20 volumes of PBS. This was centrifuged at 8000 x g for 5 minutes. The resulting pellet was then resuspended in PBS by homogenisation, filtered through 60µm nylon mesh, and diluted to between 1 and 5 million particles/ml, as estimated approximately, using a haemocytometer. A portion of the suspension was viewed by light, polarising, and fluorescence microscopy to check the selectivity of staining. The sample was frozen in small aliquots at -40°C to prevent dissociation of dye from tissue particles. Immediately before sorting, the sample was thawed on ice, and gently dispersed using 5 strokes of a glass on glass homogeniser.

#### **4.2.2.4 Methods employed to increase the proportion of tangles and plaques in sample before sorting**

The following 'pretreatments' were tested on the initial homogenates, in an attempt to increase the ratio of tangles and plaques to background tissue, present in the sample before preparation for fluorescence activated sorting. After the pretreatment, the sample was stained and processed for FACS according to methods of 4.2.2.2(b) and 4.2.2.3.

i) Fixation - Finely chopped grey matter was fixed for 24-28 hours in 0.5% glutaraldehyde/2% paraformaldehyde. 25-500 mg of this fixed brain tissue was washed twice in PBS then homogenised and processed for FACS.

ii) Alkaline pre-treatment - Plaques and tangles have been shown to be partially insoluble in 0.2M NaOH (Chapter 3, this thesis). The brain tissue used for FACS (brain no. 20) showed that 49% of tangles were insoluble in 0.2 M NaOH. For the purposes of FACS, a further solubility experiment was carried out on this brain; the procedure being identical to that described in section 3.2, with the exception that 0.025M NaOH instead of 0.2M NaOH, was used as the solubilising agent. 96% of tangles in this brain were found to be insoluble in 0.025 M NaOH. Therefore, the latter could be used to selectively solubilise other tissue in the homogenate less resistant than tangles to alkaline treatment. Grey matter was homogenised in approximately 5 volumes of 0.025M NaOH, and was incubated at room temperature for one minute, before staining and processing for FACS.

iii) Pepsin digestion - According to Bancroft (1975), amyloid is resistant to protease digestion, compared to other tissue components. Therefore, a pepsin digest was carried out using a modification of Bancroft's methods for the demonstration of amyloid. 100mg of pepsin (EC.3.4.23.1, 1:2500, Sigma Chem. Co) was dissolved in 20ml 0.02M HCl, 250-500mg brain tissue was homogenised in 10 volumes of this solution and incubated overnight at 37°C.

#### **4.2.2.5 Microscopy**

Before fluorescent sorting, samples were examined microscopically using i) crossed polarisation microscopy for the presence of plaques and tangles; ii) light microscopy and iii) fluorescence microscopy to check the selectivity of staining. After sorting, fractions were restrained with Congo red, and checked for the presence of tangles and plaques using crossed polarisation microscopy. See Fig. 4.2.

#### **4.2.3 Fluorescence Activated Cell Sorting procedure**

The principle of FACS is described in section 2.2.10. Briefly, it involves the sorting of cells or tissue particles on the basis of their fluorescence and/or light scattering properties. The sorting procedure can be divided into 3 stages: i) analysis of sample, and identification of cells or subcellular particles, ii) choice of sorting parameters, iii) sorting.

This three stage procedure was carried out for each of eleven experiments, in which aspects of the staining and sorting methods were varied, one at a time, in order to determine the optimal tangle sorting protocol.

#### **4.2.3.1 Analysis (fig. 4.4)**

This was carried out as described in Section 2.2.10. Samples were initially assessed for fluorescence using light scatter as the trigger. This showed the fluorescence profile of the whole sample. With trigger on fluorescence the dot plot of the number of particles vs. fluorescence was examined for a peak or shoulder corresponding to more highly fluorescent particles namely tangles and plaques. The dot plot of the number of particles vs. forward-angle light scatter was examined, enumerated per channel and printed out. This dot plot was compared with the print-out of an analysis of a solution containing 1.5 $\mu$ m diameter fluorescent beads which gave peaks corresponding to 1.5, 3 and 6 $\mu$ m. However, for the reasons described in section 2.2.10, this technique provided only an approximate estimate of the size of the sorted particles.

#### **4.2.3.2 Sorting parameters**

For each experiment, the sorting parameters were chosen on the basis of the initial analysis. The peak or shoulder of highly fluorescent particles, if present on analysis, was collected, see fig. 4.4. In later sorts only larger particles were collected (channels 30-255). A comparison fraction of low fluorescence particles, of an equal size to that of the tangle fraction was also collected in experiments 10 and 11.

#### **4.2.3.3 Sorting**

Fractions were thawed in aliquots of 0.5 ml and kept on ice during sorting. The latter was performed at a rate approximately between 100 and 300 particles per second.

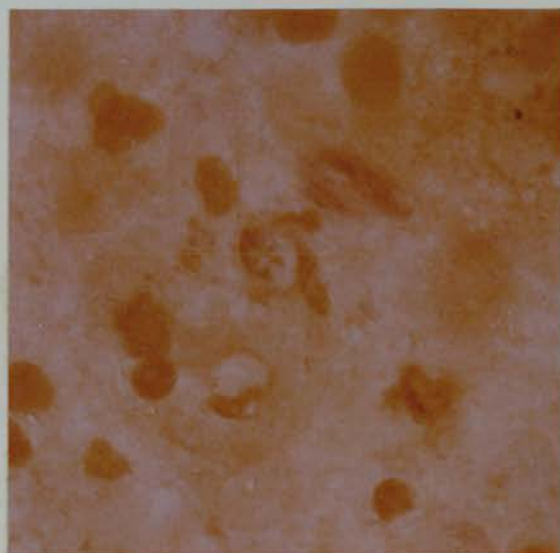
#### **4.2.4 Investigation of the effect of autofluorescence and non-specific staining**

After the sorting technique and parameters had been established an experiment to assess the contribution of autofluorescence, and the contribution of non-selective (i.e. non-tangle or plaque) staining by Congo red was performed. Three tissue suspensions were prepared for FACS: unstained ATD brain, ATD brain stained as described in Section 4.2.2.2.b; and control brain (normal non-ATD brain) stained in a similar fashion. The differentiation step on the control brain was performed by having previously noted the exact time required to differentiate the ATD brain, then incubating the control brain in differentiating solution for the same time period. The stained ATD brain suspension was subjected to analysis as described in section 4.2.3.1, and the channels for sorting selected. Then all three tissue suspensions were sorted under identical conditions, using FACS. This enabled a comparison to be made between the numbers of particles sorted into the 'tangle' and 'comparison' fractions in the three different tissue suspensions. The results of this procedure show that in the first run of experiment 11 (figure 4.5) which provided the photos in fig, 4.2, 18.1% of particles sorted in the stained ATD brain arrived in the 'tangle fraction', whereas, 7.9% and 4.9% of particles sorted arrived in the tangle fractions of the stained control brain and unstained ATD brain, respectively. Therefore, this showed that autofluorescence and non-specific staining was contributing to particles



Figure 4.2

a



b



c



d

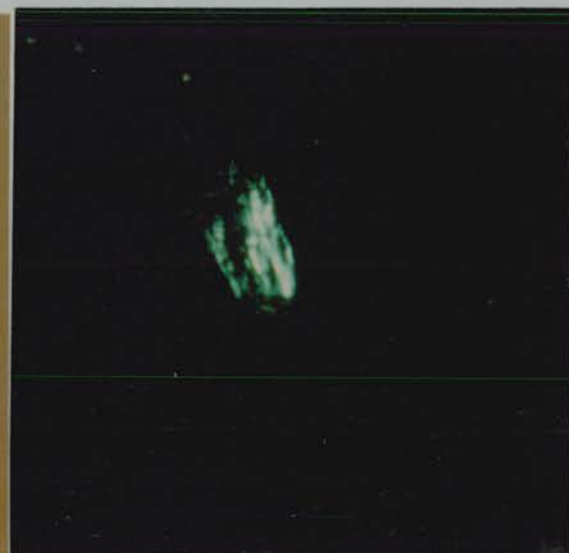
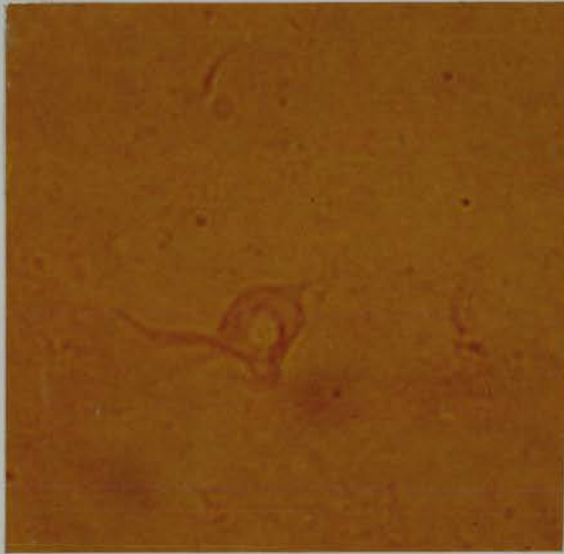


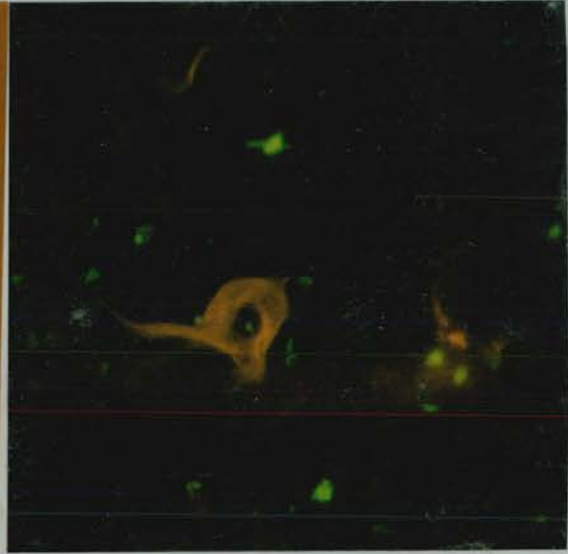


Figure 4.2

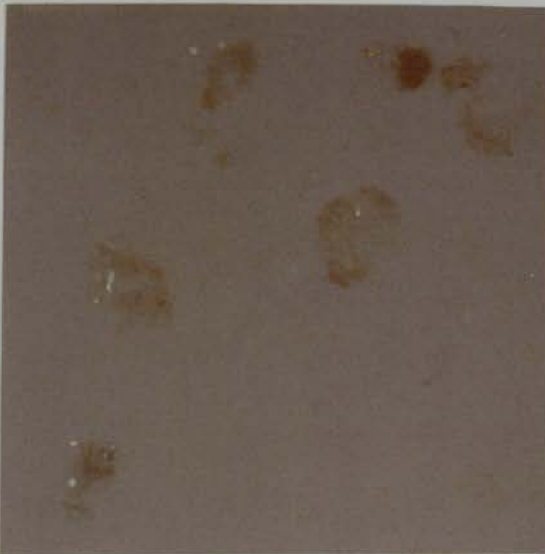
e



f



g



h

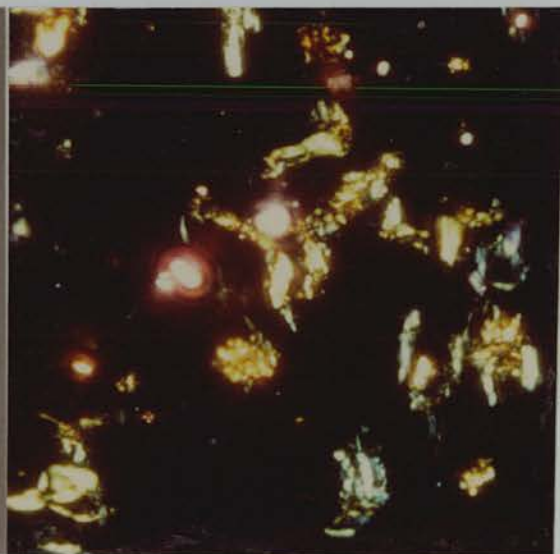


Figure 4.2 PHOTOMICROGRAPHS OF AN ATD BRAIN PREPARATION  
BEFORE AND AFTER FACS SORTING

Before Sorting:

- (a) and (b) Stained homogenate of ATD brain before differentiation of Congo red staining by 0.01 M NaOH. The same field viewed by (a) light microscopy and (b) crossed polarisation microscopy.
- (c) (d) (e) and (f) Sample prepared for FACS as described in Section 4.2.2.3: Stained dispersed pellet from ATD brain homogenate after differentiation of Congo red staining by 0.01M NaOH showing selective staining of tangles by Congo red.
- (One field viewed by (c) light microscopy and (d) crossed polarisation microscopy).
- (Another field viewed by (e) light microscopy and (f) fluorescence microscopy).

After Sorting:

- (g) Low fluorescence, larger sized particles (comparison fraction,  $\delta$ , in Fig 4.4.c) viewed under crossed polarisation microscopy, showing non-birefringent particles.
- (h) High fluorescence, larger sized particles (tangle fraction,  $\gamma$ , in Fig. 4.4.c) viewed under crossed polarisation microscopy, showing green birefringent tangles.

Magnification x 620.

sorted in the tangle fraction though this contribution was less than half of the fraction. None of the particles in the 'tangle' fraction collected from the control brain were plaques or tangles. A few of these particles could be identified as pieces of connective tissue. In the sorted samples of the unstained ATD brain, plaques and tangles were present in the 'tangle' and 'comparison' fractions in approximately the same proportions.

#### 4.3. RESULTS AND DISCUSSION

In the series of experiments described here (1-11) Fig. 4.3, using different combinations of sample preparation, staining, analysis and sorting techniques, resulted in a final method (11) which yielded a fraction rich in tangles and plaques.

##### 4.3.1 Comments on figure 4.3

Experiment 3 showed that Congo red staining was more intense in unfixed homogenates, than in homogenates which had been fixed overnight in 10% formalin, (experiments 1 and 2). This observation is in accord with the report (Puchtler et al, 1962), that formalin binds to amyloid, excluding the dye Congo red. Counter staining of the Congo red stained suspensions with toluidine blue, methylene blue or haematoxylin, yielded few birefringent particles in the collected 'tangle' fraction. Whereas, the Congo red alkaline differentiation method, produced more intense, more selective, and more reproducible staining, (experiments 6-11). The introduction of a larger pore

Figure 4.3

Development of method for separation of tangles from ATD and Down's syndrome brain using FACS

EXPERIMENT NO.	TREATMENT OF HOMOGENATE	STAIN [Congo Red = CR].	PARTICLE FILTER SIZE (μm)	GATE ON SCATTER	EXCITATION WAVELENGTH (nm) [BARRIER FILTER = 515nm]	DESCRIPTION OF FRACTIONS COLLECTED		
						TANGLE FRACTION (γ)	COMPARISON FRACTION (δ)	
1.	Fixed	CR <sup>+</sup> Counterstain	20	NO	480	+	+	not collected
2.	Fixed	CR <sup>+</sup> Counterstain	20	NO	457.9	+	+	not collected
3.	None	CR <sup>+</sup> Counterstain	20	NO	457.9	+	++	not collected
4.	Pepsin digest	CR <sup>+</sup> Counterstain	20	NO	457.9	++	+	not collected
5.	Pepsin digest	CR <sup>+</sup> counterstain	20	NO	370	±	±	not collected
6.	None	CR <sup>+</sup> differentiation	20	NO	370	+	++	not collected
7.	None	CR <sup>+</sup> differentiation	60	NO	370	±	+	not collected
8.	Pepsin digest	CR <sup>+</sup> differentiation	60	YES	370	++	++	not collected
9.	Pepsin digest	CR <sup>+</sup> differentiation	60	YES	457.9	+++	+	not collected
10.	Alkaline	CR <sup>+</sup> differentiation	60	YES	457.9	+++	+	±
11.	None	CR <sup>+</sup> differentiation	60	YES	457.9	+++	+	±

\* Bir. = birefringent particles, Non-Bir. = non-birefringent particles.

Figure 4.3 THE DEVELOPMENT OF A METHOD FOR THE SEPARATION OF TANGLES FROM ATD AND DOWN'S SYNDROME BRAIN USING FACS.

The table shows the sequence of experiments in which the variables of: pre-treatment, staining, filter size, gates and exciting wavelength were altered in order to arrive at the optimum conditions for FACS. These conditions were achieved in experiments 10 and 11.

Tangle fractions were assessed using crossed polarisation microscopy. They were graded with regard to the numbers of tangles and plaques (birefringent) and other particles (non-birefringent) present, on a semiquantitative scale of +, ++, +++ (+ = very few; +++ = numerous).

filter (experiment 7) enabled larger tangles to pass through the filter prior to sorting and collection in the tangle fraction. In experiments 8-11, in which gates on forward angle light scatter were inserted in addition to gates selecting for fluorescence, very small fluorescent particles were not collected. This improved sorting efficiency by concentrating on particles in the appropriate size range. Prior experiments, using a fluorescence spectrophotometer showed the maximum excitation wavelength of Congo red to vary between 400 and 500 nm. Using a fluorescence microscope, Congo red stained, tangles and plaques were best viewed with an excitation wavelength between 390 and 440 nm. When FACS sorting was performed using the nearest wavelength to this, obtainable from the laser (457.9nm) results were good. The use of an excitation beam of 480 nm produced less good results. Pretreatment of the homogenate with pepsin or 0.025 M NaOH increased the proportion of tangles and plaques relative to other tissue particles before sorting. However the incubation of the homogenate in 0.01M NaOH during the stain differentiating procedure could be expected to have a similar, though lesser effect.

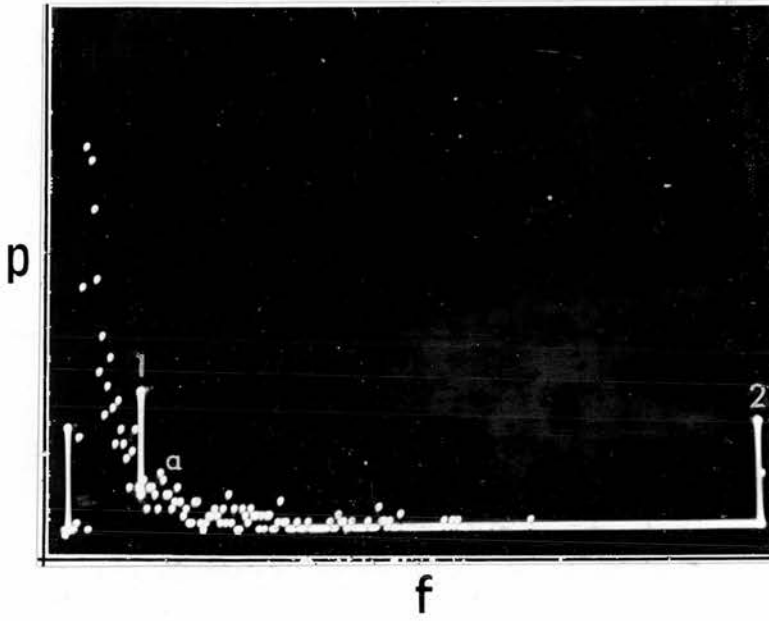
Thus these studies showed that the optimal conditions were those used in experiments 10 and 11. These were:

- (i) Pepsin or alkali pre-treatment of sample. (Not critical: may be omitted).
- (ii) Congo red staining alone, with aqueous alkaline differentiation.
- (iii) Use of 60 $\mu$ m filter before sorting.
- (iv) Use of 457.9nm as the exciting wavelength.
- (v) Use of a 'scatter gate' to eliminate very small particles (in addition to the gate on fluorescence).



Figure 4.4

a



b

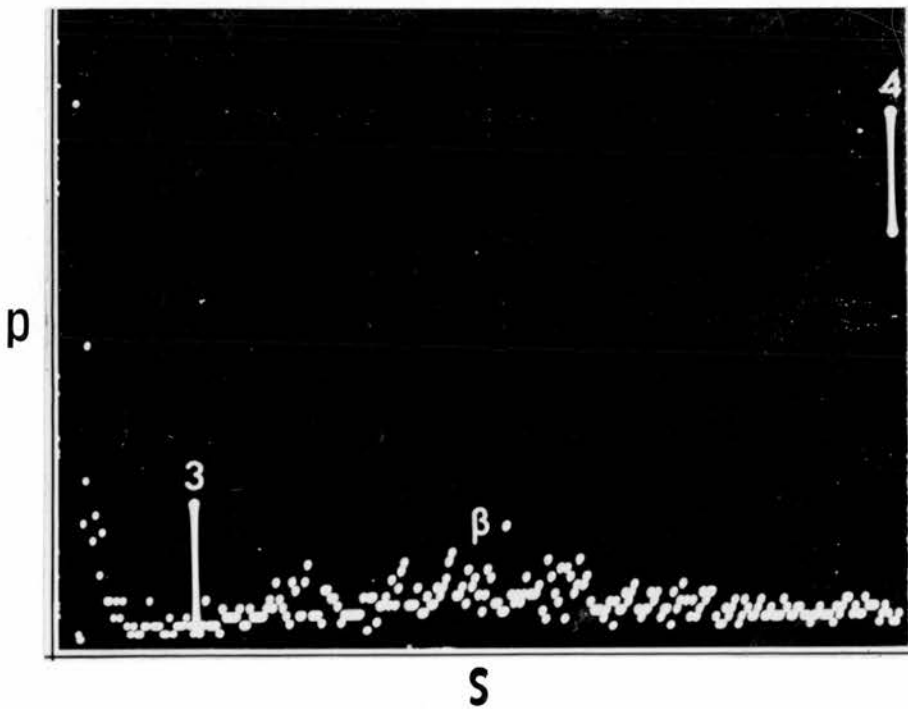
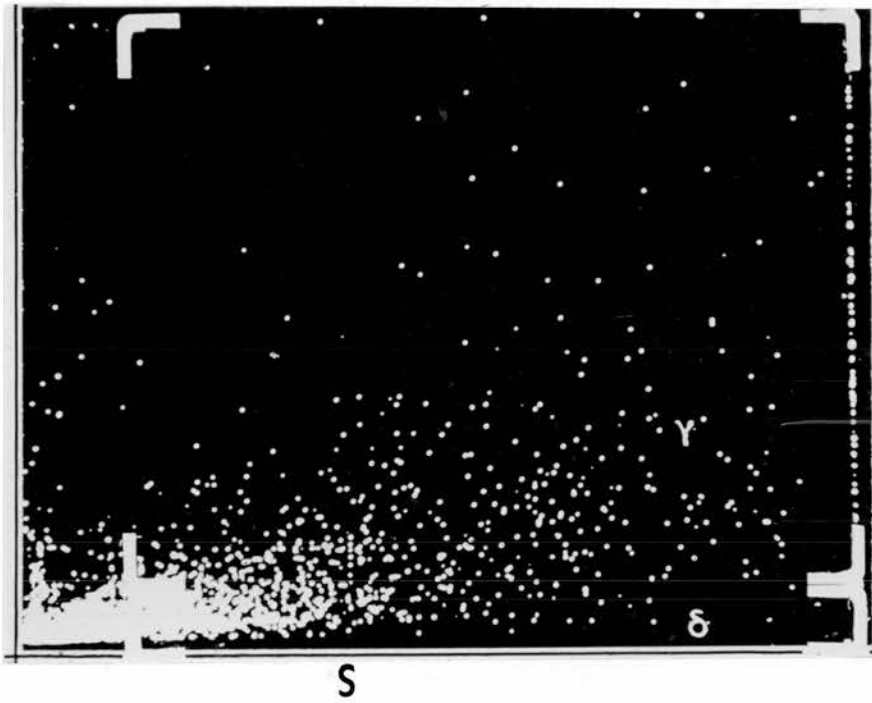


Figure 4.4

c

f



d

p

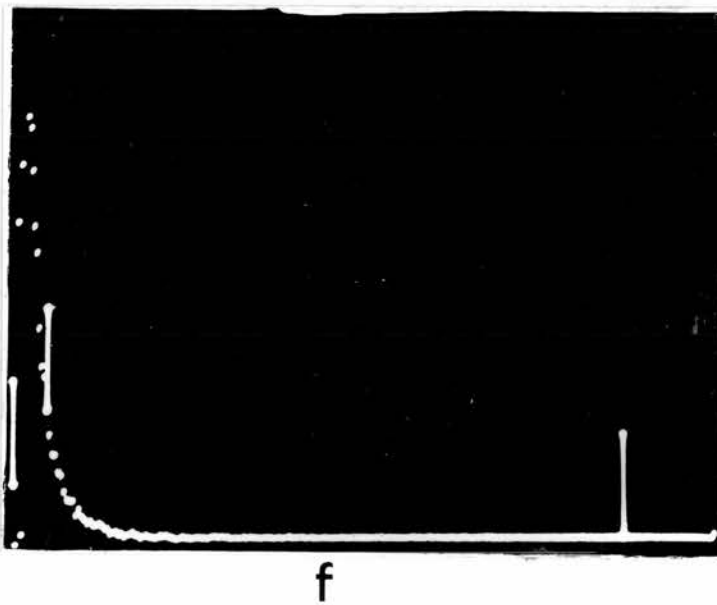


Figure 4.4 DOT PLOTS OBTAINED FROM THE FACS CONSOLE.

- (a) Stained ATD brains, experiment 11. Number of particles (p) vs. fluorescence intensity (f). Small peak (a) indicates minor population of more highly fluorescent particles. Lines 1 and 2 represent gates, particles within these gates were collected.
- (b) Stained ATD brain; experiment 11. Number of particles (p) vs. forward-angle light scatter (s), with lazer focused on fluorescence. Gates were set at approximately  $6\mu\text{m}$  (line 3) and  $60\mu\text{m}$  (line 4) to collect fraction.
- (c) Stained ATD brain, experiment 11. Forward-angle light scatter (S) vs. fluorescence intensity (f). The two sets of gates (Fig. 4.4a 1 and 2; Fig. 4.4.b, 3 and 4) which formed a window encompassing large highly fluorescent particles which were collected as the tangle fraction,  $\gamma$ . Another window was inserted to collect a fraction consisting of particles of similar size but lower fluorescence intensity (the comparison fraction,  $\delta$ ).
- (d) Stained control brain. Number of particles (p) vs. fluorescence intensity (f). cf. with Fig. 4.4a.

Figure 4.5 FACS ANALYSIS OF SAMPLES

Brain Sample	No. of particles in channels 1-6*	No. of particles in channels 6-255	No. of particles in channels 6-255 as a % of total no. of particles sorted
Unstained	a) 23979	1232	4.9
Alzheimer	b) 25632	1152	4.3
	c) 23295	1278	5.2
Stained	a) 24772	2068	7.7
Control	b) 25470	2215	8.0
	c) 22943	2104	8.4
Stained	a) 22695	5017	18.1
Alzheimer	b) 20756	5060	19.6
	c) 18250	5732	23.9

Counts shown above are from 3 FACS sorts performed under the conditions described in experiment 11 (Fig. 4.3).

Channels 6-255 are collecting the more highly fluorescent particles.

The numbers of particles in channels 6-255 as a percentage of the total numbers of particles sorted, are highest in the stained Alzheimer samples.

a) shows the counts from the first run of experiment 11, photomicrographs and dot plots of which are displayed in fig. 4.2 and 4.4 respectively. b) and c) show counts from repeat runs of experiment 11, using separately stained samples of the SAME brains. The small variations seen here in the results can be attributed to the subjective nature of the assessment of intensity of staining, prior to FAC sorting.

Other factors tested hindered the sorting, and were avoided:

(i) The use of ethanol as a staining or differentiating medium - this produces irreversible clumping of the particles.

(ii) Use of a counterstain.

(iii) Fixation of sample.

Taking these factors into consideration, it is possible to produce a very good result. Yet the technique could still be much improved and it is important to consider the problems encountered in the method, some of which have been overcome, whilst others remain (see section 4.3.3).

#### **4.3.2 Assessment of sorted fraction in final experiment.**

(fig. 4.3, no.11)

The total number of particles sorted in the first minute of experiment no. 11 was 380,000 consisting of 150,000 particles in the tangle fraction ( $\gamma$ ) and 230,000 in the comparison fraction ( $\delta$ ). The number of particles below channel 30 in the waste fraction was 1,184,749. Two repeat runs of experiment 11, using the same brain, showed these counts to be fairly reproducible (fig. 4.5).

Centrifugation of the tangle and comparison fractions produced by FACS, resulted in tiny pellets (approximately 0.25mg wt) which were restained and viewed under crossed polarisation microscopy. The comparison fraction contained amorphous material (unidentifiable cell fragments) with very few birefringent particles (Fig. 4.2g). The tangle fraction contained a large proportion of birefringent to non-birefringent particles compared with the original tissue

homogenate (Fig. 4.2h compared with Fig. 4.2a & b). These birefringent particles consisted largely of tangles with a few plaque cores, the latter estimated at 20-30% of the fraction. A sample of Down's brain containing tangles processed and sorted in the same way, also yielded a tangle-rich fraction.

#### **4.3.3. Unresolved problems encountered during staining and sorting**

##### **(i) Congo red stain:**

Congo red is not an absolutely specific stain for tangles and plaques. This may explain why Congo red did not produce a sharp peak on the scatter grams, which would be indicative of a distinct population of fluorescent particles. It was, therefore, difficult to decide exactly where to sort. Although aqueous Congo red staining with alkaline differentiation produced selective and reproducible staining, due to assessment of the staining being subjective, it was not possible to achieve exact reproducibility of stain intensity. This necessitated the determination of fluorescence sorting parameters, on the basis of analysis, for each stained sample. Also some non-specific staining of tissue still occurred, as shown by the collection of a significant number of particles in the 'tangle fraction' of the control brain sample (fig. 4.5).

##### **(ii) Sample**

In the use of FACS as a separation method for tangles, tangle-rich brain tissue was a pre-requisite. With tissue



poor in tangles, there were insufficient numbers to show up clearly as a sub-population on analysis.

Plaques and tangles in the tissue suspension were found to have a wide size range, approximately between 5 and 40 $\mu$ m. Although very small particles could be excluded using a gate on light scatter, the wide size range meant that plaques and tangles did not appear as discrete population on forward angle light scatter dotplots (fig. 4.4.).

#### (iii) FACS machine

During FACS, it would have been preferable to excite at a number of intermediate wavelengths between 370, 457.9 and 480, but this was not possible using the argon laser. In addition, the laser generated only 0.2 watts at the wavelength (457.9nm) used during these sorting experiments. When compared with the 100 watt mercury source of the fluorescence microscope this seems weak. However, the FACS and the fluorescence microscope are not directly comparable, as in the latter 100 watts produces the entire spectrum; whereas the laser in the former instrument produces a single wavelength. Though, results may be improved by using a more powerful laser.

#### 4.4 DISCUSSION

Despite the problems encountered above, the final method enabled preparation of a fraction enriched in neurofibrillary tangles from Alzheimer and Down's brain

without the use of strong surface-active agents. Contamination with amyloid core plaques was minimised by using brain tissue which contained many tangles and fewer plaques. The described FACS method yielded a useful tangle fraction, of at least 1 mg, after 16 hours sorting. As a preparation method it had two advantages over other published methods. Firstly, it could be used on very small amounts of material in comparison to the methods of Selkoe et al (1983) and Iqbal et al (1984) in which it is necessary to use between 40 and 60 grams of tissue. The non-denaturing PHF preparation method of Selkoe et al (1982) although using only 2 g of tissue is less efficient in that tangles are discarded in the pellet produced by the initial centrifugation (Chapter 5, this thesis) and only free PHF are retained for purification. As SDS solubilised a percentage of tangles and alters PHF ultrastructure (Chapter 3, this thesis); future biochemical and structural investigations of PHF will be facilitated by the use of non-denaturing preparation methods.

CHAPTER 5

THE PREPARATION OF NEUROFIBRILLARY TANGLES (NFT) BY DENSITY  
GRADIENT CENTRIFUGATION TECHNIQUES

## THE PREPARATION OF NEUROFIBRILLARY TANGLES (NFT) BY DENSITY GRADIENT CENTRIFUGATION TECHNIQUES

### 5.1 INTRODUCTION

#### 5.1.1. Centrifugation theory

The Sedimentation rate ( $v$ ) of a sphere in a centrifugal field, can be expressed as:

$$v = \frac{d^2 (\rho_p - \rho_i) \times g}{18n} \quad \text{(Svedberg equation)}$$

where:

$d$  = diameter of sphere

$\rho_p$  = density of sphere

$\rho_i$  = liquid density of medium

$n$  = viscosity of medium

$g$  = centrifugal force

This has been exploited, in both analytical and preparative ultracentrifugation for the analysis and preparation of biological substances.

Density gradient centrifugation in the preparative centrifuge can be divided into three categories:

1. Stabilised moving boundary centrifugation which is analogous to classical ultra-centrifugation experiments aimed at determining the sedimentation coefficient.

2. Zone centrifugation in which particles with different sedimentation rates are completely separated. Each substance with a different sedimentation rate, will form a band or zone in the gradient. These zones are separated by distances related to the sedimentation rates of the substances.
3. Isopycnic gradient centrifugation. With this method separation is based on the differing densities of the substances undergoing centrifugation. The gradient column should encompass the density range of all particles being separated, and sedimentation should be of sufficient force and time, that particles reach the position at which the density of the surrounding gradient media is equal to their own.

This last method is a commonly used technique for subcellular fractionation, and has been used as the main basis for the preparative experiments described in this chapter.

#### **5.1.2. The use of density gradient centrifugations as a preparation method for intermediate filaments and PHF**

The intermediate filaments, neurofilaments and the larger microtubules, are found in abundance in neurones (see section 1:12). Neurofilaments can be prepared in a very pure form by density gradient centrifugation (Carden et al, 1983), whereas microtubules are best prepared by repeated polymerisation and depolymerisation cycles (Shelanski et al, 1973). Other methods of preparing neurofilaments make use of the low density of myelin sheath by using axonal flotation, (Yen et al, 1976) though the preparation obtained in this way is less pure.

An early published preparation method for PHF (Selkoe et al, 1982) was based on a neurofilament preparation method, and included incubation with Triton X-100, with centrifugation conditions similar to those used in the preparation of neurofilaments. In the same publication the authors noted the resistance of PHF to denaturing agents, particularly SDS (see Section 1:11). Subsequent preparation methods using centrifugation can be divided into those in which SDS was used during the procedure to increase purity, and, non-denaturing methods in which SDS was not used. Methods in which SDS was used, resulted in purer preparations than methods in which SDS was omitted. This chapter describes studies on the use of discontinuous and continuous sucrose density gradient centrifugation, and the self forming gradient material Percoll as a continuous density gradient medium, for the separation of tangles from human brain tissue.

#### 5.1.3 Percoll, a continuous self-forming gradient medium

Percoll is a silica colloid self-forming gradient medium. It has a low viscosity and exerts no osmotic effect on tissue particles. When a solution of Percoll in 0.15 M NaCl or 0.25M sucrose is centrifuged at  $>10,000 \times g$  or  $25,000 \times g$  respectively, in an angle head rotor, the particles begin to sediment. The resulting uneven distribution of particles forms a density gradient. The polydisperse nature of the colloid means that the gradient is very smooth because of the different sedimentation rates of the particles. The gradient is sigmoid in shape, and becomes steeper with increased time



or force (fig. 5.2), (Pertoft et al, 1978). The flat area of the curve, where a small difference in density of the media is represented by a large distance along the tube, will give the best resolution. Therefore, ideally the particles of interest should resolve in this region. The type of rotor and tube size have an effect on the gradient shape, so comparative experiments should be performed in one rotor. Fixed angle rotors are always used for gradient formation and fractionation with Percoll. The more vertical the tubes, the more rapidly the gradient is formed, as the gradient path length is shorter and the g force more nearly equal along the tube. Due to the self-forming nature of Percoll a continuous gradient is usually used for fractionation experiments. Discontinuous density Percoll gradients can be prepared, though due to the nature of the Percoll colloid, these tend to merge their interfaces, becoming continuous gradients.

## 5.2 MATERIALS AND METHODS

5.2.1 The preparation of Neurofibrillary tangles using Percoll  
Materials were obtained as described in section 2.1.5. and centrifugation was carried out as described in section 2.2.6.  
A set of experiments was designed to separate tangles on Percoll gradients. Centrifugation conditions were varied. In each experiment the location of plaques and tangles was monitored by fractionating the gradient into 1.5ml fractions, and collecting visible bands whole. 100 $\mu$ l from each fraction was then diluted with 9 volumes of distilled water containing

0.1% Congo red, and centrifuged for 10 minutes at 8,000 x g in an Eppendorf centrifuge. The pellet was smeared on a microscope slide, air dried, dehydrated and mounted. The pellets were then viewed by light microscopy and assessed for the presence of plaques, tangles and other tissue.

All experiments were performed in parallel with control tubes, in which density marker beads were used instead of tissue. Thus the gradient formed during experiments, could be plotted and the position of tissue bands calculated (Kagedal et al, 1978).

#### 5.2.1.1 Percoll gradient formation

Firstly, experiments were carried out to establish the correct conditions for the formation of a Percoll gradient suitable for the separation of NFT:

##### (i) Average density of Percoll solution

A number of initial experiments were performed in order to ascertain the isopycnic density of tangles (fig 5.1.a). 0.5ml portions of ATD brain homogenate (200mg of tissue in 1ml 5mM Tris, pH 7.5, homogenised with 20 strokes, glass on glass) were dispersed in Percoll solutions, of a range of average density between 1.027 g/ml and 1.06g/ml. Parallel samples in which density marker beads were used in place of homogenate were prepared in each case. Samples were centrifuged at 10,000 x g for 45 min, after which, gradient curves were plotted from the marker beads, and gradients were fractionated and analysed microscopically, as described above. The density at which tangles were found was recorded. The gradient most suited for the resolution of particles at this density was

ascertained, by noting that the gradients form isometrically around the starting density of the Percoll solution (Percoll booklet: Pharmacia). Therefore, the best gradient for the resolution of particles of a particular density is one in which the starting density of the Percoll solution is equal to the particle density.

#### (ii) Shape of Percoll gradient

The appropriate Percoll solution (starting density of solution equal to density at which tangles banded) was then subjected to centrifugation for periods varying from 45-75 minutes (fig. 5.1.b). The best resolution of particles on a gradient occurs when the central portion of the sigmoid curve is most nearly horizontal. As stated above, gradients form isometrically around the starting density of the Percoll solution and became progressively steeper with time. Therefore, as expected, the most suitable gradient curve was created by centrifuging for the least amount of time (45 minutes).

#### 5.2.1.2. The use of Pre-formed Percoll gradients

In the experiments described above, brain homogenate was dispersed within the Percoll solution before gradient formation. In the following experiments, brain homogenate was centrifuged more slowly, on pre-formed gradients. By centrifuging on a pre-formed gradient at a slower speed for a range of time periods, the sedimentation of tangles could also be investigated as a rate zonal phenomenon (fig. 5.1.c). Whereas, because of the higher g force required to form the Percoll gradient in the experiments previously described, it was only possible to study tangle sedimentation as an isopycnic phenomenon.

A Percoll gradient of average density 1.034 g/ml was pre-formed by centrifuging at 10,000 x g for 45 minutes; gradient formation was monitored by a control tube, containing density marker beads.

0.5 ml of ATD brain homogenate was subsequently loaded on to the pre-formed gradient, and both tubes were centrifuged at 400 x g in a swing out rotor for time periods ranging from 10 - 120 minutes. The resulting gradients were fractionated and examined as before.

#### 5.2.2. The preparation of neurofibrillary tangles using sucrose density gradients

##### 5.2.2.1 Discontinuous density gradients

Sucrose solutions were used as discontinuous density gradient media. Unlike Percoll, sucrose solutions exert an osmotic effect on tissue particles; and are highly viscous, which affects the sedimentation of particles during centrifugation. Discontinuous density gradients were prepared in polypropylene tubes. The various concentrations of sucrose were made up in distilled water containing 0.001% azide. The gradients were left all day (6 hours) at 4°C to allow merging of interfaces before the sample was applied. 0.5g of ATD brain was homogenised (20 strokes, glass on glass) in 1 ml of 5mM Tris pH7, and this homogenate was applied to the top of the gradient using a fine glass pipette.

A set of experiments was performed in which the following centrifugation conditions were varied, and the effect on tangles studied:

- 1) Tissue loading
- 2) Pre-spin through 1.1M sucrose
- 3) Time and g force of centrifugation
- 4) The presence or absence of SDS in the sucrose gradient
- 5) Gradient composition

In each experiment, samples of cortical grey matter from ATD or Down's brain, and control brain (of equal wet weights), were processed in parallel. After centrifugation the gradient was fractionated into its constituent layers, collecting the interfaces separately. This was done by drawing off each layer of sucrose, and each interface, with a glass pipette. Tissue bands seen at any position in the gradient were also collected separately. All volumes were recorded. A 100  $\mu$ l portion of each fraction from the gradient was diluted with 9 volumes of distilled water, containing 0.1% Congo red and centrifuged for 5 minutes at 8,000 x g in an Eppendorf centrifuge. The pellet was smeared on a microscope slide and mounted. Slides prepared from each gradient fraction were assessed by light microscopy with regard to the amount of tissue, and the relative proportions of tangles, plaques, nuclei and other cellular fragments. Protein concentration was measured using the method of Petersen et al, (1977).

A further experiment was performed, in which a discontinuous gradient was formed, and the interfaces allowed to merge for 60 hours, in order to produce a more continuous gradient. Brain homogenate was loaded on to the gradient, and this was centrifuged at 50,000 x g for 50 hours, and analysed as described above, (fig. 5.4).

Each gradient fraction was dialysed before protein measurement, or EM, as described in section 2.

#### 5.2.2.2 Continuous density sucrose gradient centrifugation

A continuous sucrose density gradient was made up using an LKB gradient mixer and peristaltic pump. A continuous linear gradient with a density range between 1.2M and 2M sucrose, was prepared using 8 ml of 1.2 M sucrose in the one chamber and 8 ml of 2 M sucrose in the other chamber of the mixer. ATD and control brain homogenates were layered on to these gradients. Centrifugation at 50,000 g for 50 hours was performed.

#### 5.2.3 The preparation of neurofibrillary tangles using a rapid denaturing method

1g of ATD cortex, rich in tangles and containing few plaques, was homogenised in 0.5% SDS/0.01%  $\beta$ ME in distilled water. This was spun down for 10 minutes at 8,000g, the supernatant poured off and conserved, and the pellet removed intact from the centrifuge tube.

Upon removal, the pellet showed a clearly demarcated division between a dark lower layer and a paler upper layer. The pellet was cut along this division using a scalpel blade.

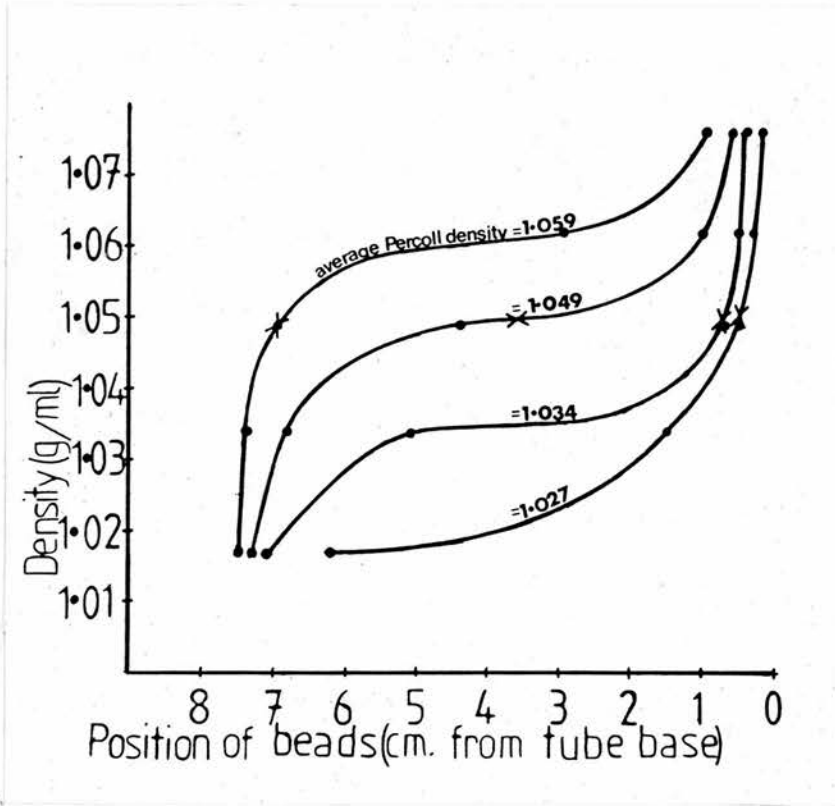
#### 5.2.4 An investigation of Selkoe et al's (1982) PHF preparation method

PHF were prepared according to the method of Selkoe et al (1982). All fractions were reserved for microscopy and the final pellet subjected to EM.



Figure 5.1

a



b

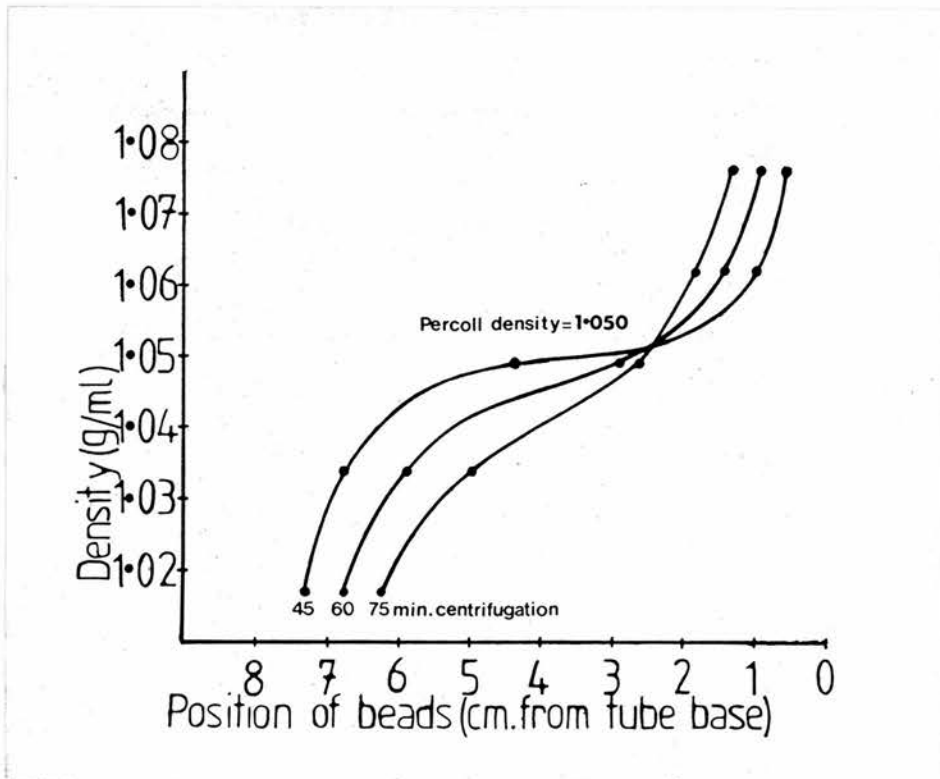
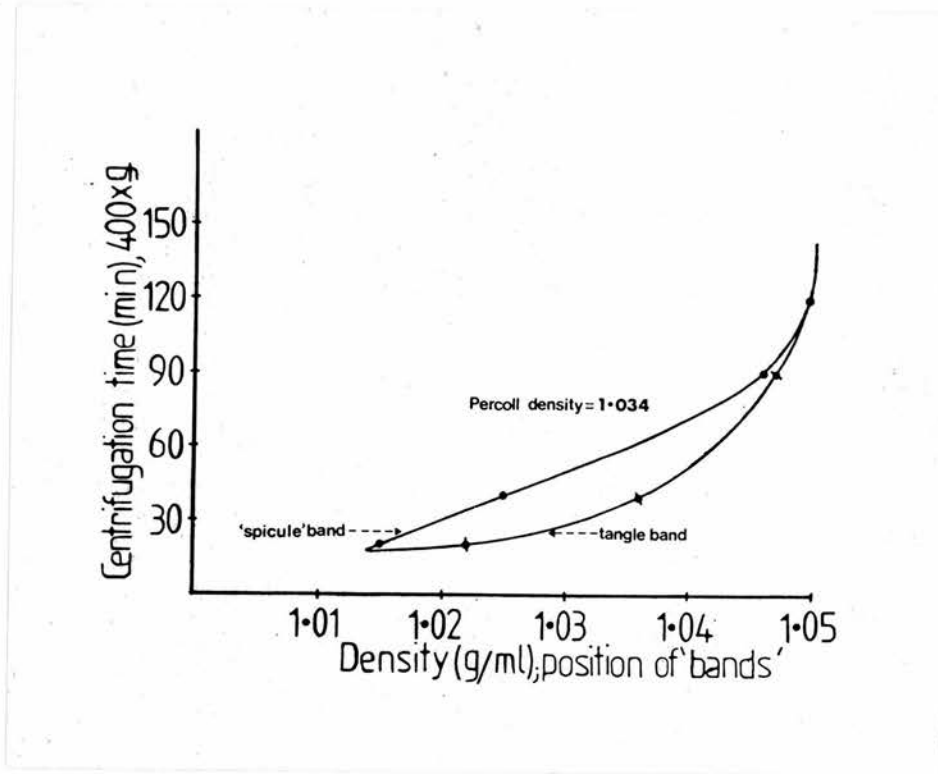


Figure 5.1

c



#### PERCOLL GRADIENT CENTRIFUGATION

- Centrifugation of ATD brain homogenate on 5 different densities of Percoll solution. A tissue band containing tangles, indicated by a cross on the figure, occurred at 1.050g/ml in the gradients (on average). Therefore a Percoll solution of starting density 1.050g/ml was deemed the most suitable for tangle separation procedures.
- Centrifugation of Percoll solution for 3 different time periods shows steepening of the gradient with increasing centrifugation time.
- Centrifugation of ATD brain homogenate of pre-formed Percoll gradients shows separation of tissue into 2 bands, which, with increasing centrifugation time, eventually reunite.

All gradients = 16ml

### 5.3 RESULTS AND DISCUSSION

#### 5.3.1 The preparation of neurofibrillary tangles using Percoll

##### 5.3.1.1. Percoll gradient formation. Average density of Percoll solution

As seen in fig 5.1. a dense tissue band containing plaques and tangles were formed between 1.049 and 1.0505, (average 1.050) in each of the four gradients. A few tangles were present above these bands, i.e. above 1.050 g/ml, however, no tangles were noted below the bands in any of the gradients. Centrifugation under the conditions depicted in gradient fig 5.1 b (10,000 x g for 45 minutes; average Percoll density 1.050) produced a diffuse band containing large amounts of tissue, and plaques and tangles, with no significant separation of these elements. Plaques, and nuclei tended to occupy the bottom portion of the band, and tangles the top, although there was no discrete division between these particles. A few tangles were present above, although most were present within, the tissue band. The average protein content of this band, over 3 repeat experiments, was 11.4mg/ml in 330 $\mu$ l for ATD brain. Tubes containing identically prepared control brain, centrifuged in parallel, showed similar bands, though these, obviously, did not contain plaques and tangles. The average protein content of the control brain band, over 3 repeat experiments was 13.3mg/ml in 293 $\mu$ l.

Further tubes containing a 1.050 g/ml Percoll solution were centrifuged; in one tube the homogenate was carefully layered on top of the Percoll solution, and in the other the homogenate was layered below the Percoll solution. Whereas,

previously, the homogenate has been dispersed within the Percoll solution. These alterations in method had no effect on the final position of bands containing whole tangles, or on the purity of the tangle containing fraction.

#### 5.3.1.2 The use of pre-formed Percoll gradients

Centrifugation of brain homogenate for time periods below those required to sediment particles at their isopycnic density, produced 2 tissue bands (fig 5.1.c). The upper of which contained small tangles, birefringent spicules, and other tissue components; the lower of which contained larger tangles, plaques, and other tissue including large numbers of nuclei.

Therefore using Percoll in NaCl under isopycnic conditions, most tangles banded with other tissue particles at an average density of 1.050 g/ml; with a small number of tangles situated just above this band. Separation of tangles from other tissue particles was poor. There are a number of possible reasons for this; Firstly, the gradient produced using Percoll may have been too steep with too wide a density range; despite the fact that the gradient was formed to be as shallow as possible (fig. 5.1.b). Secondly, tissue in the homogenate may well have aggregated, and thus been prevented from separating satisfactorily on the gradient. Thirdly, the densities of large subcellular particles, in particular, tangles, may vary due to other proteins attached to, or trapped within them. Within the band formed at 10,000 x g for 45 minutes, plaques, nuclei and larger tangles tended to occupy the lower part, indicating that these are probably more dense than smaller tangles and birefringent spicules.

The fact that tangles and birefringent spicules do fall into two populations, at least in terms of size, is confirmed by the results shown in fig. 5.1c, in which, under rate zonal conditions, two separate bands are formed. However, when the tube is centrifuged for long enough to create isopycnic conditions, the two bands are found to have merged to form one band.

### **5.3.2 The preparation of neurofibrillary tangles using sucrose density gradients**

The results of the discontinuous sucrose density gradient experiments are shown in Figs 5.2, 5.3 and 5.4. As described, the fractions taken from each gradient were assessed for the presence of tangles by light microscopy and also by electron microscopy in some cases. The assessment of a preparation as "partially purified" indicated a band very enriched in tangles with few other microscopic cell particles. In particular, in such preparations, nuclei and plaques were separated from the tangle fraction.

The five variables tested in the method (section 5.2.2.1) were found to be important in the production of more highly purified neurofibrillary tangle preparations.

#### **1) Tissue loading**

All experiments were performed with two tissue loadings, 0.25g wet weight tissue/15ml gradient and 1.0g wet weight tissue/15ml gradient. Both produced good separation of tangles using methods 5.2.d (or e), the former loading appearing to give a marginally better, i.e. microscopically more pure, preparation. However, there were drawbacks using

this lighter loading, in that the bands of interest were poorly visible, and yielded small quantities of material. The heavier tissue loading also produced very good separation, and clearly visible bands which were easy to fractionate. Therefore, 1g wet weight of tissue per 15ml gradient was used routinely.

## **2) Pre-spin through 1.1M sucrose**

Tangle separation was improved by first removing lipid material, this was done by pre-spinning the brain homogenate on sucrose. The homogenate was laid on to a single sucrose pad and centrifuged at 200,000 g x 2 hours. A range of densities between 0.5M and 1.5M sucrose were used. 1.1M sucrose was found to be the density at which lipid material floated, and all birefringent material was found in the pellet. If the sucrose molarity used was greater than 1.1M, some birefringent spicules stayed on top of the pad. If a density lower than 1.1M was used, this allowed lipid material to penetrate the sucrose. The pellet was then rehomogenised, and applied to a discontinuous sucrose density gradient.

## **3) Time and g force of centrifugation**

To effect successful isopycnic separation on gradients with a range of 1.2-2M sucrose, it was found to be necessary to spin for the order of 50,000 x g for 50 hours; or the equivalent. Centrifugation in excess of this, failed to alter the position of tissue bands formed. (Fig. 5.3).

## **4) Presence or absence of SDS within the gradient**

Experiments in which SDS/ $\beta$ ME was included in the gradient (figs. 5.2 e) and 5.4b)). produced purer tangle preparations,



as nuclei were removed, and the amount of amorphous unidentifiable tissue was reduced. In the discontinuous gradients, tangles banded at the 1.6-2M interface in gradients, both with and without SDS/ $\beta$ ME. In the experiment (fig 5.4) in which the gradient was more continuous, bands richest in tangles were formed around the level of the merged 1.4/2M sucrose interface; although, the tangle enriched band was narrower and much more well defined in the gradient which included SDS.

#### 5) Gradient composition

It can be seen from figures 5.2, 5.3 and 5.4 that the two most suitable gradients for separating tangles were achieved by using a discontinuous gradient of 1.2, 1.4, 1.6 and 2M sucrose, in which tangles banded at the 1.6-2M interface (fig 5.2 d) and e)) or a more continuous gradient with merged interfaces (figure 5.4) in which tangles banded above the level of the merged 2M layer. Tangles did not penetrate 2M sucrose in any gradients, although some tangles penetrated the 1.8M sucrose layer. It can also be seen that tangles were less dense than plaques or nuclei, both of which penetrated 2M sucrose. In fig. 5.2 d) and e) and fig 5.3 c), bands formed at all the sucrose interfaces. The band at the 1.2-1.4M interface contained most of the tissue loaded on to the gradient. The other bands contained far less material in comparison. This 1.2-1.4 interface band consisted of lipid and myelin sheath components from the white matter, and cellular debris. The band at 1.4 - 1.6 contained some whole tangles, and large numbers of birefringent spicules

Figure 5.2

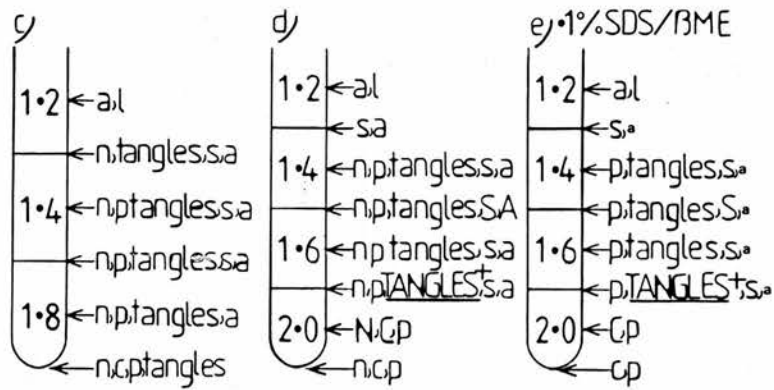
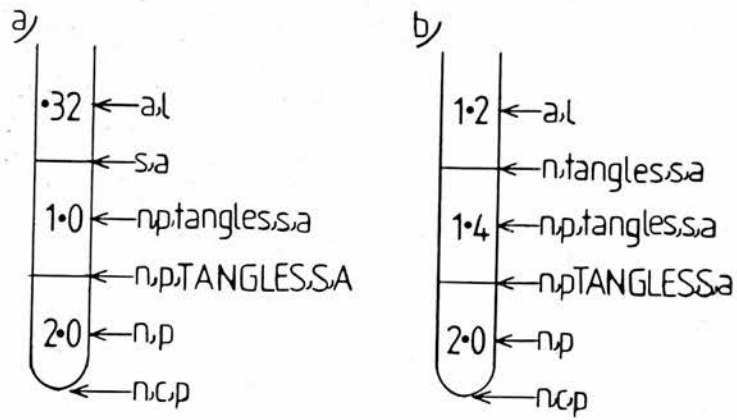


Figure 5.2 SUCROSE DISCONTINUOUS DENSITY GRADIENT CENTRIFUGATION - EFFECT OF GRADIENT COMPOSITION.

a) b) c) and d) Centrifugation of ATD brain homogenate on discontinuous gradients. These were the main steps taken to arrive at the final gradient, d), which produced a highly tangle-enriched fraction at the 1.6 - 2M interface.

e) gradient of identical composition to that of d), except in this case 1% SDS/0.1% B mercaptoethanol was included in the sucrose layers. This produced a highly tangle-enriched fraction at the 1.6 - 2M interface, with very little other contaminating protein.

Key:

n = nuclei, c = connective tissue, p = plaques,  
s = spicules, a = amorphous (unidentifiable) tissue,  
l = lipid.

As assessment of the fractions was entirely qualitative, a quantitative estimation of different tissue components has not been attempted: except, where very large amounts of a tissue component have sedimented in a particular fraction, it has been represented as a capital letter (or word) e.g. S = large amounts of spicules. Where the tissue component has dominated the fraction, almost to the exclusion of other particles, a plus sign has been added, e.g. TANGLES + = tangles comprising of most of the fraction. Also, where very small amounts of a tissue type have been present, the component has been represented by an extra-small letter, e.g. amorphous tissue was only present in very small quantities in the 1.6 - 2 M interface fraction in e).

Protein estimations for Fig.5.2.d and e for ATD and control brains (Average of 3 experiments). (Gradients using control brain homogenate were run in parallel with ATD brain homogenate in all experiments in Fig.5.2.).

Fig.5.2.d;

1.4-1.6 interface: ATD = 0.352mg/ml in 0.481ml  
Control = 0.253mg/ml in 0.458ml  
1.6-2.0 interface: ATD = 0.415mg/ml in 0.452ml  
Control = 0.234mg/ml in 0.391ml

Fig.5.2.e;

1.4-1.6 interface: ATD = 1.059mg/ml in 0.377ml  
Control = 0.980mg/ml in 0.374ml  
1.6-2.0 interface: ATD = 0.603mg/ml in 0.380ml  
Control = 0.376mg/ml in 0.354ml

500mg tissue loaded on to 16 ml gradients.

Figure 5.3

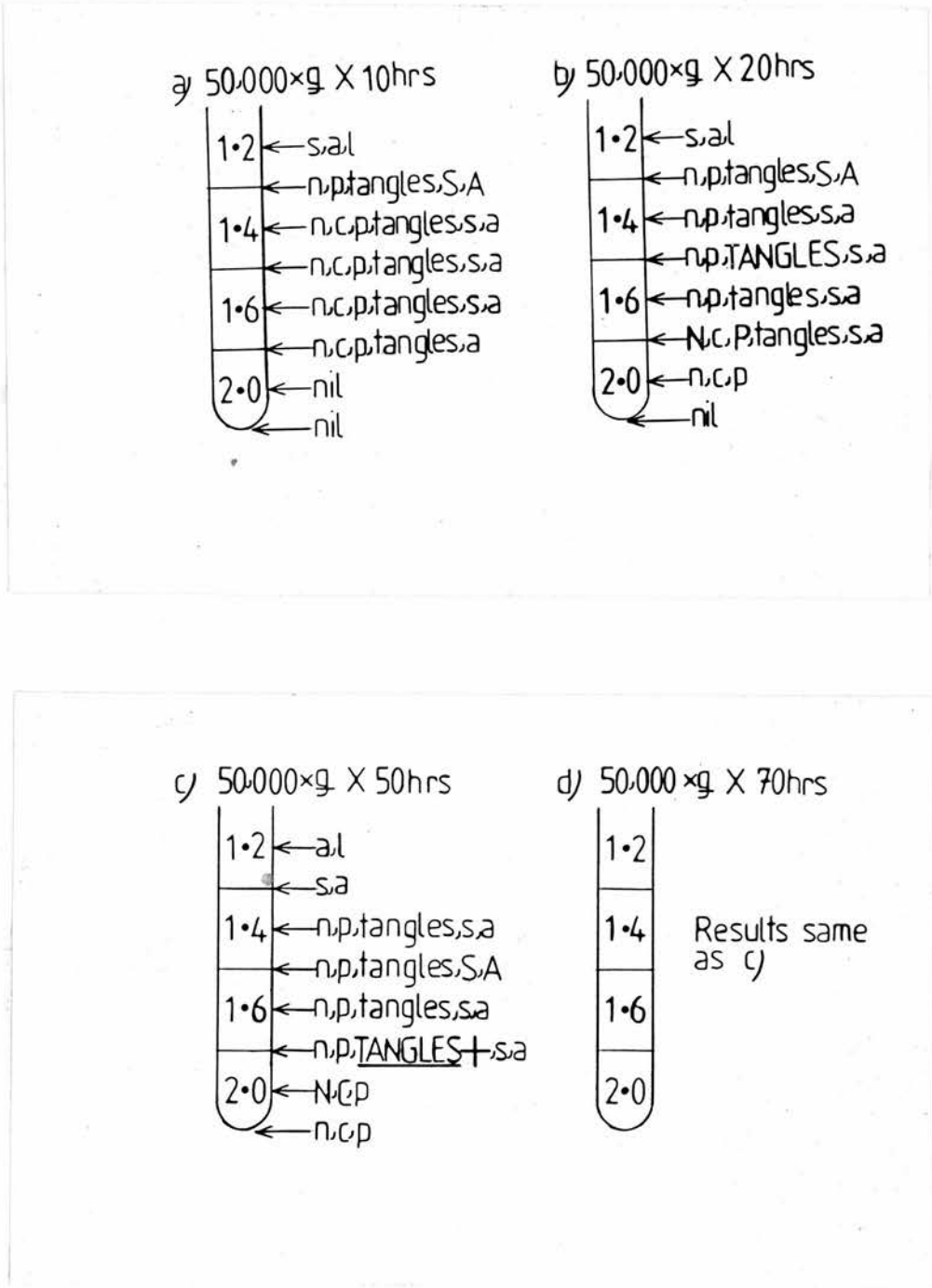


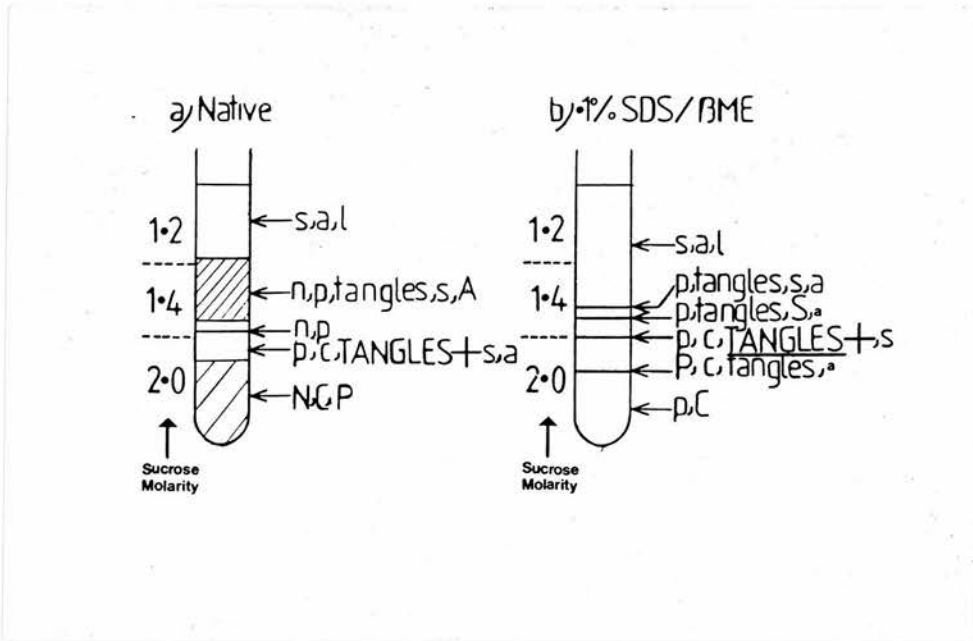
Figure 5.3 SUCROSE DISCONTINUOUS DENSITY GRADIENT  
CENTRIFUGATION - EFFECT OF CENTRIFUGATION TIME.

a) b) and c) Organelles are spread throughout the gradient after 10 and 20 hours of centrifugation. After 50 hours most tangles have sedimented at the 1.6 - 2 M interface, and significant numbers of plaques, nuclei and pieces of connective tissue have penetrated the 2 M layer.

d) Centrifugation for 40 hours does not appear to significantly alter the composition of bands seen after 50 hours.

Key: As for figure 5.2

Figure 5.4  
SUCROSE DISCONTINUOUS DENSITY GRADIENT CENTRIFUGATION - EFFECT  
OF INTERFACE MERGING



Bands seen on SDS discontinuous density gradient centrifugation of ATD brain, with interfaces left to merge for 60 hours before use.

a) Bands formed in native gradient.

b) Discrete narrow bands formed in SDS gradient, with a highly tangle enriched band formed at the level of the 1.4 - 2M interface.

(Bands are indicated by lines, and shaded areas).

Protein estimations for Fig. 5.4.a and b, for ATD brains only  
(Average of 3 experiments)

Fig. 5.4.a;

Tangle band at the level of the 1.4-2.0 interface = 0.127mg/ml  
in 0.974 ml

Fig. 5.4.b;

Tangle band at the level of the 1.4-2.0 interface - 0.473mg/ml  
in 0.279ml.



Figure 5.5 PHOTOMICROGRAPHS OF TANGLE ENRICHED FRACTIONS  
PRODUCED BY CENTRIFUGATION OF ATD BRAIN HOMOGENATE

a) and b) Congo red stained ATD brain homogenate prior to density gradient separative procedures; viewed by light and crossed polarisation microscopy.

c) Fraction from band obtained by centrifugation on Percoll gradient. It can be seen that this fraction was not significantly tangle enriched compared to b) the original homogenate.

d) Fraction from band at 1.6 - 2M interface obtained by centrifugation on SDS discontinuous density sucrose gradient, as specified in fig. 5.3e). This shows a significantly tangle enriched fraction compared to b) the original homogenate.

Magnification:

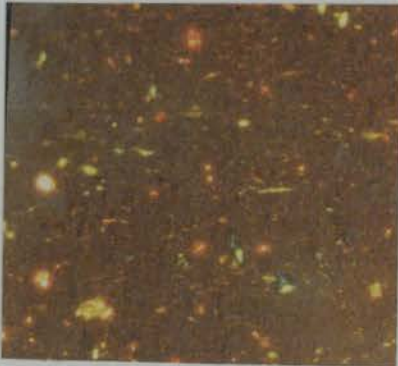
a-d1= x 200

d2 = x 620

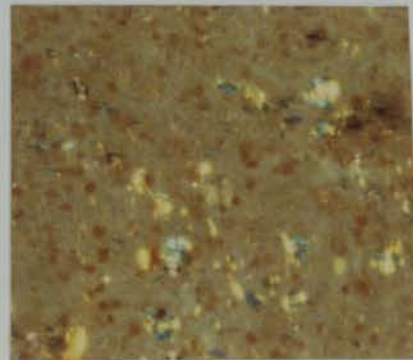
a



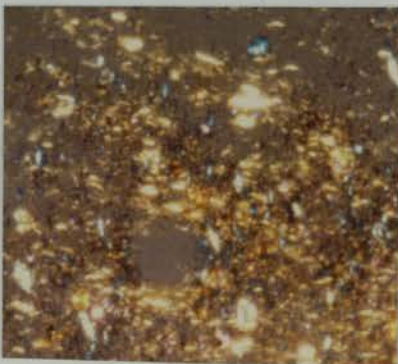
b



c



d1



d2



corresponding in shape to parts of tangles. Only very occasional intact plaques were present. The 1.6 - 2M interface contained large numbers of intact tangles, with occasional plaques, nuclei or connective tissue fragments, and very small amounts of amorphous unidentifiable tissue (Fig. 5.5.d). All fractions showing tangles or spicules under light microscopy, showed PHF under EM, with variable amounts of other contaminating protein. In the native discontinuous sucrose density gradient preparations, PHF was a minor constituent, with a moderate amount of other protein present in both 1.6 - 2 and 1.4 - 1.6M interface fractions. Most of this contaminating protein was unidentifiable, although occasional collagen fibrils and groups of amyloid fibrils were noted in the 1.6 - 2M fraction. However, a few PHF were seen on every grid square. The SDS treated discontinuous density gradient preparations showed PHF to be a major constituent of the fraction. Contaminating proteins present consisted of a small quantity of unidentifiable material in both 1.6 - 2M and 1.4 - 1.6M interface fractions. The 1.6 - 2M interface fraction also showed a few collagen and amyloid fibrils. Numerous PHF were seen on every intact grid square.

The pellet (below 2M sucrose) consisted mainly of fibrous connective tissue with many nuclei and some plaques. As stated above, in discontinuous sucrose gradients, the upper band at the 1.4 - 1.6M interface position contained many spicules, which resembled tangle fragments. It was also possible that these fragments were from neuritic plaques. As electron microscopy of this fraction showed numerous PHF, with

no amyloid fibrils, these spicules may have been fragments of tangles or of neuritic plaques, but they were not fragments of amyloid plaques. This phenomenon, i.e. PHF sedimenting at both 1.4-1.6 and 1.6-2M interfaces, was noted in discontinuous gradients both with and without SDS/ $\beta$ ME (figure 5.2 d) and e).

#### **5.3.3. The preparation of neurofibrillary tangles using continuous sucrose density gradient centrifugation.**

Both control and ATD brain homogenates showed multiple small bands on continuous density gradient centrifugation. Several bands mainly between 1.34 and 1.83 M sucrose contained tangles. The lower bands (at a density of more than 1.6M contained more plaques than those higher in the tube.

#### **5.3.4 Rapid denaturing method for the preparation of neurofibrillary tangles**

The dark lower layer of the pellet contained vessels, connective tissue fragments and some amyloid core plaques. EM of this fraction showed collagen fibrils, amyloid fibrils and some PHF. The pale upper layer contained numerous tangles, occasional amyloid core plaques and a small amount of unidentifiable tissue. EM of this fraction showed numerous PHF, with occasional collagen and amyloid fibrils, and some unidentified protein.

#### **5.3.5 The preparation of neurofibrillary tangles using Selkoe's (1982) method**

The initial pellet which is formed by centrifuging twice at 500 x g for 10 min, and then discarded in Selkoe's method, was found to contain numerous tangles. No tangles were seen under light microscopy in the supernatant of the initial

centrifugation, or in the final pellet of the preparation, using congo red staining. At EM, in the final pellet some filamentous structures, probably PHF, were seen to be present; although sections of the tiny pellet were difficult to interpret. Therefore, the PHF prepared by this method, are presumably detached from tangles during the initial homogenisation. As this method discards all intact tangles in the first step of the procedure, it therefore gives a low yield of PHF.

#### 5.4 DISCUSSION

On the basis of light and electronmicroscopic assessment the best methods for preparing tangles were found to be the spin through 1.1M sucrose, followed by 50 hours centrifugation at 50,000 g in either a 2 M/1.6 M/1.4 M/1.2 M sucrose/SDS discontinuous density gradient; or a 2 M/1.4 M/1.2 M/SDS gradient left to merge for 60 hours. In the former method the 1.6/2 M interface appeared to be composed almost entirely of PHF at electron microscopy. Also numerous PHF were seen at the 1.4/1.6 M interface. The reason for the banding of whole tangles at the 1.6/2 M interface, and tangle fragments or 'spicules' at the 1.4/1.6 M interface was unclear. As additional centrifugation, a further 20 hours, did not alter the position of the bands, it is reasonable to assume that particles had reached their equivalent densities. Therefore, it was possible, either that there was a difference in density between whole tangles and spicules or that other protein was

attached to whole tangles, making them behave as denser particules. The absence of this finding in the isopycnic Percoll experiments can be attributed to the fact that separation of all subcellular particles was extremely poor, most of the tissue forming a single band at 1.050 g/ml. As previously discussed, the formation of two bands on pre-formed Percoll gradients (fig. 5.1.c) was due to separation of particles in the basis of size. In the sucrose gradient with merged interfaces (fig, 5.4), the upper of the two bands formed at the level of the 1.4 - 2M interface also appeared to be composed almost entirely of PHF at electron microscopy. The reason for 'tangle' bands being more discrete in denaturing as opposed to the native gradients, may have been due to the removal of proteins from outside of tangles by SDS, thus altering their density. Alteration in viscosity in the gradient medium caused by the addition of SDS, may have also contributed to this finding.

Therefore, tangles appear to be distributed over a wide density range within the gradient. However, they do form tangle enriched bands. One suggestion for the banding of tangles at differing densities is that either tangles, or PHF themselves may sometimes have other attached proteins, which alter their sedimentation properties. Despite this functional variation in the density of tangles, discontinuous sucrose gradient centrifugation produced a partially purified tangle fraction above the 2.0M sucrose layer.

The continuous sucrose density gradient used, proved to be an inferior method of tangle preparation compared to

discontinuous methods, producing numerous bands containing tangles and other organelles. Continuous methods were, therefore, abandoned as a method of tangle purification.

These findings concur with those of other authors, who used similar, though not identical, gradient for tangle separation (Ihara et al 1983, Iqbal et al, 1984). The latter group, when using their 'short' procedure, similarly found there to be two tangle fractions within the gradient, corresponding to the tangle enriched (1.6 - 2 M interface) and spicule enriched (1.4 - 1.6M interface) bands. They postulated that this separation was on the basis of size, although did not test this hypothesis. However, these authors agree that tangles do not readily form a single band on sucrose density gradient centrifugation, although, using this method a partially purified tangle preparation can be produced.



## CHAPTER 6

### SPECTRAL STUDIES ON PURIFIED PREPARATIONS OF PHF

## SPECTRAL STUDIES ON PURIFIED PREPARATIONS OF PHF

### 6.1 INTRODUCTION

#### 6.1.1. Fluorescence spectra

Protein chromophores can be divided into three classes: the peptide bond itself, amino acid side chains, and prosthetic groups. The peptide bond absorption is maximal at about 190 nm. Certain amino acid side chains including Asp, Gly, Asn, Gln, Arg and His have absorption bands in the same region, i.e. under 230nm, and these are masked by the presence of the peptide bond. Aromatic amino acids, mainly tyrosine and tryptophan absorb strongly at a higher wavelength (about 280 nm), where peptide bond absorption is reduced to negligible values. The contributions of the aromatic amino acids to the spectra of PHF and control brain preparations have been looked at in the experiments described in this Chapter.

Spectra produced by a fluorescent spectrophotometer are 'uncorrected'. This means that the wavelength distribution of the emissivity of the xenon arc lamp, the efficient of the photomultiplier, and the wavelength distribution of the light losses from the monochromator and dispersing grating, have not been corrected for. Thus the intensity of the spectrum at different wavelengths is not accurately proportional to the quantum yield at those wavelengths. Therefore the spectra obtained here have been used for qualitative observations and for comparison of samples.

### 6.1.2 Circular dichroism

Most biological molecules including proteins, are optically active, due to dissymmetry of the molecule. One of the effects exhibited by optically active molecules is the phenomenon of circular dichroism (CD); this measures the absorption difference between left-hand and right-hand circularly polarised light. Plane polarised light is broken down into left and right-hand circularly polarised light and the optical activity of the protein molecule results in a difference in molar absorptivity between the left and right-hand portions. This results in an ellipticity of the beam, which is recorded by the instrument.

### 6.1.3 Vibrational spectra - Infra red

The infra red spectra of proteins and polypeptides are characterised by three main bands. These three arise from the peptide backbone, and can be attributed to: 1) the N-H stretch at  $3,300\text{ cm}^{-1}$ , 2) the C = O stretch at  $1,630$  to  $1,550\text{ cm}^{-1}$ , (amide I), and 3) the N-H deformation at  $1,520 - 1,550\text{ cm}^{-1}$  (amide II). The value of these measurements is that they depend on the secondary structure of the protein and thus indicate whether the protein consists of  $\alpha$  helix or  $\beta$  sheet. Hydrogen bonding shifts the energies of the three vibrations, moving the two stretch bands to lower energy and the N-H deformation to higher energy. Under good conditions, e.g. pure sample, known orientation of sample, the technique is capable of showing up other peptide bands, and bands from various side chains. Also proteins can be studied in solution or in solid form, this fact has been particularly useful in studying PHF preparations.

## 6.2 METHODS

### 6.2.1 Fluorescence spectra

Samples were prepared from ATD and control brains for spectroscopy by discontinuous density gradient centrifugation under the conditions illustrated in figure 5.2.e. In all studies performed (including infra red and CD), tangle-enriched and control brain preparations were compared, and the differences between the two attributed to the presence of tangles or PHF in the former fraction. As it was, obviously, important to exclude amyloid from the tangle-enriched preparations; firstly, brain rich in tangles and poor in plaques and blood vessel amyloid was chosen; secondly, the 1.4 - 1.6 M interface band of the sucrose gradient was culled. As described in Chapter 5, this "spicule rich" band is almost free from plaques, and on electron microscopy shows no amyloid fibrils. Before subjecting the dialysed samples to spectroscopy, in order to prevent scatter, they were centrifuged at 8,000 x g for 5 minutes to remove large tissue particles (spectra shown in fig 6.1). EM of this supernatant showed moderate numbers of PHF in the tangle fraction, and a little amorphous protein in the control fraction. On a subsequent occasion, the dialysed samples were left to settle for one hour before spectroscopy, without centrifugation (Spectra shown in fig 6.2). EM of this supernatant showed considerably larger numbers of PHF in the tangle fraction, and slightly more (though still a small amount) of the amorphous protein in the control fraction.

### 6.2.2 Circular dichroism

Samples were prepared as described in 6.2.1. Before spectroscopy they were centrifuged at 8,000 x g for 30 seconds. EM of the tangle-enriched fraction supernatant showed large numbers of PHF, and of the control fraction showed a little unrecognisable protein. Protein concentration was measured by absorption at 210 nm.

### 6.2.3 Infra red spectra

Samples were prepared as described in 6.2.1. They were not centrifuged before spectroscopy, instead the preparations in suspension were smeared and air dried on to calcium fluoride windows, as described in section 2.2.11.

## 6.3. RESULTS AND DISCUSSION

### 6.3.1 Fluorescence spectra

Fig. 6.1 shows spectra obtained on tangle-enriched and control preparation supernatants (8,000 x g for 5 minutes). These show similar profiles, with maximum absorption at approximately 285 nm, and maximum emission at approximately 330 - 335 nm. The ATD trace shows overall hyperchromicity.

Fig 6.1.c shows the emission spectra obtained by exciting at 280 nm, the supernatants of preparations left to settle at unit gravity for one hour, without centrifugation. The tangle-enriched fraction shows a double peak at approximately 307 and 335 nm. The control fraction shows a somewhat flattened peak. The PHF spectrum is also hyperchromic.

Figure 6.1

a

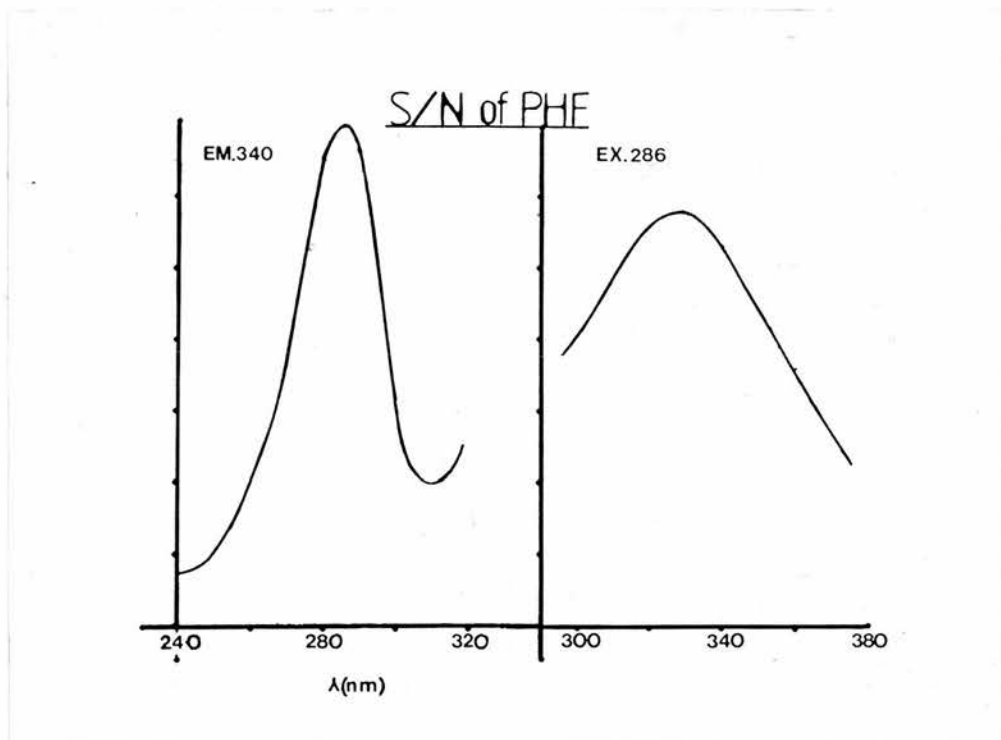




Figure 6.1

b

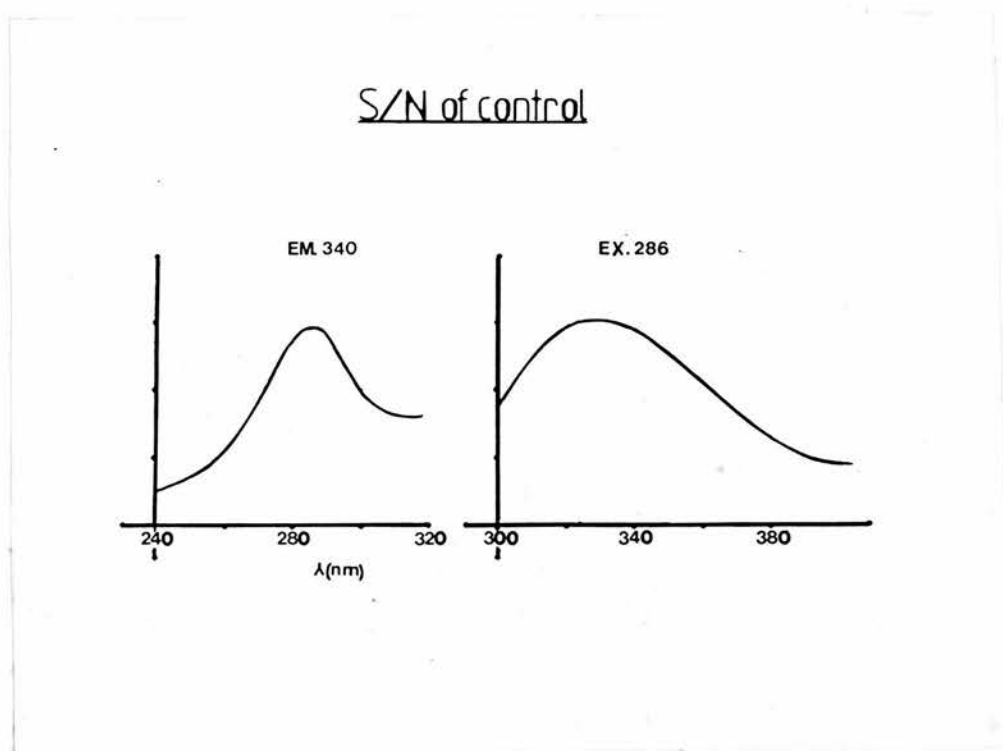


Figure 6.1

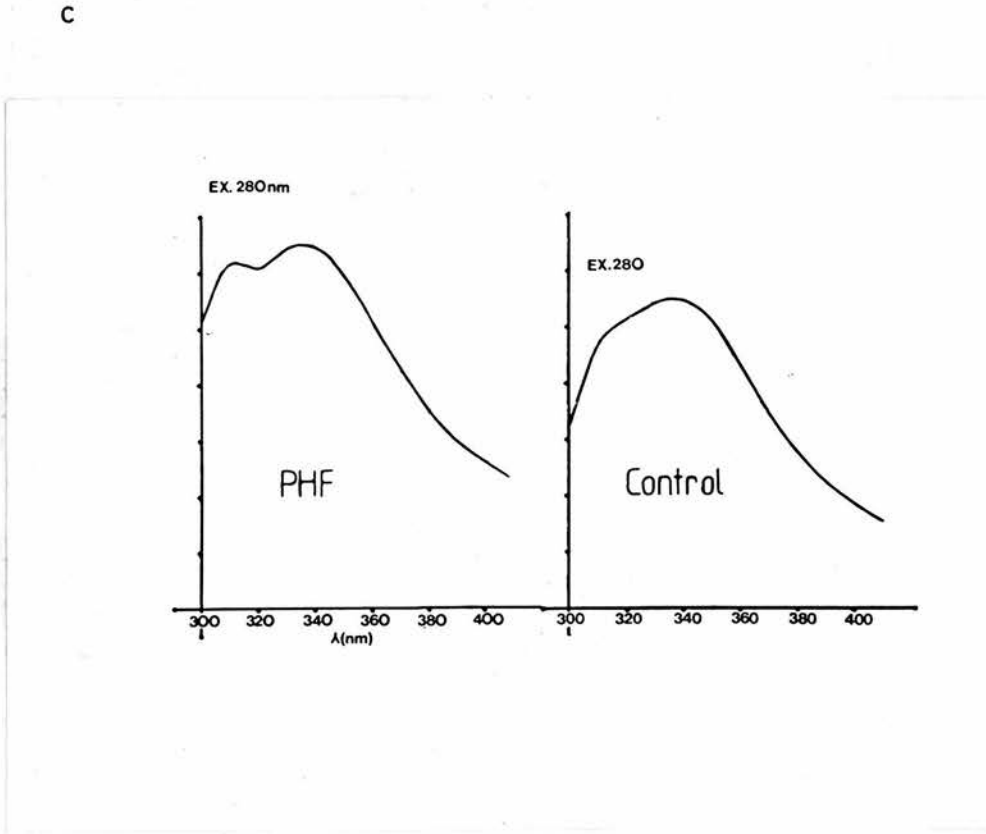


Figure 6.1 FLUORESCENCE SPECTRA

a) and b) Absorption and emission spectra (8000 x g, for 5 minute supernatants) of ATD and control brain preparations.

c) Emission spectra of supernatants of ATD and control brain preparations, left to settle at unit gravity for 1 hour.

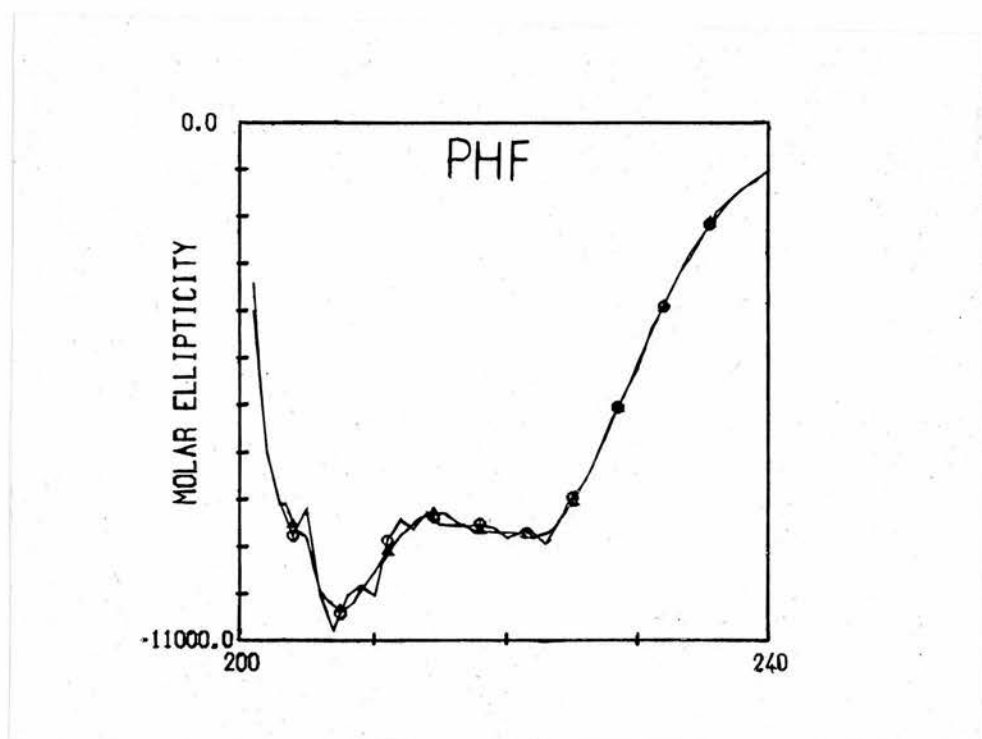
Hyperchromicity of the tangle fraction spectra in comparison to the control, is suggestive of  $\beta$  structure, as opposed to  $\alpha$  helix, in the former (Gratzer, 1967). However, the possibility that this feature is due to an excess of random coil in the tangle fraction could not be excluded without quantitative data which it is not possible to achieve with such impure fractions. The two peaks seen in fig. 6.1.c almost certainly correspond to tyrosine and tryptophan; the former's absorption maximum being 274 nm, and emission maximum 303 nm; the latter's absorption maximum being 280 nm and emission maximum 348 nm. Although tyrosine is a weaker emitter than tryptophan, it is usually present in larger numbers, however, tyrosines are often quenched by any nearby tryptophans, and fluorescence spectra tend to be dominated by tryptophan. As this has not occurred in the tangle fraction spectrum (fig. 6.1.c) the distinction of the two peaks would argue against a coiled secondary structure, particularly  $\alpha$  helix: and is compatible with, but not diagnostic of  $\beta$  conformation.

### 6.2.3 Circular dichroism

The two control samples gave values for  $[\theta]_{222}$  of  $-9400^\circ$  and  $-9060^\circ$ ; the two ATD samples gave values of  $-8330^\circ$  and  $-7600^\circ$ . As the situation is complex, i.e.  $\alpha$  helix content is low, one control and one ATD spectrum were read off, and put through the Provencher and Glockner programme (1981). This uses elastic standards and provides a best fit (fig. 6.2), based on a set of 25 proteins of known structure, which the programme combines on a least squares basis, and then averages

Figure 6.2

a



b

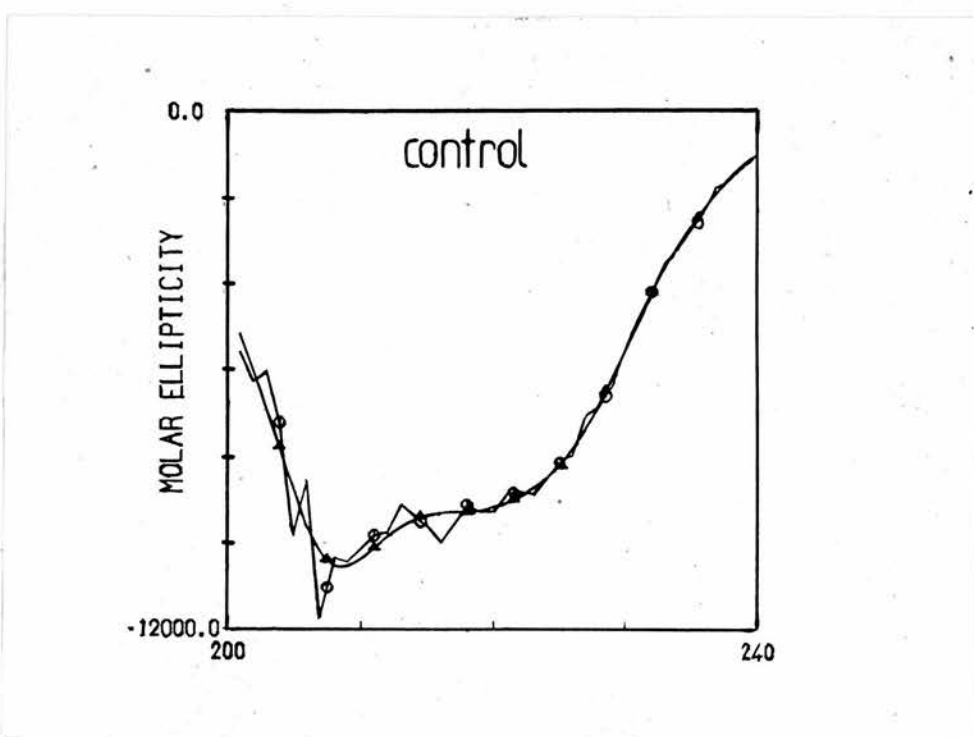



Figure 6.2 CIRCULAR DICHROISM SPECTRA

- a) ATD brain preparation, with 'best fit' curve.
- b) Control brain preparation, with 'best fit' curve.

Best fit curve obtained by method of Provencher and Glockner (1981).

Key:

CD tracing = 

Best fit = 

the conformation. This is very reliable for  $\alpha$  helix, though less so for  $\beta$  sheet and random coil. The best fit for the ATD fraction ( $[\theta]_{222}$  of  $-8300^\circ$ ) was:

$\alpha$  helix 22%;  $\beta$  sheet 48%; remainder 30%.

The best fit for the control brain fraction, ( $[\theta]_{222}$  of  $-9600^\circ$ ) was:

$\alpha$  helix 27%;  $\beta$  sheet 39%; remainder 34%.

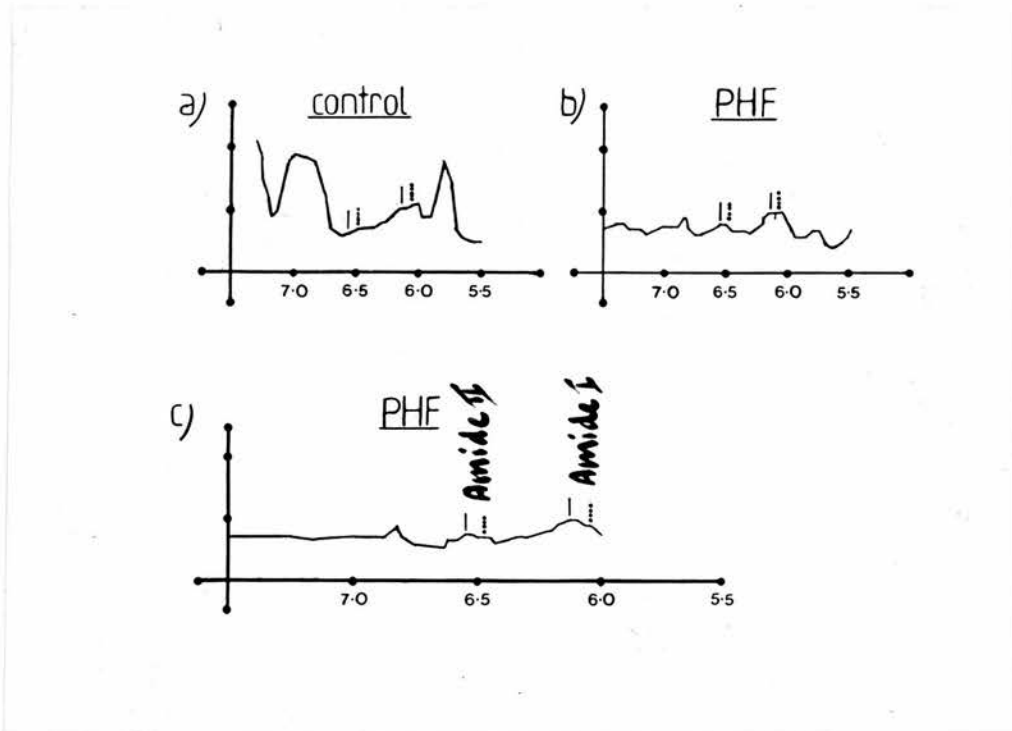
Judging by the  $[\theta]_{222}$  values, one would anticipate that the  $\alpha$  helix and  $\beta$  sheet contents would differ more in the remaining ATD and control fractions ( $[\theta]_{222}$  of  $-7600^\circ$  and  $-9400^\circ$  respectively).

### 6.3.3 Infra red spectra

Fig. 6.4.a) and b) shows the spectra obtained from ATD and control samples; 6.4c) shows a rerun of the ATD sample on a larger scale baseline. Amide I can be seen as a double peak in both ATD and control samples. The first peak corresponds to  $\beta$  sheet at a wavelength of  $6.126\mu$  (a frequency of  $1,6\text{ cm}^{-1}$ ), and the second peak corresponds to  $\alpha$  helix at a wavelength of  $6.05\mu$  (a frequency of  $1,652\text{cm}^{-1}$ ). The amide I  $\beta$  sheet frequency is more pronounced in the ATD tracings, and the amide I  $\alpha$  helix frequency is more pronounced in the control. However, as has been found using CD,  $\alpha$  helix content is low, and random coil probably accounts for some of the  $\alpha$  helix peak. Amide II can be seen as a lesser feature on the tracings; consisting of a peak corresponding to  $\beta$  sheet at a wavelength of  $6.55\mu$  (a frequency of  $1,526\text{ cm}^{-1}$ ), and a peak corresponding to a  $\alpha$  helix at a wavelength of  $7.475\mu$  (a frequency of  $1,544\text{ cm}^{-1}$ ). Overall the amide II band is much



Figure 6.3



Key: — =  $\beta$  sheet  
 ..... =  $\alpha$  helix

Figure 6.3 INFRA RED SPECTRA

a) Spectrum of control brain preparation.

b) and c) Spectrum of ATD brain preparation.

c) shows 2 x scale on Y axis.

Frequencies at which the  $\alpha$  helical and  $\beta$  sheet components of amide bands I and II occur are marked on each tracing.

(Y axis shows scale (metres), the reciprocal of which = frequency (cm⁻¹)).

more apparent in the ATD sample; in particular the amide II  $\beta$  sheet frequency is far more evident.

#### 6.4. DISCUSSION

These results suggest that the difference between tangle and control spectra are consistent with the presence of excess  $\beta$  sheet in the tangle fraction. This can be attributed to the presence of PHF in the tangle fraction (see section 6.2.1), and implies that  $\beta$  sheet predominates in the secondary structure of PHF protein. This is in concurrence with observations on staining (see Chapter 4), and the X-ray diffraction studies of Kirschner et al (1986) who showed PHF to have cross  $\beta$  conformation. Tryptic cleavage of NF produces 'head regions' which are thought to contain the side arms seen along NF borders. X-ray diffraction studies have shown the head regions to consist of 40%  $\beta$  sheet. As MAPS are associated with NF side arms, this may be relevant to PHF, in view of recent immunocytochemical findings (see section 1.8). Though it is also possible that  $\beta$  sheet is induced when PHF are formed, rather than predominating prior to this, in the subunits which are assembled into PHF.

**Note:** See bibliography for texts consulted on theory and practice of Optical Methods.

## SUMMARY

Congo red is a better stain for tangles and plaque cores, and silver a better stain for neuritic plaques. Future quantitative assessments of plaques and tangles should take this finding into consideration and choose the staining method appropriate to the requirements of any proposed studies; or if necessary, use both staining methods.

Tangles are soluble to a varying degree in SDS and 0.2 M NaOH. Numbers of insoluble tangles within any one brain are inversely related to the duration of dementia. The effect of SDS on isolated PHF is to increase the repeat length. Investigation of an 'aged' sample of PHF revealed an increase in numbers of morphologically unusual PHF with variable disruption of helical structure, and the apparent formation of protein projections along the periphery of PHF loops, in some cases. These observations cannot be directly extrapolated to the in vivo situation. Though it can be hypothesised that tangles from brains with longer durations of dementia become more susceptible to endogenous proteolytic processes within brain. This may be due to the increased neuronal death in AD resulting in the appearance of extracellular tangles, which are more easily broken up than intracellular tangles.

The electronmicroscopic visualisation of PHF apparently undergoing disintegration in the 'aged' preparation, raises the possibility that in vivo, significant numbers of PHF may be broken up and completely digested. Such indications that any of the pathological features of AD may be reversible are

interesting, because of the possible therapeutic implications. A new method of tangle separation using FACS has been developed in this thesis. This technique can be used on small amounts of ATD cerebral cortex, and can be performed more quickly than tangle preparation using centrifugation. As it is described in Chapter 4, the method is practical, and produces a tangle-enriched fraction. Though in future, it may be possible to further improve the purity of the tangle yield by using an intrinsic property of the tangle for sorting; for example 90 degree light scatter, rather than a fluorescent label.

Centrifugation using Percoll and sucrose gradients, was investigated as a tangle separation method. Only sucrose discontinuous gradients proved successful. Tangles were found to band over a wide density range, with smaller tangles and 'spicules' banding at lower densities than larger tangles, despite reaching isopycnic conditions during centrifugation. This finding may reflect changes in the density of the actual PHF; or the trapping of miscellaneous structures and proteins within the tangle, (eg. neurofilaments).

Spectral studies showed that tangle-enriched fractions contain an excess of  $\beta$  sheet, compared to control fractions. This concurs with previously published staining and X-ray diffraction data on the secondary structure of PHF.

BIBLIOGRAPHY

Adolfsson, R., Gottfries, C.G., Ross B.E., Winblad, B. (1979) Changes in brain catecholamines in patients with dementia of the Alzheimer type. *Brit. J. Psychiatry* 135: 216-223.

Allsop, D., Landon, M., Kidd, M. (1983) The isolation and amino acid composition of senile plaque core protein. *Brain Res.* 259: 349-352.

Alzheimer, A. (1907a) Ueber eine eigenartige Erkrankung der Hirnrinde. *Allgemeine Zeitschrift fur Psychiatrie* 64: 146-8.

Alzheimer, A. (1907b) Ueber eine eigenartige Erkrankung der Hirnrinde. *Zentralblatt fur die gesamte Neurologie und Psychiatrie* 18; 1977-9.

Anderton, B.H., Breinburg, D., Downes, M.L.J., Green, P.J., Tomlinson, B.E., Ulrich, J. et al (1982) Monoclonal antibodies show that neurofibrillary tangles and neurofilaments share antigenic determinants. *Nature (Lond)* 298: 84-6.

Ball, M/J. (1978) Neuronal loss, neurofibrillary tangles and granulovacuolar degeneration in the hippocampus with aging and dementia. *Acta Neuropathol.* 37: 111-118.

Ball, M.J. (1978) Topographic distribution of neurofibrillary tangles and granulovacuolar degeneration in hippocampal cortex of aging and demented patients. A quantitative study. *Acta Neuropathol.* 42: 73-80.

Ball et al (1985) A new definition of Alzheimer's disease: a hippocampal dementia. *Lancet* 1: 14-16.

Bancroft (1975) *Histochemical Techniques.* 2nd edn. Butterworths, Lond.

Beck, R., Mathews, W.B., Stevens, D.L., Alpers, M.P., Ashers D.M., Gajdusek, D.C. and Gibbs C.J. (1969) Creutzfeldt-Jakob disease. The neuropathology of a transmission experiment. *Brain* 92: 699-716.

Bennhold, E. (1922) The use of congo red for histological staining of amyloid. *Muchn. Med. Wschr* 2: 1537.

Benton, J.S., Bowen, D.M., Allen, S.J. et al (1982) Alzheimer's disease as a disorder of the isodendritic core. *Lancet* i: 456.

Berger, B., Escourolle, R., Moyne, M.A. (1976) Axones catecholaminergiques du cortex cerebral humain. *Rev. Neurol. (Paris)* 132: 183-194.



Bignami, A., Selkoe, D.J., Dahl, D. (1984) Amyloid-like (Congophilic) neurofibrillary tangles do not react with neurofilament antisera in Alzheimer's cerebral cortex. *Acta Neuropathol (Berl)* 64:(3) 243-250.

Bizzi, A., Crane, R., Yoon, M., Autilio-Gambetti, L., Gambetti, P. (1983) The axonal transport of neurofilaments is impaired in aluminium intoxication. *J Neuropathol. Exp. Neurol.* 42: 331.

Black, M.M., Lasek, R.J. (1980) Slow components of axonal transport: Two cytoskeletal networks. *J. Cell Biol.* 86: 616-623.

Blessed, G., Tomlinson, B.E., Roth, M. (1968) The association between quantitative measures of dementia and of senile change in the cerebral grey matter of elderly subjects. *Brit. Psychiatry* 114: 7970811.

Borthwick, N.M., Yates, C.M., Gordon, A. (1985) Reduced proteins in temporal cortex in Alzheimer's disease - An electrophoretic study. *J. Neurochem* 44.

Bowen, D.M., Smith, C.B., White, P., Davison, A.N. (1976) Neurotransmitter-related enzymes and indices of hypoxia in senile dementia and other abiotrophies. *Brain* 99: 459-96.

Bowen, D.M., Smith, C.B., White, P., Flack, R.H.A., Carrasco, L.H., Gedy, J.L., Davison, A.N. (1977) Chemical pathology of the organic dementias. *Brain* 100: 427-53.

Braak, H., Braak, E., Grundke-Iqbal, I., Iqbal, K. (1986) Occurrence of neuropil threads in the senile human brain and in Alzheimer's disease: a third location of paired helical filaments outside the neurofibrillary tangles and neuritic plaques. *Neurosci Lett* 65: 351-355.

Bradford, M.M. (1976) A rapid and sensitive method for the quantification of microgram quantities of protein utilising the principle of protein dye binding. *Anal Biochem.* 72: 248-254.

Bramhall, S., Noack, N., Wu, M. et al (1969) A simple colorimetric method for determination of protein. *Anal. Biochem.* 31: 146-148.

van Broeckhoven C., Genthe, A.M., Vandenberghe, A., Horsthemkes, B., et al (1987) Failure of Familial Alzheimer's disease to segregate with the A4-amyloid gene in several European families. *Nature* 329: 153-156.

von Braunmuhl, A. (1928) Zur Histopathologie der umschriebenen Grosshirnatrophie (Pick'sche Krankheit). *Virchows Archiv fur pathologische Anatomie und Physiologie und fur klinische Medizin* 270: 448-86.

- Brion, J.P., Couck, A.M., Passareiro, W.J., Flament-Durant, J. (1985) Neurofibrillary tangles of Alzheimer's disease: an immunohistochemical study. *J. Submicrosc. Cytol.* 17: 89-96.
- Brody, H. (1955) Organisation of the cerebral cortex. III. A study of aging in the human cerebral cortex. *Comparative Neurol.* 102: 511-56.
- Brody, H. (1976) An examination of cerebral cortex and brain stem aging. In *Aging*, vol. 3: *Neurobiology of Aging* (Ed. Terry R.D. and Gershon, S). pp.177-83. Raven Press, New York.
- Brown, P., Salazar, A.M., Gibbs, C.J.Jr., Gajdusek, D.C. (1982) Alzheimer's Disease and Transmissible Virus Dementia (Creutzfeldt-Jakob Disease). *Ann N.Y. Acad. Sci.*
- Brun, A., Englund, E. (1981) Regional pattern of degeneration in Alzheimer's disease: neuronal loss and histopathological grading. *Histopathol.* 5: 549-564.
- Buell, S.J., Coleman, P.D. (1979) Dendritic growth in the aged brain and failure of growth in senile dementia. *Science* 206: 854-6.
- Bugiani, O., Salvarini, S., Perdelli, F., Mancardi, G.D., Leonardi, A. (1978) Nerve cell loss with ageing in the putamen. *European Neurol.* 17: 286-91.
- Burger, P.G., Vogel, F.S. (1973) The development of the pathologic changes of Alzheimer's disease and senile dementia in patients with Down's syndrome. *Amer. J. Pathol.* 73: 457-468.
- Carden, M.J., Eagles, P.A.M. (1983) Neurofilaments of ox spinal nerves - isolation, disassembly, reassembly and cross-linking properties. *Biochem. J.* 215: 227-237.
- Carlsson, A., Adolfsson, R., Aquilonius, S.M., Gottfries, C.G., Oreland, L. et al (1980) Biogenetic amines in human brain in normal aging, senile dementia and chronic alcoholism. In: *Ergot Compounds and Brain Function*. Goldstein et al (ed) pp.295-304. Raven Press NY.
- Chin, R.K., Eagles, P.A.M., Maggs, A. (1983) The proteolytic digestion of ox neurofilaments with trypsin and  $\alpha$  chymotrypsin.
- Chou, S.M., Hartmann, H.A. (1964) Axonal lesions and waltzing syndrome after IDPN administration in rats. *Acta Neuropathol.* 3: 428-450.
- Chou, S.M., Hartmann, H.A. (1965) Electron Microscopy of focal neuroaxonal lesions produced by IDPN in rats. *Acta Neuropathol.* 4: 590-603.

Chou, S.M., Martin, J.D. (1971) Kuru plaques in a case of Creutzfeldt-Jakob disease. *Acta Neuropathol. (Berl)* 11: 150-155

Cooper, J. (1974) Selective amyloid staining as a function of amyloid composition and structure. *Lab. Invest.* 31: 232-238.

Constantinidis, J. (1978) Is Alzheimer's disease a major form of senile dementia? Clinical, anatomical and genetic Data. In: *Aging Vol. 7*, eds. Katzman, Terry and Bick. Raven Press, N.Y.

Cook, R.H., Ward, B., Austin, J.H., Robinson, A. (1978) Familial Alzheimer's disease: its relation to cytogenetic abnormality and transmissible dementia. *Neurol. (Minneap.)* 28: 353.

Corsealis, J.A.N., Bruton, C.J., Freeman-Browne, D. (1973) The aftermath of boxing. *Psychological Medicine* 3: 270-303.

Cross, A.J., Crow, T.J., Perry, E.K., Perry, R.H., Blessed, G., Tomlinson, B.E. (1981) Reduced dopamine- $\beta$ -hydroxylase activity in Alzheimer's disease. *BMJ* 282: 93-94.

Crowther, R.A., Wischik, C.M. (1985) Image reconstruction of the Alzheimer paired helical filament. *EMBO J* 4/13B: 3661-3665.

Dahl, D., Selkoe, D.J., Pero, R.T., Bignami, A. (1982) Immunostaining of neurofibrillary tangles in Alzheimer's senile dementia with a neurofilament antiserum. *J. Neurosci.* 2: 113-119.

Daniel, M.W. (1978) *Applied non-parametric statistics*. Houghton Mifflin, Boston, p.231.

Davies, P., Maloney, A.J.F. (1976) Selective loss of central cholinergic neurons in Alzheimer's disease. *Lancet* 2, 1403.

Davies, P., Katzman, R., Terry, R.D. (1980) Reduced somatostatin-like immunoreactivity in cases of Alzheimer's disease and Alzheimer-senile dementia. *Nature* 288: 279-280.

Dayan, A.D., Ball, M.J. (1973) Histometric observations on the metabolism of tangle bearing neurons. *J. Neurol. Sci.* 19: 422-426.

De Boni, U., Crapper McLachlan, D.R. (1985) Controlled induction of PHF of the Alzheimer type in Cultured Human Neurons, by Glutamate and Aspartate. *J. Neurol. Sci.* 68: 105-118.

Divry, P. (1927) Etude histo-chimique des plaques seniles. *Journal Belge de Neurologie et de Psychiatrie* 27: 643-57.

- Elliott, A., Offer, G. (1978) Shape and flexibility of the myosin molecule. *J. Mol. Biol.* 123(4): 505-519.
- Ellis, W.G., McCulloch, J.R., Corley, J. (1984) Presenile dementia in Down's syndrome: Ultra structural identity with Alzheimer's disease. *Neurol.* 24: 101-106.
- Feldman, R.G., Chandler, K.A., Levyl et al (1963) Familial Alzheimer's Disease. *Neurol. (Minneap.)* 13: 811-824.
- Ferrier, I.N., Cross, A.J., Johnson, J.A. et al (1983) Neuropeptides in Alzheimer type dementia. *J. Neurol. Sci.* 62: 159-170.
- Forno, L.S. (1978) The locus coeruleus in Alzheimer's disease. *J. Neuropathol. Exp. Neurol.* 37: 614.
- Fowler, M., Robertson, E.G. (1959) Observations on Kuru, III. Pathological features in five cases. *Australas. Ann. Med.*, 8: 16-26.
- Fuchs, E., Hanukoglu, I. (1983) Unravelling the structure of the intermediate filaments. *Cell* 34(2): 332-334.
- Gajdusek, D.C., Gibbs, C.J., Alpers, M. (1966) Experimental transmission of a kuru-like syndrome to chimpanzees. *Nature (Lond)* 209: 794-796.
- Gambetti, P., Velasco, M.E., Dahl, D., Bignami, A., Roessmann, U., Sindely, S.D. (1980) Alzheimer's neurofibrillary tangles: an immuno-histochemical study. In: *Aging, vol. 13, Aging of the Brain and Dementia* (Eds. Amaducci, L., Davison, A.N. and Antuono, P.) pp.55-63. Raven Press, New York.
- Gambetti, P., Skecket, G., Ghetti, B., Hirano, A., Dahl, D. (1983) Neurofibrillary changes in human brain. An immunocytochemical study with a neurofilament antiserum. *J. Neuropathol. Exp. Neurol.* 42: 69-79.
- Geisler, N., Plessmann, V., Weber, K. (1982) Related amino acid sequences in neurofilaments and non-neuronal intermediate filaments. *Nature* 296: 448-450.
- Geisler, N., Weber, K. (1981) Comparison of the proteins of two immunologically distinct intermediate size filaments by amino acid sequence analysis: desmin and vimentin. *Proc. Natl. Acad. Sci (USA)* 78: 4120-4123.
- Geisler, N., Weber, K. (1981) Self-assembly in vitro of the 68,000 molecular weight component of the mammalian neurofilament triplet proteins into intermediate sized filaments. *J. Mol. Biol.* 151(3): 565-571.



Gibbs, C.J.Jr., Gajdusek, D.C., Asher, D.M., Alpers, M.P., Beck, E., Daniel, P.M., Matthews, W.B. (1968) Creutzfeldt-Jakob disease (spongiform encephalopathy): transmission to the Chimpanzee. *Science* 161: 388-9.

Gibson, P.H. (1985) Relationship between numbers of cortical argentophilic and congophilic senile plaques in the brains of elderly people with and without senile dementia of Alzheimer type. *Gerontology* 31: 321-324.

Glenner, G.G., Wong, C.W. (1984) Alzheimers Disease Initial Report of the purification and characterisation of a novel cerebrovascular amyloid protein. *Biochem. Biophys. Res. Comm.* 120: 885-890.

Gonatas, N.K., Anderson, A., Evangelista, I. (1976) The contribution of altered synapses in the senile plaque: an electronmicroscopic study in Alzheimer's dementia. *J. Neuropathol. Exp. Neurol.* 26: 25-39.

Gorevic, P.D., Goni, F., Estel, B.P., Alvarez, F., Peress, N.S., Frangione, B. (1986) Isolation and partial characterisation of Neurofibrillary Tangles and Amyloid Plaque Core in Alzheimer's disease: Immunohistological studies. *J. Neuropathol. Exp. Neurol.* Vol. 45, 6: 647-664.

Gottfries, C.G., Roos, B.E., Winblad, B. (1976) Monoamines and monoamine metabolites in the post mortem human brain in senile dementia. *Aktuelle gerontol* 6: 429-435.

Gottfries, C.G., Adolfsson, R., Aquilonius, S.M., Carlsson, H., Eckernas, S.A. et al (1983) Biochemical changes in dementia disorders of Alzheimer type (AD/SDAT) *Neurobiol. Aging* 4: 261-271.

Griffin, J.W., Fahnestock, K.E., Price, D.L., Hoffman, P.N. (1983) Microtubule - neurofilament segregation produced by B,B IDPN: Evidence for the association of fast axonal transport with microtubules. *J. Neurosci* 3: 557-566.

Griffin, J.W., Hoffman, P.N., Clark, A.W., Carroll, P.T., Price, D.L. (1978) Slow axonal transport of NF proteins: Impairment by  $\beta,\beta$  IDPN administration *Science* 202: 633-635.

Gratzer, W.B. (1967) Ultraviolet absorption spectra of polypeptides. In: *Poly x amino acids*. G.D. Fasman (ed). Marcel Dekker, N.Y. pp.177-238.

Grundke-Iqbal, I., Iqbal, K., Quinlan, M., Turg, Y-C., Zaidi, M.S., Wisniewski, H.M. (1986) Microtubule-associated protein tau: a component of Alzheimer paired helical filaments. *J. Biol. Chem.* 261: 6084-6089.

Grundke-Iqbal, I., Johnson, A.B., Terry, R.D., Wisniewski, H.M., Iqbal, K. (1979) Alzheimer neurofibrillary tangles antiserum and immunohistological staining. *Ann Neurol.* 6: 532-9.

- Grundke-Iqbal, I., Iqbal, K., Tung, Y-C., Wisniewski, H.M. (1984) Alzheimer paired helical filaments: immunochemical identification of polypeptides. *Acta Neuropathol. (Berl)* 62: 259-267.
- Hachinski, V.C., Lassen, N.A., Marshall, J. (1974) Multi-infarct dementia - a cause of mental deterioration in the elderly. *Lancet* 2: 207-9.
- Hadlow, W.J. (1959) Scrapie and kuru. *Lancet* 2: 89-90.
- Hardy, J., Adolfsson, R., Alafuzoff, J. et al (1985) Transmitter deficits in Alzheimer's disease. *Neurochemistry international* 7: 545-563.
- Heston, L.L., Mastri, A.R., Anderson, V.E., White, J. (1981) Dementia of the Alzheimer type. *Arch. Gen. Psychiatry* 38: 1085-1090.
- Heyman, A., Wilkinson, W.E., Hurlritz, B.J., Schmechel, D., Sigmon, A.H., Weinberg, T. et al (1983) Alzheimer's disease: genetic aspects and associated clinical disorders. *Ann. Neurol.* 14: 507-515.
- Highman, (1946) Improved methods for demonstrating amyloid in paraffin sections. *Arch. Path.* 41: 559-565.
- Hirano, A., Dembither, H.M., Juitland, L.T., Zimmerima, H.M. (1968) The fine structure of some intraganglionic alterations. *J. Neuropathol. and Exp. Neurol.* 27: 167-182.
- Hirano, A., Malamud, N., Kurland, L.T. (1961) Parkinsonism - dementia complex, an endemic disease on the island of Guam. *Brain* 84: 662-79.
- Hoffman, P., Lasek, R. (1975) The slow component of axonal transport. *J. Cell Biol.* 66: 351-366.
- Hubbard, B.M., Anderson, J.M. (1981a) Age, senile dementia and ventricular enlargement. *Neurol. Neurosurg. and Psychiatry* 44: 631-57.
- Hubbard, B.M., Anderson, J.M. (1981b) A quantitative study of cerebral atrophy in old age and senile dementia. *J. Neurol. Sci.* 50: 135-45.
- Ihara, Y., Abraham, C., Selkoe, D.J. (1983) Antibodies to paired helical filaments in Alzheimer's disease do not recognise normal brain proteins. *Nature* 304: 727-730.
- Ihara, Y., Nukina, N., Miura, R., Ogawarra, M. (1986) Phosphorylated tau protein is integrated into paired helical filaments in Alzheimer's disease. *J. Biochem.* 99: 1807-1810.



Iqbal, K., Zaidi, T., Thomson, C.H., Merz, P.A., Wisniewski, H.M. (1984) Alzheimer paired helical filaments: bulk isolation, solubility and protein composition. *Acta Neuropathol (Berl)* 62: 167-177.

Iqbal, K., Grundke-Iqbal, I., Zaidi, T., Ali, N., Wisniewski, H.M. (1986) Are Alzheimer neurofibrillary tangles insoluble polymers? *Life Sci* 38: 1695-1700.

Ishii, T. (1966) Distribution of Alzheimer's neurofibrillary changes in the brain stem and hypothalamus of senile dementia. *Acta Neuropathol (Berl)* 6: 181-187.

Ishii, T., Haga, S., Tobutake, S. (1971) Presence of neurofilament protein in Alzheimer's neurofibrillary tangles (ANF): an immunofluorescent study. *Acta Neuropathol (Berl)* 48: 105-42.

Jamada, M., Mehraein, P. (1968) Verteilung smuster der senilen. Veränderungen in gehirn. *Archiv fur Psychiat und Zeitschrift fur ges amte Neurol* 211: 308-24.

Jarvik, L.F., Puth, V., Matsuyalma, S.S. (1980) Organic brain syndrome and aging: a six year follow-up of surviving twins. *Arch. Gen. Psychiatry* 37: 280-286.

Jellinger K. (1976) Neuropathological aspects of dementias resulting from abnormal blood and cerebrospinal fluid dynamics. *Acta Neurologica Belgica* 76: 83-102.

Kallman, R.J., Sander, G. (1949) Twin studies of senescence. *Amer. J. Psychiatry* 106: 26-36.

Kay, D.W.K., Beamish, P., Roth, M. (1964) Old age mental disorders in Newcastle upon Tyne. Part 1: A Study of prevalence. *Brit. J. Psychiatry* 110: 146.

Kidd, M. (1963) Paired helical filaments in electron microscopy of Alzheimer's disease. *Nature* 197: 192-193.

Kidd, M. (1964) Alzheimer's disease. An electron microscopical study. *Brain* 87: 307-20.

Kidd, M., Allsop, D., Landon, M. (1985) Senile plaque amyloid paired helical filaments and cerebrovascular amyloid in Alzheimer's disease are all deposits of the same protein. *Lancet* 1: 278.

Kirschner, D.A., Abraham, C., Selkoe, D.J. (1986) X-ray diffraction from intraneuronal paired helical filaments and extra neuronal amyloid fibres in Alzheimer's disease indicates cross- $\beta$  conformation.

Klatzo, L., Wisniewski, H., Streicher, E. (1965) Experimental production of neurofibrillary degeneration 1. Light Microscopic observations. *J. Neuropathol. Exp. Neurol.* 24: 187-199.

Kosik, K.S., Duffy, K., Dowling, M., Abraham, C., McCluskey, A., Selkoe, D.J. (1984) Microtubule-associated protein 2: monoclonal antibodies demonstrate the selective incorporation of certain epitopes into Alzheimer neurofibrillary tangles. *Proc. Natl. Acad. Sci. USA* 81: 7941-7945.

Kosik, K.S., Ihara, Y., Abraham, C., Rasool, C.G., McCluskey, A., Selkoe, D.J. (1984) Neurochemical studies of Alzheimer-type neurofibrillary degeneration and a related experimental model. *Comparative patho-biology of major Age-Related Diseases: Current Status and Research Frontiers*. pp.373-384. Pub Liss Inc., N.Y.

Kosik, K.S., Joachim, C.L., Selkoe, D.J. (1986) The microtubule-associated protein, tau, is a major antigenic component of paired helical filaments in Alzheimer's disease. *Proc. Natl. Acad. Sci. USA* 83: 4044-4048.

Laemmli, U.F. (1970) Cleavage of structural proteins during the assembly of the head of bacteriophage T4. *Nature (Lond)* 227: 680-685.

Larsson, T., Sjogren, T., Jacobsen, G. (1963) Senile dementia. *Acta Psychiatrica Scandinavica* 39, suppl. 167.

Lindwall, G., Cole, R.D. (1984) Phosphorylation affects the ability of tau protein to promote microtubule assembly. *J. Biol. Chem.* 259: 5301-5305.

McGeer, P.L., McGeer, E.C., Suzuki, J., Dolman, C.E., Magai, T. (1984) Aging, Alzheimer's disease and the cholinergic system of the basal forebrain. *Neurology* 34: 741-745.

Malamud, N. (1972) Neuropathology of organic brain syndromes associated with aging. In *Advances in Behavioural Biology*, vol. 3, Aging and the Brain (Ed. Geitz, F.M.) pp 63-87. Plenum Press, New York.

Mandybur, T.I. (1975) The incidence of cerebral amyloid angiopathy in Alzheimer's disease. *Neurology* 25: 125-6.

Mann, D.M.A., Lincoln, J., Yates, P.O., Stamp, J.E., Toper, S. (1980) Changes in the monoamine containing neurones of the human CNS in senile dementia. *Brit. J. Psychiatry* 50: 341-344.

Mann, D.M.A., Yates, P.O., Marcyniuk, B. (1984) Age and Alzheimer's Disease. *Lancet* 1: 281-282.

Mann, D.M.A., Yates, P.O., Marcyniuk, B. (1985) Some morphological observations on the cerebral cortex and hippocampus in presenile Alzheimer's disease, senile dementia of Alzheimer type and Down's syndrome in middle age. *J. Neurol. Sci.* 69: 139-159.

Martland, H.S. (1978) Punch drunk. J.A.M.A. 91: 1103-1107.

Masters, C.L., Gajdusek, D.C., Gibbs, C.J.Jr. (1981a) Creutzfeldt-Jakob disease virus isolations from the Gerstmann-Straussler syndrome. With an analysis of the various forms of amyloid plaque deposition in the virus-induced spongiform encephalopathies. Brain 104: 559-88.

Masters, C.L., Gajdusek, D.C., Gibbs, C.J.Jr. (1981b) The familial occurrence of Creutzfeldt-Jakob disease and Alzheimer's disease. Brain 104: 353-58.

Masters, C.L., Weinmann, N.A., Multhaup, G., McDonald, B.L., Beyreuther, K. (1985a) Amyloid plaque core protein in Alzheimer's disease and Down's syndrome. Proc. Natl. Acad. Sci. USA 82: 4245-4249.

Masters, C.L., Malthamp, G., Sims, G., Pottgiesser, J., Martins, R.N., Beyreuther, K. (1985b) Neuronal origin of a cerebral amyloid: neurofibrillary tangles of Alzheimer's disease contain the same protein as the amyloid of plaque cores, and blood vessels. EMBO J 4: 2757-2763.

Mehraein, P., Yamada, M., Tarhowska-Dzidusko, E. (1975) Quantitative studies on dendrites in Alzheimer's disease and senile dementia. In Physiol. and Pathol. of dendrites. Kreutzberg, O.W. (ed) pp.453-458. Raven Press, New York.

Merz, P.A., Somerville, R.A., Wisniewski, H.M., Iqbal, K. (1981) Abnormal fibrils from scrapie-infected brain. Acta Neuropathol. (Berl) 54: 63-74.

Merz, P.A., Somerville, R.A., Wisniewski, H.M. (1983) Scrapie associated fibrils in Creutzfeld-Jakob disease. Nature 306: 474-478.

Mesulam, M.M., Mutson, E.J., Levey, A.I., Wainer, B.H. (1984) Atlas of cholinergic neurons in the forebrain and upper brainstem of the macaque. Neuroscience 12: 669-686.

Metuzals, J., Clapin, D.F., Montpetit, V. (1984) Formation of paired helical filaments in Alzheimer disease. Proc. Ann EMSA Meeting 42: 302-303.

Miller, C.C.J., Brion, J.P., Calvert, R., Chin, T.K., Eagles, P.A.M., Downes, M.J.J., Flamend-Durand, J., Haugh, M., Kahn, J., Probst, A., Ulrich, J., Anderton, B.H. (1986) Alzheimer's paired helical filaments share epitopes with neurofilament side arms. EMBO J 5/2: 269-276.

Morel, F., Wildi, E. (1982) General and cellular pathochemistry of senile and presenile alterations of the brain. In Proc. First Jnt Congr. Neuropathol. Vol. 2: 347-74.

Morrissey, J.H. (1981) Silver stain for proteins in polyacrylamide gels: a modified procedure with enhanced uniform sensitivity. *Anal. Biochem.* 117: 307-310.

Mountjoy, C.Q., Rosser, M.N., Iverson, L.L., Roth, M. (1984) Correlation of cortical cholinergic and GABA deficits with quantitative neuropathological findings in senile dementia. *Brain* 107: 507-518.

Mountjoy, C.Q., Roth, M., Evans, N.J.R., Evans, H.M. (1983) Cortical neuronal counts in normal elderly controls and demented patients. *Neurobiology of Aging* 4: 1-11.

Mountjoy, C.Q., Tomlinson, B.E., Gibson, P.H. (1982) Amyloid and senile plaques and cerebral blood vessels. A semi-quantitative investigation of possible relationship. *Neurol. Sci.* 57: 89-103.

Norton, W.T., Goldman, J.E. (1980) Neurofilaments. In *Proteins of the Nervous System*, 2nd edn. Bradshaw and Schneider (eds) pp 301-329. Raven Press, New York.

O'Brien, L., Shelley, K., Towfughi, J., McPherson, A. (1980) Crystalline ribosomes are present in brains from senile humans. *Proc. Natl. Acad. Sci. USA* 77: 2260-2264.

Okamoto, K., Hirano, A., Yamaguchi, H., Hirai, S. (1983) The fine structure of eosinophilic stages of Alzheimer's neurofibrillary tangles. *J. Clin. Electron Microsc.* 16: 77-82.

Pauling, L., Corey, R.B. (1951) Configuration of polypeptide chains with favored orientations around single bonds. Two new pleated sheets. *Proc. Natl. Acad. Sci. USA* 37: 729-740.

Porath, J., Flodin, P. (1959) Gel filtration: A method for desalting and group preparation. *Nature* 183: 1657-1659.

Pertoft, H., Laurent, T.C., Laast, et al (1978) Density gradients prepared from colloidal silica particules coated by polyvinyl pyrrolidone (Percoll). *Anal. Biochem.* 88: 271-282.

Perry, E.K., Blessed, G., Tomlinson, B.E., Perry, R.H., Crow, T.J. et al (1981) Neurochemical activities in human temporal lobe related to aging and Alzheimer type changes. *Neurobiol Aging* 2: 251-256.

Perry, E.K., Tomlinson, B.E., Blessed, G., Bergman, K., Gibson, P.H., Perry, R.H. (1978) Correlation of cholinergic abnormalities with senile plaques and mental test scores in senile dementia. *BMJ* ii: 1457-1459.

Perry, E.K., Tomlinson, B.E., Blessed, G., Perry, R.G., Crow, T.J. (1981) Neuropathological and biochemical observations on the noradrenergic system in Alzheimer's disease. *Neurol. Sci.* 51: 279-287.



Perry, G., Rizzuto, N., Autilio-Gambetti, L., Gambetti, P. (1985) Alzheimer's paired helical filaments contain cytoskeletal components. *Proc. Natl. Acad. Sci. USA* 82: 3916-1920.

Peterson, G.L. (1977) A simplification of the protein assay method of Lowry et al., which is more generally applicable. *Anal. Biochem.* 83: 346-356.

Probst, A., Basler, V., Bron, B., Ulrich, J. (1983) Neuritic plaques in senile dementia of the Alzheimer type: a golgi analysis in the hippocampal region. *Brain Res.* 268: 249-254.

Probst, A., Ulrich, J., Hietz, Ph.U. (1982) Senile dementia of the Alzheimer type: astroglial reaction to extracellular neurofibrillary tangles in the hippocampus. *Acta Neuropathol (Berl)* 57: 75-79.

Pruisner, S.B. (1982) Novel porteinaceous infectious particles cause scrapie. *Science* 216: 136-144.

Pruisner, S.B., McKinley, M.P., Bowman, K.A. et al (1983) Scrapie prions aggregate to form amyloid-like birefringent rods. *Cell* 35: 57-62.

Puchtler H., Sweat, F., Levine, M. (1962) On the binding of congo red by amyloid. *J. Histochem. Cytochem.* 10: 355-364.

Puchtler, H., Sweat, F. (1965) Congo red as a stain for fluorescence microscopy of amyloid. *J. Histochem. Cytochem.* 13: 693-694.

Rasool, C.G., Selkoe, D.J. (1984) Alzheimer's disease: exposure of neurofilament immunoreactivity in SDS insoluble paired helical filaments. *Brain Res.* 322: 194-198.

Roberts, A.H. (1969) Brain damage in Boxers. A study of prevalence of traumatic encephalopathy among ex-professional boxers. Pitman, London.

Roberts, G.W., Crow, T.H., Polak, J.M. (1985) Location of neuronal tangles in somatostatin neurones in Alzheimer's disease. *Nature* 314: 92-94.

Rogers, D.H. (1965) Screening for amyloid with thioflavine T fluorescent method. *Amer. J. Clin. Path.* 44: 59.

Ropper, A.H., Williams, R.S. (1980) Relationships between plaques, tangles and dementia in Down's syndrome. *Neurol.* 30: 639-44.

Rosser, M.N., Emson, P.C., Mountjoy, C.Q., Roth, M., Iversen, L.L. (1980) Reduced amounts of immunoreactive somatostatin in the temporal cortex in senile dementia of the Alzheimer-type. *Neurosci. Lett.* 20: 373-377.

Roth, M., Tomlinson, B.E., Blessed, G. (1966) Correlation between scores for dementia and counts of 'senile plaques' in cerebral grey matter of elderly subjects. *Nature (Lond)* 209: 109-110.

Rubenstein, R., Kascsak, R.J., Merz, P.A., Wisniewski, H.M., Carp, R.I., Iqbal, K. (1986) Paired helical filaments associated with Alzheimer disease are readily soluble structures. *Brain Res* 372: 80-88.

Rubenstein, R. (1987) The solubility controversy of paired helical filaments: a commentary. *Neurochem. Res.* 12: 93-95.

Sajdel-Sulkowska, E.M., Coughlin, J.F., Staton, D.M., Marotta, C.A. (1983) In vitro protein synthesis by messenger RNA from the Alzheimer disease brain. In *Biological Aspects of Alzheimer's Disease*, Banbury Report 15. (Ed. Katsman, R.) pp.193-200. Cold Spring Harbor Laboratory, Cold Spring Harbor, N.Y.

Scheibel, M.E., Scheibel, A.B. (1975) Structural changes in the aging brain. In: Brody H, Harmand, K., Ord, J.M. (eds) *Ageing*, 1. Raven Press, New York.

Schlaepfer, W.W., Freeman, L.A. (1978) Neurofilament proteins of rat peripheral nerve and spinal cord. *J. Cell Biol.* 78: 653-662.

Schlaepfer, W.W. (1978) Observations on the disassembly of isolated mammal neurofilaments. *J. Cell Biol.* 76: 50-60.

Schellman, J.A., Schellman, C. (1962) The proteins. H. Neuroth (ed) New York Acad. Press. 2nd edn. vol. 2 pp. 1.

Schlote, W. (1965) Die Amyloid natur der kongophilen drüsigen Entartung der Hirnarterien (Scholz) in Senium. *Acta Neuropath.* 4: 449-68.

Schochet, S.S. Jr., Lampert, P.W., Earle, K.M. (1968) Neuronal changes induced by intrathecal vincristine sulfate. *Neuropathol. Exp. Neurol.* 27: 645-58.

Scholz, W. (1938) Studien zur Pathologie der Hirngefasse. II. Die dursige Entartung der Hirnarterien und Capillaren. *Zeitschfrit fur die gesamte Neurologie und Psychiatrie* 162: 694-715.

Selkoe, D.J., Abraham, C.R., Podlisney, M.B., Duffy, L.K. (1986) Isolation of low molecular-weight proteins from amyloid plaque fibres in Alzheimer's disease. *J. Neurochem* 146: 1820-1834.

Selkoe, D.J., Ihara, Y., Salazar, F.J. (1982) Alzheimer's disease: insolubility of partially purified paired helical filaments in sodium dodecyl sulphate and urea. *Science* 215: 1243-1245.



Selkoe, D.J., Liem, R.K.H., Yen, S.H., Shelanski, M.L. (1979) Biochemical and immunological characterisation of neurofilaments in experimental neurofibrillary degeneration induced by aluminium. *Brain Res* 163: 235-252.

Sharp, G.A., Shaw, G., Weber, K. (1982) Immunoelectron-microscopical localization of the three neurofilament triplet proteins along neurofilaments of cultured dorsal root ganglion neurones. *Exp. Cell Res.* 137: 403-413.

Shelanski, M.L., Gaskin, F., Cantor, C.R. (1973) Microtubule assembly in the absence of added nucleotides. *Proc. Nat. Acad. Sci (USA)* 70: 765-768.

Silverman, B.W. (1981) Using kernel density estimates to investigate multimodality. *J.R. Statist Soc.[B]* 43: 97-99.

Simchowicz, T. (1911) Histological Studien uber die senile Demenz. *Histologische und histopathologische Arbeiten uber die Grosshirnrinde* 4: 267-444.

Sjogren, R., Sjogren, D., Lindgren, A.G.M. (1952) Morbus Alzheimer and morbus Pick. A genetic clinical and patho-anatomical study. *Acta Psychiat et Neurol Scand, Suppl.* 82: 1-115.

Smith, C.C.T., Bowen, D.M., Sims, N.R., Neary, D., Davidson, A.N. (1983) Amino acid release from biopsy samples of temporal neocortex from patients with Alzheimer's disease. *Brain Res.* 264: 138-141.

Sofroniew, M.V., Pearson, R.C.A., Eckenstein, F., Cuello, A.C., Powell, T.P.S. (1983) Retrograde changes in cholinergic neurons in the basal forebrain of the rat following cortical damage. *Brain Res.* 289: 370-374.

Tanzi, R.E., St. George Hyslop, P.H., Haines, J.L., Polinsky et al (1987) The genetic defect in Familial Alzheimer's disease is not tightly linked to the amyloid  $\beta$  protein gene. *Nature* 329: 156-157.

Terry, R.D. (1983) The fine structure of neurofibrillary tangles in Alzheimer's disease. *Neuropathol. Exp. Neurol.* 22: 629-642.

Terry, R.D., Fitzgerald, C., Peck, A., Millner, J., Farmer, P. (1977) Cortical cell counts in senile dementia. *J. Neuropathol. Exp. Neurol.* 36: 633.

Terry, R.D., Peck, A., DeTeresa, R., Schechter, R. (1981) Some morphometric aspects of the brain in senile dementia of the Alzheimer type. *Ann Neurol.* 10: 184-92.

Terry, R.D., Pena, C. (1965) Experimental production of neurofibrillary degeneration. 2. Electronmicroscopy, phosphatase histochemistry and electron probe analysis. *J. Neuropathol. Exp. Neurol.* 24: 200-10.

Terry, R.D., Wisniewski, H.M. (1972) Ultrastructure of senile dementia and of experimental analogs. In *Advances in Behavioural Biology*, vol. 3, Aging and the Brain. Gaitz, C.M. (ed) pp 89-116. Plenum Press, New York.

Terry, R.D., Wisniewski, H. (1970) The ultrastructure of the neurofibrillary tangle and the senile plaque. In *Ciba Foundation on A.D. and related conditions*. Wolstenholme and O'Connor (eds) pp 145-168. Churchill Livingstone, London.

Thase, M.E., Liss, L., Schmelzer, D., Maloon, J. (1982) Clinical evaluation of dementia in Down's syndrome. *J. Mental Deficiency Res.* 26: 239-44.

Tombs, M.P., Souter, F., MacLagan, N.F. (1959) The spectrophotometric determination of protein at 210m $\mu$ . *Biochem. J.* 73: 167-171.

Tomlinson, B.E., Blessed, G., Roth, M. (1968) Observations on the brains of non-demented old people. *J. Neurol. Sci.* 7: 331-56.

Tomlinson, B.E., Blessed, G., Roth, M. (1970) Observations on the brains of demented old people. *J. Neurol. Sci.* 11: 205-42.

Tomlinson, B.E., Corsellis, J.A.N. (1985) Ageing and the dementias. In: Hume Adams, J., Corsellis, J.A.N., Duchon, L.W. (eds) *Greenfield's neuropathology*. Arnold, London, pp 958-959.

Torack, R.M. (1978) Current evaluation of pathological correlates of dementia. In: Torack R.M. (ed) *The pathologic physiology of dementia*. Springer, Berlin.

Troncosco, J.C., Price, D.L., Griffin, J.W., Parhad I.M. (1982) Neurofibrillary axonal pathology in aluminum intoxication. *Ann. Neurol.* 12: 278-283.

Uemura, E., Hartmann, H.A. (1978) RNA content and volume of nerve cell bodies in human brains. I. Prefrontal cortex in aging and demented subjects. *J. Neuropathol. Exp. Neurol.* 37: 487-97.

Vassar, P.S., Culling, C.F.A. (1959) Fluorescent stains with special reference to amyloid and connective tissue. *Arch. Path. (Chicago)* 68: 487.

Wang, G.P., Gunke-Iqbal, I., Kascsak, R.J., Wisniewski, H.M. (1984) Alzheimer neurofibrillary tangles; monoclonals to interent antigens. *Acta Neuropathol.* 62: 268-275.

Weber, K., Osbourn, M. (1969) The reliability of molecular weight determination by SDS-polyacrylamide gel electrophoresis. *J. Biol. Chem.* 244: 4406-4412.

Wheeler, L. (1959) Familial Alzheimer's Disease. *Ann Human Genetics* 23: 300-310.

Whitehouse, P.J., Price, D.L., Clark, A.W., Coyle, J.T., DeLong, M.R. (1981) Alzheimer's disease: evidence for selective loss of cholinergic neurons in the nucleus basalis. *Ann Neurol.* 10: 122-126.

Whitehouse, P.J., Price, D.L., Struble, R.G., Coyle, J.T., DeLong, M.A. (1982) Alzheimer's disease and senile dementia - loss of neurons in the basal forebrain. *Science* 215: 1237-1239.

Wilcock, G.K., Esiri, M.M. (1982) Plaques, tangles and dementia: a quantitative study. *J. Neurol. Sci.* 56: 343-56.

Wilcock, G.K., Esiri, M.M., Bowen, D.M., Smith, C.C.T. (1982) Alzheimer's disease. Correlation of cortical choline acetyltransferase activity with the severity of dementia and histological abnormalities. *J. Neurol. Sci.* 57: 407-419.

Willard, M., Simon, C. (1981) Antibody decoration of neurofilaments. *J. Cell Biol.* 89: 198-205.

Wischik, C.M., Crowther, R.A., Stewart, M., Roth, M. (1985) Subunit structure of paired helical filaments in Alzheimer's disease. *J. Cell Biol.* 100: 1905-1912.

Wisniewski, H.M., Bruce, M.E., Fraser, H. (1975) Infectious etiology of neuritic (senile) plaques in mice. *Science* 190: 1108-10.

Wisniewski, H.M., Ghetti, B., Terry, R.D. (1973) Neuritic (senile) plaques and filamentous changes in aged rhesus monkeys. *J. Neuropathol. Exp. Neurol.* 32: 566-84.

Wisniewski, H.M., Iqbal, K., Grundke-Iqbal, I., Rubenstein, R. (1987) The solubility controversy of paired helical filaments: a commentary. *Neurochem. Res.* 12: 93-95.

Wisniewski, H.M., Merz, P.A., Iqbal, K. (1984) Ultrastructure of paired helical filaments of Alzheimer's neurofibrillary tangle. *J. Neuropathol. Exp. Neurol.* 43: 643-656.

Wisniewski, H.M., Merz, G.S., Merz, P.A., Wen, G.Y., Iqbal, K. (1983) Morphology and biochemistry of neuronal paired helical filaments and amyloid fibres in humans and animals. *Prog. Neuropathol.* 5: 139-150.

Wisniewski, H.M., Narang, H.K., Terry, R.D. (1976) Neurofibrillary tangles of paired helical filaments. *J. Neurol. Sci.* 27: 173-181.

Wisniewski, H.M., Shelanski, M.L., Terry, R.D. (1964) Effects of mitotic spindle inhibitors on neurotubules and neurofilaments in anterior horn cells. *J. Cell Biol.* 39: 224-229.

Wisniewski, H.M., Terry, R.D. (1967) Experimental colchicine encephalopathy. I. Introduction of neurofibrillary degeneration. *Laboratory Investigations* 17: 577-87.

Wisniewski, H.M., Terry, R.D. (1973) Pathogenesis of senile plaques. *Prog. in Neuropathol.* pp.501.

Wisniewski, H.M., Wen, G.Y. (1985) Substructures of paired helical filaments from Alzheimer's disease neurofibrillary tangles. *Acta Neuropathol. (Berl)* 66: 173-176.

Wong, C.W., Quaranta, Glenner, G.G. (1985) Neuritic plaques and cerebrovascular amyloid in Alzheimer's disease are antigenically related. *Proc. Natl. Acad. Sci. USA* 82: 8729-8732.

Woodard, J.S. (1962) Clinico-pathologic significance of granulovacuolar degeneration in Alzheimer's disease. *J. Neuropathol. Exp. Neurol.* 21: 85-91.

Wuerker, R.B., Kirkpatrick, J.B. (1972) Neuronal microtubules, neurofilaments and microfilaments. *Int. Rev. Cytol.* 33: 45.

Yates, C.M., Ritchie, I.M., Simpson, J., Maloney, A.F.J., Gordon, A. (1981) Noradrenaline in Alzheimer-type dementia in Down's syndrome. *Lancet* ii, 39-40.

Yates, C.M., Simpson, J., Gordon, A., Maloney, A.F.J., Allison, Y., Ritchie, I.M., Urquhart, A. (1983) Catecholamines and cholinergic enzymes in pre-senile and senile Alzheimer-type dementia and Down's syndrome. *Brain Res.* 280: 119-26.

Yates, C.M., Simpson, H., Maloney, A.F.J., Gordon, A. (1980) Some neurochemical observations in a case of Pick's disease. *J. Neurol. Sci.* 48: 257-263.

Yen, S.H., Crowe, A., Dickson, D.W. (1985) Monoclonal antibodies to Alzheimer's neurofibrillary tangles. 1. Identification of polypeptides. *Am. J. Pathol.* 120: 282-291.

Yen, S.H., Dahl, D., Schachner, M.L. (1976) Biochemistry of the filaments of brain. *Proc. Natl. Acad. Sci. (USA)* 73: 529-533.

Yen, S.H., Gaskin, , Terry, R.D. (1981) Immunocytochemical studies of neurofibrillary tangles. *Am. J. Pathol.* 104: 77-89.

Yen, S.H., Kress, Y. (1983) The effect of chemical reagents or proteases on the ultrastructure of paired helical filaments. In: Banbury Report 15: Biological Aspects of Alzheimer's Disease. Katzman, R. (ed) N.Y.: Cold Spring Harbor Lab. pp.155-165.

Yoshimura, N. (1984) Evidence that paired helical filaments originate from neurofilaments. Clin. Neuropathol. 3: 22-27.

## APPENDIX TO BIBLIOGRAPHY

### REFERENCE TEXTS USED FOR CHAPTER 6

Jirgensons, B. (1973) Optical activity of proteins and other macro molecules. Chapman and Hall: London

d'Albis, A., Gratzer, W.B. (1974) Electronic spectra and optical activity of proteins. In: Bull, A.T., Lagnado, J.R., Tipton, K.F., Thomas, J.Q. (eds) Companion to Biochem. Longman, Lond.

Cantor, C.R., Schimmel, P.R. (1980) Biophysical Chemistry Part III. The behaviour of Biological Macromolecules. W.H. Freeman.

Provencher, S.W., Glockner, J. (1981) Estimation of globular protein secondary structure from circular dichroism. Biochemistry 1981 20:(1) 33-37.



## APPENDIX

### SDS-PAGE DISSOLVING BUFFER

5 ml	1M Tris pH 8.8
27 ml	10% SDS
18 ml	Glycerol
250 ml	10% azide
2.5 ml	$\beta$ Mercepto-ethanol ( $\beta$ ME)
0.5 mg	Bromophenyl blue

### GEL STAIN-COOMASSIE BLUE

0.5% (W/V) Coomassie brilliant blue R250  
45.5:9.0:45.5 (V/V/V) methanol/acetic acid/water

### GEL DESTAIN

7.5:5.0:87.5 (V/V/V) methanol/acetic acid/water

### GEL RUNNING BUFFER (Laemmli, 1970)

0.025M Tris  
1.92M Glycine  
0.1% (W/V) SDS

### SDS TREATMENTS

0.1%  $\beta$  mercaptoethanol was added to all SDS solutions used for solubilising proteins.